

UNIVERSITY OF SOUTHERN CALIFORNIA  
DEPARTMENT OF CIVIL ENGINEERING

UNIFORM RISK SPECTRA OF STRONG  
EARTHQUAKE GROUND MOTION:  
NEQRISK

by

V. W. Lee and M. D. Trifunac

Report No. CE 85-05

October 1985



## CONTENTS

ABSTRACT.....	i
1. INTRODUCTION.....	1
2. MODEL OF SEISMICITY.....	4
2.1 Types of Faults.....	4
2.2 Estimation of Seismicity.....	5
2.3 The Source Elements.....	7
3. ATTENUATION OF RISK FUNCTIONALS FROM THE SEISMIC SOURCES.....	12
3.1 Previous Work .....	12
3.2 The New Scaling Functions.....	15
3.3 Comparison of the Old and New Scaling Functions.....	18
3.4 Derivation of the Function $q_{ij}(S(\omega))$ .....	23
4. MODEL OF SEISMIC RISK.....	27
4.1 The Uniform Risk Spectra.....	27
4.2 Formulation of the Risk Model.....	28
4.3 Characterizing Uncertainties of Seismicity.....	35
4.4 The Probability of Exceedance $P[S(\omega)]$ .....	41
4.5 Literal Seismicity.....	46
4.6 Summary.....	52
5. THE COMPUTER PROGRAM.....	53
5.1 Introduction.....	53
5.2 Input Data.....	56
5.3 The Flow Chart and Program Description.....	64
5.4 Listing of Sample Inputs.....	74
5.5 Listing of Printer Output.....	83

6. CASE STUDIES AND AN APPLICATION.....	91
6.1 Introduction: Models I, II, III and IV.....	91
6.2 Seismic Risk Spectra at 6 Sites.....	95
6.3 Comparison of Different Models.....	95
6.4 An Application.....	106
ACKNOWLEDGEMENTS.....	119
REFERENCES.....	120

## ABSTRACT

The concept of uniform risk spectra of Anderson and Trifunac (1977) has been generalized to include (1) more refined description of earthquake source zones, (2) the uncertainties in estimating seismicity parameters  $a$  and  $b$  in  $\log_{10} N = a - bM$ , (3) to consider uncertainties in estimation of maximum earthquake size in each source zone, and to (4) include the most recent results on empirical scaling of strong motion amplitudes at a site.

Examples of using to new NEQRISK program are presented and compared with the corresponding case studies of Anderson and Trifunac (1977). The organization of the computer program NEQRISK is also briefly described.



## 1. INTRODUCTION

Earthquakes are natural phenomena occurring in many parts of the world and can adversely affect all societies. Even though the annual losses due to earthquakes are smaller than those caused by other natural disasters like wind and flood, it is the unforeseeable nature and destructive power of a major earthquake that commands serious attention. With rapidly evolving modern technology the society's vulnerability to earthquakes will increase with time, as our activities become more dependent on new sources of power, communication and complex technological systems. Earthquakes can cause extensive loss of lives through collapses of buildings, dams, bridges and other man-made structures. They are but one hazard against which design provisions must be made. To this end considerable emphasis on earthquake prediction research in the U.S. has been initiated by seismologists in the 1970's. Up till now, the development of earthquake prediction techniques is far from complete. However, we note that even a successful prediction cannot eliminate the physical damages of an earthquake. Even if the entire population were to be evacuated to safety and, in time, the destruction of the structures that remain behind could still result in a major loss and a serious blow to the region's economy. It is thus necessary to apply effectively the knowledge of balanced earthquake resistant design through seismic risk analyses, to minimize the collapse or destruction of structures, through rational and economically balanced design codes.

Seismic risk analyses are capable of estimating the probability of experiencing a given earthquake of given size during the expected life of a structure. It should be noted that designing an earthquake resistant structure may add substantially to the cost of construction, and yet the

probability that any given structure will ever be adversely affected by a major earthquake is typically low. Earthquake resistant design thus aims at obtaining an optimum balance between the expected benefits and increased costs of construction.

The objective of a seismic risk analysis is to describe the nature and probability of possible future shaking. Methods for this evaluation have been developed and used as a useful engineering and seismological tool for over a decade now. As pointed out earlier, much work still remains to be done before seismologists can predict, accurately the large future earthquakes which will occur and cause strong shaking at a given site. The same applies for providing a precise description of what the shaking will be. The locations and characteristics of future earthquakes affecting a region are, in general, still in many ways a "random process" and their analysis can only be formulated on a probabilistic basis. In any case, the problem involved is to derive, from available seismological and geological information, the nature of the ground motion to be expected at the site during possible future strong-motion earthquakes. This information is then used as the input for quantifying the seismic loads required in the design of structures.

Early analytical methods to determine the seismic risk at a site were discussed by Cornell (1968). The results are often presented in terms of one ground motion parameter, such as peak acceleration, as a measure of some characteristic of shaking, and the return period is frequently calculated versus that parameter. Other ground motion parameters like magnitude, some peak amplitude of ground shaking and Modified Mercalli Intensity at the site have also been used (Milne and Davenport, 1969; Liu and Fagel, 1972; Dalal, 1973; DeCapua and Liu, 1974; Douglas and Ryall,



1975; Algermissen and Perkins, 1976). In such studies, the detailed spectral nature of ground motion is not considered. The probability that such a spectral amplitude will be exceeded during future earthquakes does depend on wave frequency (McGuire, 1974; Trifunac, 1977).

Implicit in most early analyses is the assumption that the total energy released during an earthquake is released from the focal point of the earthquake, and hence there are "point-source models." Der-Kiureghian and Ang (1977) proposed a risk model based on the assumption that an earthquake originates at the focus and propagates as an intermittent series of fault ruptures or slips in the ruptured zone. The peak intensity of ground shaking at a site is determined by the slip that is closest to the site. Der-Kiureghian and Ang studied the level of risk independently for maximum acceleration, velocity and displacement and discussed how a response spectrum derived from the three peak values changes shape with changes in the seismicity distribution and levels of risk.

Anderson and Trifunac (1977) generalized these methods to a functional of shaking,  $S(\omega)$ , which can represent any functional of strong ground motion at frequency  $\omega$  (like Fourier amplitude, response spectral amplitude, peak response amplitude of any particular instrument, or duration of strong shaking). Their work also incorporated a more realistic model for describing the seismicity and proposed two independent methods to obtain uniform risk functionals: one assuming that the seismicity which is the input to the model is treated as the mean of a Poisson sequence, and the other one assuming it be taken literally.

The present effort is an extension of previous analyses on seismic risk and represents the second generation of the results based on the previous work of Anderson and Trifunac (1977). It incorporates into the

model the uncertainties involved in the characterization of seismicity. It uses the new frequency-dependent attenuation function (Trifunac and Lee, 1985a), and the new method for scaling Fourier and response spectral amplitudes (Trifunac and Lee, 1985b,c).

## 2. MODEL OF SEISMICITY

Following Anderson and Trifunac (1977), the seismicity here refers to the description of where earthquakes occur, the frequency of their occurrence and sizes (magnitudes or intensities), and the determination of the largest events expected to occur in any particular region or on any particular fault. The uncertainties involved in such description are also considered.

### 2.1 Types of Faults

The spatial distribution of earthquakes in any region can be divided into different source geometries according to their shape and pattern of seismicity. For this purpose, five types of sources are considered: point source, line source, areal source (diffused zone), dipping plane source, and volume (diffused) source.

#### (a) Point Source

The point source is used to describe concentrated seismicity, such as a geothermal area or a distant volcanic source, or in general when the source is far from the site.

#### (b) Line Source

A line source is used to model regions where the recorded seismic events lie fairly well along a line of shallow faults or when the faults are at considerable distance from the site.

(c) Areal Source (diffused zone)

An areal source describes areas where the faults are too numerous, randomly oriented and too small to describe individually, areas where the faults are not well defined, and where earthquakes have not been associated with faults.

These three types of sources all assume that the focal depth is small or unimportant for analysis and is thus taken as zero.

(d) Dipping Plane Source

A dipping source models the seismicity near large faults on which the activity is recorded over a depth range. The faults are modeled by planes which can be vertical or dipping at an angle.

It is assumed, in general, that the focus of an earthquake is equally likely to occur anywhere on a given fault surface.

(e) Volume Source

This model of the seismicity is to be employed where the relative depths of the earthquakes are important but cannot be constrained to a fault surface. It allows for the modeling of faults on which the activity is recorded over an area and within a certain depth. As pointed out by Anderson and Trifunac (1977), the general formulation of this type of source will become more important as more strong-motion data for deep earthquakes become available.

## 2.2 Estimation of Seismicity

There are several ways in which seismicity may be estimated. Whichever method is used, the outcome of a seismic risk analysis will depend critically on such description of seismicity surrounding the site. In

a large enough region, the occurrence rate of earthquakes is often well known. But seismic risk analysis at a specific site is more sensitive to seismic activities near the site, particularly within 25 to 50 km (Trifunac and Anderson, 1977). For such small regions, "historical seismicity" based on felt reports is often incomplete and may not represent the true seismicity of the region. In such cases, the knowledge of fault slip rates or regional strain rates from plate tectonics theory may be used to estimate "geological seismicity." This helps to increase the reliability of the description of seismicity in a region (Anderson, 1979a).

For any single source zone, let  $\mathcal{N}(e)$  be the estimated number of earthquakes with size greater than or equal to  $e$  that is to be expected in a specified time period. Here  $e$  is a general scalar variable describing the size of the earthquake, such as magnitude,  $M$ , or maximum intensity  $I_{\max}$ , for example. It can also be used as a vector variable when more parameters are involved, like for example, magnitude, rupture length, seismic moment and stress drop.

For the case of scaling in terms of magnitude or maximum intensity, the frequency of occurrence of different magnitudes (Richter, 1958) versus magnitude, giving the probability of different earthquake sizes may be used. This states that in a given period of time, the occurrence of an earthquake in a source zone can be approximated by

$$\log_{10} \mathcal{N}(M) = a - bM \quad (2.2.1)$$

where  $\mathcal{N}(M)$  is defined above and  $M$  could mean either magnitude or maximum intensity, "a" and "b" are parameters to be estimated, often from past seismicity. The earthquake size can be specified to be within a range  $[M_{\min}, M_{\max}]$ . More precisely, (2.2.1) can be rewritten as

$$\log_{10} \mathcal{N}(M) = \begin{cases} a - bM & M_{\min} \leq M \leq M_{\max} \\ 0 & M_{\max} < M \end{cases} \quad (2.2.2)$$

Here  $M_{\min}$  denotes the smallest magnitude of concern to engineering (like 3 or 3.5), and  $M_{\max}$  the upper bound magnitude which depends on each source region.

The parameters "a" and "b" can be estimated by regression analysis of the number and size of past earthquakes from the source zone in question. Using the relationship between the seismic moment rate and relative slip rate as given by Brune (1970), the parameter "a" can also be estimated indirectly from the seismic moment rate (Anderson, 1979a) in the area.

For the purposes of this discussion the estimation of seismicity thus involves the estimation of the parameters "a," "b" and " $M_{\max}$ ." It requires the use of historical and geological data combined with subjective judgment. Uncertainties in this estimation thus should be included in subsequent analysis. The parameters  $M_{\max}$  and  $\mathcal{N}(M)$  will be treated as random variables each described by an appropriate probability distribution function.

### 2.3 The Source Elements

For each source zone, starting with  $\mathcal{N}(M)$ , the estimated number of earthquakes with size greater than or equal to  $M$ , within the time period of (2.2.1) and a size  $M_j$ , we define  $N(M_j)$  to be the estimated number of earthquakes with sizes inside  $[M_j - \delta M_j / 2, M_j + \delta M_j / 2]$ . Then

$$N(M_j) = \mathcal{N}(M_j - \delta M_j / 2) - \mathcal{N}(M_j + \delta M_j / 2) \quad (2.3.1)$$

As in Anderson and Trifunac (1977), the earthquake size  $M$  will be discretized. For scaling with magnitudes, one half of magnitude unit, will be used for basic interval. Earthquakes of size  $M_j$  will thus mean earthquakes of size within  $[M_j-.25, M_j+.25]$ . For scaling with intensities, the Modified Mercalli Intensities are already discretized. The discretized values ( $M_j, j = 1$  to  $J$ ) will be used in subsequent analysis.

The total seismicity of a region will be modeled by a superposition of different types of source zones in the region. To evaluate the risk, each of the zones will be divided into small source elements, and to each of these source elements, say the  $i$ -th element, we will assign  $n_{ij}$ , the estimated number of earthquakes of size  $M_j$  which occur in the  $i$ -th element within the chosen time period.

$n_{ij}$  is derived from  $N(M_j)$  for different geometries of source zones, as discussed in Section 2.1. The detailed manner in which the source parameters are related to the shaking at the site will affect the way  $n_{ij}$  is evaluated. One earlier approach is to consider only the epicentral distance from the fault to the site. In this case then,  $n_{ij}$  will represent the estimated number of earthquakes with epicenters in the  $i$ -th element. Such approach has been proposed and used by Cornell (1968), for example. Dalal (1973) and McGuire (1974) also used this form. For such approach,  $n_{ij}$  is defined as follows:

(a) Point Source: If there are  $N(M_j)$  events of size  $M_j$ , and the point source is the  $i$ -th element, then  $n_{ij} = N(M_j)$ .

(b) Line Source: If the  $i$ -th element has a length  $L_i$  and is part of a line source of length  $L$ , then  $n_{ij} = N(M_j)L_i/L$ .

(c) Areal Source: If the  $i$ -th element has an area  $A_i$ , and is part of an areal source (diffused zone) of total area  $A$ , then  $n_{ij} = N(M_j)A_i/A$ .

(d) Dipping Surface: This case is analogous to that of an areal source. If the  $i$ -th element has area  $\Sigma_i$ , and is part of a dipping surface of total area  $\Sigma$ , then  $n_{ij} = N(M_j)\Sigma_i/\Sigma$ .

(e) Volume Source: If the  $i$ -th element has volume  $V_i$ , and is part of a volume source of total volume  $V$ , then  $n_{ij} = N(M_j)V_i/V$ .

Alternatively, if one considers not the epicentral distance but the distance to the closest point of rupture on the fault, for example, then  $n_{ij}$  represents the estimated number of earthquakes which have their closest point of rupture to the site in the  $i$ -th element. In this approach, both the magnitude and rupture length or area of the events are considered.

The assumptions that the rupture is unilateral and the direction of rupture may be random is often used with this approach. Der-Kiureghian and Ang (1975), Douglas and Ryall (1975), and Anderson and Trifunac (1977) all used a similar approach. The following is a description of how  $n_{ij}$  is derived for each source type:

(a) Point Source: The formulation of the point source model is identical to that of the first approach.

(b) Line Source: The following formulation has been used by Anderson and Trifunac (1977) in their computer program "EQRISK." The line source of total length  $L$  is described by a set of straight lines, which are input as a consecutive sequence of coordinates in terms of their latitudes and longitudes. The program then represents the line source as a sequence of

$N_L$  equally spaced points along the fault. The spacing  $\delta L = L/(N_L - 1)$  between the points is small enough so that this is equivalent to discretizing the line source in terms of  $N_L$  points. For an earthquake of size  $M_j$  (magnitude of maximum intensity), it is assumed that the earthquake ruptures the fault along a length  $\ell_j$ . Let  $\ell_j = k_j \delta L$ , so that the rupture zone takes up  $k_j$  segments of the discretized points. Then there are  $N_L - k_j$  "allowable" points along the fault that have equal probability of being the midpoint of a rupture zone. Each of these "allowable" points will have  $N(M_j)/(N_L - k_j)$  "allowable" events of size  $M_j$ . For each of these points, let the  $i$ -th discretized point (the  $i$ -th element) of the fault be the point on the rupture zone closest to the site where the risk is to be calculated. In this case the number  $N(M_j)/(N_L - k_j)$  is attributed to the  $i$ -th element. The total number of events,  $n_{kj}$ , of the  $i$ -th element of size  $M_j$  is built up in this way. Events with rupture length  $\ell_j$  larger than the fault length  $L$  will mean that only one of the discretized points on the fault, namely the point closest to the site, will have  $N(M_j)$  as the expected number of events of size  $M_j$ .

(c) Areal Source: Since an areal source describes surface areas where the faults are too numerous or too small to describe individually (diffused zone), or where the faults are not well defined, the program "NEQRISK" (Anderson and Trifunac, 1977) simply divides the area into small source elements and assumes the earthquakes to have equal probability of occurrence in each source element, as in the first approach.

(d) Dipping Source: The formulation for a dipping plane source is similar to that for a line source. First, the fault surface is divided into  $N_\Sigma$  equal size square elements with areas  $\delta\Sigma = \Sigma/N_\Sigma$ , where  $\Sigma$  is the



total area of the dipping source. The spacing  $\delta\Sigma$  is small enough so that this is equivalent to discretizing the dipping surface in terms of  $N_\Sigma$  points. For an earthquake of size  $M_j$ , it is assumed that the earthquake ruptures the fault along an area  $a_j$ . Then an event with area  $a_j$  must rupture  $a_j/\delta\Sigma$  adjacent fault elements. Let  $a_j = k_j\delta\Sigma$ , so that the rupture zone takes up  $k_j$  segments of the discretized points. The ruptured  $k_j$  segments will then be approximately square for small events and rectangular with the width equal to the width of the fault surface for larger events. As in the case of a line source, there are  $N_\Sigma - k_j$  "allowable" points (or discretized areas) along the fault which have equal probability of being the focus of a rupture zone. Each of these "allowable" points will have  $N(M_j)/(N_\Sigma - k_j)$  "allowable" events of size  $M_j$ . For each of these points, let the  $i$ -th discretized point ( $i$ -th element) of the surface be the point on the rupture zone closest to the site. Then  $N(M_j)/(N_\Sigma - k_j)$  events are attributed to that element. The total number of events,  $n_{ij}$ , of the  $i$ -th element of size  $M_j$  is built up in this way. Note that the number of "allowable" locations,  $N_\Sigma - k_j$ , depends on the size of the rupture area and hence on the size of the events.

(e) Volume Source: As mentioned in Anderson and Trifunac (1977), there were, and there still are at present, insufficient empirical results to formulate methods of modifying the distribution of epicenters to account for the finite dimensions of rupture in a source zone of this type. For such source zone at sufficient distance from the site, the same characterization of volume source as that of the first approach is used here.

### 3. ATTENUATION OF RISK FUNCTIONALS FROM THE SEISMIC SOURCES

#### 3.1 Previous Work

An example of previous work on a description of the attenuation of risk functionals from seismic sources used in seismic risk analysis is found in Anderson and Trifunac (1977). The risk functionals that have been used include Fourier spectral amplitudes,  $FS(T)$ , pseudo relative velocity spectral amplitudes,  $PSV(T)$ , relative velocity spectral amplitudes,  $SV(T)$  and absolute acceleration spectral amplitudes,  $SA(T)$ . For scaling of Fourier spectral amplitudes  $FS(T)$ , using earthquake magnitude, source to station distance and local geology (parameter  $s$  or  $h$ ), either the model of Trifunac (1976) or Trifunac and Lee (1978) have been used. The first model is given by (Trifunac, 1976):

$$\log_{10} FS(T)_{, \ell} = \begin{cases} M + \log_{10} A_0(R) - a(T)p_{\ell} - b(T)M_{\min} - c(T) - d(T)s \\ \quad - e(T)v - f(T)M_{\min}^2 - g(T)R, & M \leq M_{\min} \\ M + \log_{10} A_0(R) - a(T)p_{\ell} - b(T)M - c(T) - d(T)s \\ \quad - e(T)v - f(T)M^2 - g(T)R, & M_{\min} \leq M \leq M_{\max} \\ M_{\max} + \log_{10} A_0(T) - a(T)p_{\ell} - b(T)M_{\max} - c(T) - d(T)s \\ \quad - e(T)v - f(T)M_{\max}^2 - g(T)R, & M_{\max} \leq M \end{cases} \quad (3.1.1)$$

where  $T(=2\pi/\omega_n)$  is the period,  $M$  is the local magnitude of the earthquake,  $\log_{10} A_0(R)$  is a description of the attenuation with epicentral distance  $R$  as used by Richter (1958) to define the local magnitude, and  $p_{\ell}$  is a linear approximation for  $0.1 < p_{\ell} < 0.9$ , to the actual probability,  $p_a$ , say, that the spectral amplitude,  $FS(T)$ , will not be exceeded.  $s$  is a site condition of the local geology,  $s = 0$  for alluvial sites, 2 for sites on hard basement (igneous) rocks and 1 is used for sites which are on consolidated sediments or are difficult to classify because of confusing geological environment.  $v$  is a component variable set to 0 for horizontal

motion and to 1 for vertical motion. The values for  $M_{\min}$  and  $M_{\max}$  are given by

$$\begin{aligned} M_{\min} &= -b(T)/2f(T), \quad \text{and} \\ M_{\max} &= (1-b(T)/2f(T)) . \end{aligned} \quad (3.1.2)$$

The resulting spectral amplitudes grow linearly for  $M < M_{\min}$ , quadratically for  $M_{\min} \leq M \leq M_{\max}$  and stop increasing for  $M > M_{\max}$ . The coefficients  $a(T), b(T), \dots, g(T)$  are empirical "constants" estimated by regression analysis.

A more refined correlation function has been developed by Trifunac and Lee (1978). For  $M_{\min} < M < M_{\max}$ , it is given by

$$\log_{10} FS(T) = M + \log_{10} A_0(R) - b(T)M - c(T) - d(T)h - e(T)v - f(T)M^2 - g(T)R . \quad (3.1.3)$$

Here  $h$  represents the depth of alluvium, and replaces parameter  $s$ . The term  $a(T)p_{\ell}$  is dropped from this correlation, and the result is the mean estimated value of  $FS(T)$ ,  $\hat{FS}(T)$ . With  $FS(T)$  representing the actual Fourier amplitude spectra computed from recorded accelerograms, the residuals,  $\varepsilon(T)$ , were calculated, where

$$\varepsilon(T) = \log_{10} FS(T) - \log_{10} \hat{FS}(T) \quad (3.1.4)$$

describes the distribution of the observed  $FS(T)$  about the estimated  $\hat{FS}(T)$ . It is assumed that  $\varepsilon(T)$  can be described by a normal distribution function with mean  $\mu(T)$  and standard deviation  $\sigma(T)$  (Trifunac and Lee, 1978):

$$p_a = p(\varepsilon, T) = \frac{1}{\sigma(T)\sqrt{2\pi}} \int_{-\infty}^{\varepsilon(T)} \exp \left[ -\frac{1}{2} \left( \frac{x - \mu(T)}{\sigma(T)} \right)^2 \right] dx, \quad (3.1.5)$$

from which  $p_a$ , the probability that  $\log_{10}[FS(T)] - \log_{10}[\hat{FS}(T)] \leq \varepsilon(T)$ , can be determined directly.

Equations (3.1.1) and (3.1.3) have complementary uses, since in some cases, the depth of alluvium,  $h$ , is known, while in other cases, only the surface geology parameter  $s$  is available.

The regression analyses for the above equations were carried out for 186 free-field records corresponding to a total of 558 components of data from 57 earthquakes from 1933 through 1971. The same data base has been used for regression analysis on relative velocity spectral amplitudes,  $SV(T)$  (Trifunac and Anderson, 1978b), on pseudo relative velocity spectral amplitudes,  $PSV(T)$  (Trifunac and Anderson, 1978a; Trifunac and Lee, 1979), and absolute acceleration spectra amplitudes,  $SA(T)$  (Trifunac and Anderson, 1977).

The same scaling equations were used for  $SV(T)$ ,  $SA(T)$  and  $PSV(T)$  as those of  $FS(T)$ . In each case, the residuals,  $\varepsilon(T)$ , were calculated, and then described by an analytical assumed probability distribution function. For  $PSV(T)$ , for example, the distribution function derived from Rayleigh distribution is used (Trifunac and Lee, 1979):

$$p_a = p(\varepsilon, T) = [1 - \exp(-\exp(\alpha(T)\varepsilon(T) + \beta(T)))]^{N(T)} \quad (3.1.6)$$

from which  $p_a$ , the probability that  $\log_{10}[PSV(T)] - \log_{10}[\hat{PSV}(T)] \leq \varepsilon(T)$ , the difference between the calculated and estimated spectral amplitudes being less than a specified residual value, can be determined directly.

Scaling of Fourier spectral amplitudes in terms of Modified Mercalli Intensity and local geology parameters can be found in Trifunac (1979), or in Trifunac and Lee (1978) using the depth of alluvium at recording sites,  $h$ . Similarly, scaling of pseudo relative response spectral amplitudes in terms of Modified Mercalli Intensity and local geology are found in Trifunac and Anderson (1978a) or Trifunac and Lee (1979). All these scaling relationships have been used in seismic risk analyses.

### 3.2 The New Scaling Functions

Through the years new earthquake acceleration data have been recorded, digitized and added to the original database. The list of 57 earthquakes has now grown to 104, most of which occurred in the regions of northern and southern California. The original list of 186 free-field records has now grown to 438. With 3 components available for each record, this amounts to a total of 1314 acceleration components, of which there are 876 horizontal and 438 vertical components.

With this new database, Trifunac and Lee (1985a) have developed a new frequency dependent attenuation function,  $\mathcal{A}tt(\Delta, M, T)$ , to replace the Richter's attenuation function,  $\log_{10} A_0(R)$ , used previously. It takes the form

$$\mathcal{A}tt(\Delta, M, T) = \mathcal{A}_0(T) \log_{10} \Delta, \quad (3.2.1)$$

where  $\mathcal{A}_0(T)$  is an empirically determined parabolic function of period  $T$ , and  $\Delta$  is given by

$$\Delta = S \left( \ln \frac{R^2 + H^2 + S^2}{R^2 + H^2 + S_0^2} \right)^{-\frac{1}{2}}. \quad (3.2.2)$$

$\Delta$  can be thought of as a "representative distance" from the earthquake source of size  $S$ , at depth  $H$  and at distance  $R$  from the recording site.  $S_0$  is the coherence radius of the source. The definition of  $\Delta$  used has been proposed by Gusev (1983) in his descriptive statistical model of earthquake source radiation for the description of short-period strong ground motion. Detailed description and calculation for this new attenuation function are given in Trifunac and Lee (1985a).

With the new attenuation function defined, the regression equation of Fourier amplitudes now takes the form (Trifunac and Lee, 1985b):

$$\log_{10} FS(T) = \mathcal{A}(\Delta, M, T) + \begin{cases} M + C_1(T)M_{\min} + C_2(T)s + C_3(T)v + C_4(T) + C_5(T)M_{\min}^2, & M \leq M_{\min} \\ M + C_1(T)M + C_2(T)s + C_3(T)v + C_4(T) + C_5(T)M^2, & M_{\min} \leq M \leq M_{\max} \\ M_{\max} + C_1(T)M_{\max} + C_2(T)s + C_3(T)v + C_4(T) + C_5(T)M_{\max}^2, & M_{\max} \leq M \end{cases} \quad (3.2.1)$$

with all the parameters defined as before. Again,  $M_{\min}$  and  $M_{\max}$  are given by

$$\begin{aligned} M_{\min} &= -C_1(T)/2C_5(T), \quad \text{and} \\ M_{\max} &= -(1+C_1(T))/2C_5(T) \quad . \end{aligned} \quad (3.2.2)$$

$C_1(T), \dots, C_5(T)$  are "coefficients" determined by regression analyses on the new database of 1314 components of Fourier amplitude data  $FS(T)$  at 91 discrete periods  $T$  ranging from 0.04 to 15.0 sec. The same regression analysis has been also carried out with the site condition  $s$  replaced by the depth of alluvium  $h$ . The residuals  $\varepsilon(T)$  were again calculated as in the previous

analyses (equation (3.1.4)) and it was assumed that  $\epsilon(T)$  can be described by a normal distribution function with mean  $\mu(T)$  and standard deviation  $\sigma(T)$  (equation (3.1.5)).

The same scaling equations in terms of the frequency dependent attenuation functions  $\mathcal{A}tt(\Delta, M, T)$  were also developed for PSV(T) (Trifunac and Lee (1985c)). As before, the residuals,  $\epsilon(T)$ , were calculated and described by the appropriate distribution function as in equation (3.1.6).

Scaling of Fourier spectral amplitudes in terms of the Modified Mercalli Intensity (MMI) using the new database of 1314 records has also been carried out. While new instrumentation is being developed in many parts of the world, the long-term historical seismicity records continue to be available only in terms of the locally developed intensity scales and thus all risk calculations in terms of MMI scaling have been developed here as well.

The new set of earthquakes that have been added to the database through the years 1972 to 1981 have magnitudes typically below 6. For this reason the MMI levels for many of these earthquakes are either not well documented or have not been reported. A correlation of the MMI levels with the corresponding earthquake magnitudes, representative source to station distance and local site geology has been developed (Lee and Trifunac, 1985), using the following equation

$$I_{MM} = 1.5M - A - B \ln \Delta - C\Delta/100 - Ds, \quad (3.2.3)$$

where the parameters  $M$ ,  $\Delta$ ,  $s$  are defined as before, and  $I_{MM}$  is the MMI level at the site.

For scaling of Fourier amplitude spectra the following equation was employed

$$\log_{10} FS(T) = b_1(T)\hat{I}_{MM} + b_2(T)s + b_3(T)v + b_4(T) \quad (3.2.4)$$

with  $\hat{I}_{MM}$  representing the estimated level at the site computed from (3.2.3) or the reported MMI level if available. The correlation using  $h$ , the depth of alluvium, instead of  $s$ , the site parameters, was also carried out.

Correlations of pseudo relative velocity spectra in terms of intensities were also carried out (Trifunac and Lee, 1985c). In both bases, correlations using both the recording site conditions ( $s = 0, 1, 2$ ) and the depth of alluvium,  $h$ , at the site have been presented.

In summary, for both Fourier and pseudo relative velocity response spectra, correlation coefficients for the four models using the new database are available: (1) magnitude- $s$  model, (2) magnitude- $h$  model, (3) MMI- $s$  model and (4) MMI- $h$  model.

### 3.3 Comparison of the Old and New Scaling Functions

It is interesting to compare the results of the old scaling functions using Richter's attenuation function and the old database with those of the new scaling functions using the new attenuation function and the new database. Figure 3.3.1 is a plot of the estimated PSV spectra with 5% of critical damping for an event of magnitude 6.5 at a focal depth of 5 km. In this example the recording sites are assumed to have the depth of sediments of 2 km and to be at the epicentral distances of 5, 25, 50 and 100 km. The two graphs correspond respectively to the horizontal component of input (on the left) and vertical component (on the right). The solid lines on each graph represent the new results while the dashed lines correspond to old



ESTIMATED PSV SPECTRA, 5% DAMPING  
MAGNITUDE = 6.5    FOCAL DEPTH(KM) = 5.0    ALLUV. DEPTH(KM) = 2.0  
EPIC DIST (KM) = 5    25    50    100

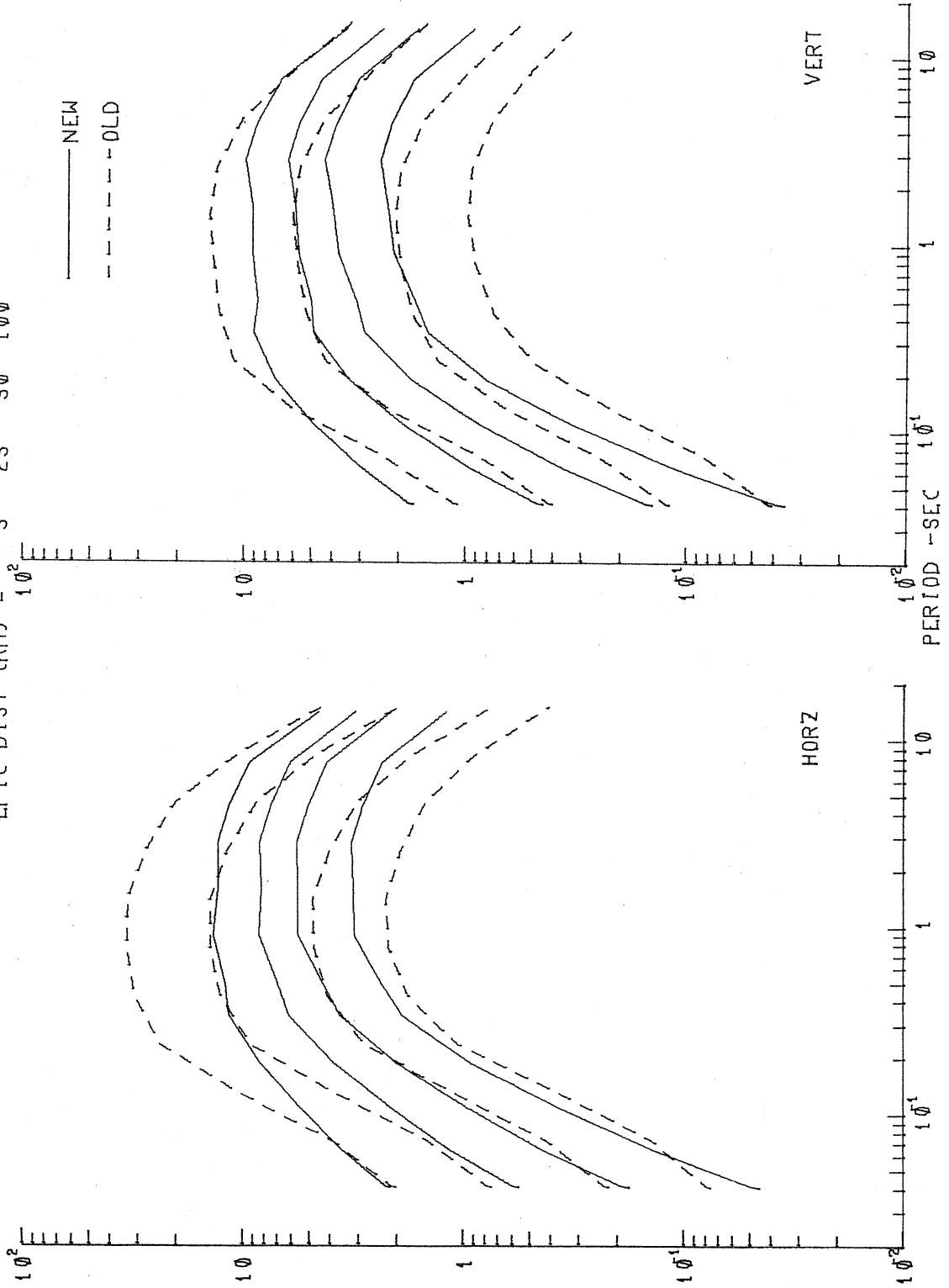


Figure 3.3.1

results. For periods between .04 and .1 seconds, the dashed lines and the corresponding solid lines are of comparable amplitudes. Beyond the period of .1 seconds, and for horizontal components the dashed lines are higher than the solid lines at sites with epicentral distances of 5 and 25 km, and vice versa at sites with epicentral distances of 50 and 100 km. For responses from the vertical accelerations at periods beyond 1 sec., the dashed line is higher than the solid line at the site with epicentral distance at 5 km, but the two sets of curves become of comparable amplitudes at a distance of about 25 km and then the trend is reversed for distances of 50 and 100 km. The observed differences between the dashed lines and solid lines are due to the differences between the old (Richter) attenuation and the new frequency dependent attenuation function.

Figure 3.3.2 is a plot of the estimated PSV spectra with 5% of critical damping at a recording site with epicentral distance of 5 km from the source. Again the recording site is assumed to have the depth of sediments equal to 2 km. The events shown have magnitudes of 5.5, 6.0, 6.5 and 7, and a focal depth of 5 km. Both the spectra from the horizontal and vertical acceleration show that for intermediate periods, the dashed lines are usually higher than the corresponding solid lines for most magnitudes. This shows that at short epicentral distances, the new frequency dependent attenuation function attenuates slower than the old Richter's attenuation function for periods greater than about .1 sec. Figure 3.3.3 is a plot of the estimated PSV spectra similar to that of Figure 3.3.2, but with the recording site this time at an epicentral distance of 100 km. Contrary to Figure 3.3.2, Figure 3.3.3 shows that for both the spectra from the horizontal and vertical acceleration, and for periods greater than about .1 sec., the dashed lines have lower

ESTIMATED PSV SPECTRA, 5% DAMPING  
FOCAL DEPTH(KM) = 5.0 ALLUV. DEPTH(KM) = 2.0 EPIC DIST(KM) = 5.0  
MAGNITUDE = 5.5, 6.0, 6.5, 7.0

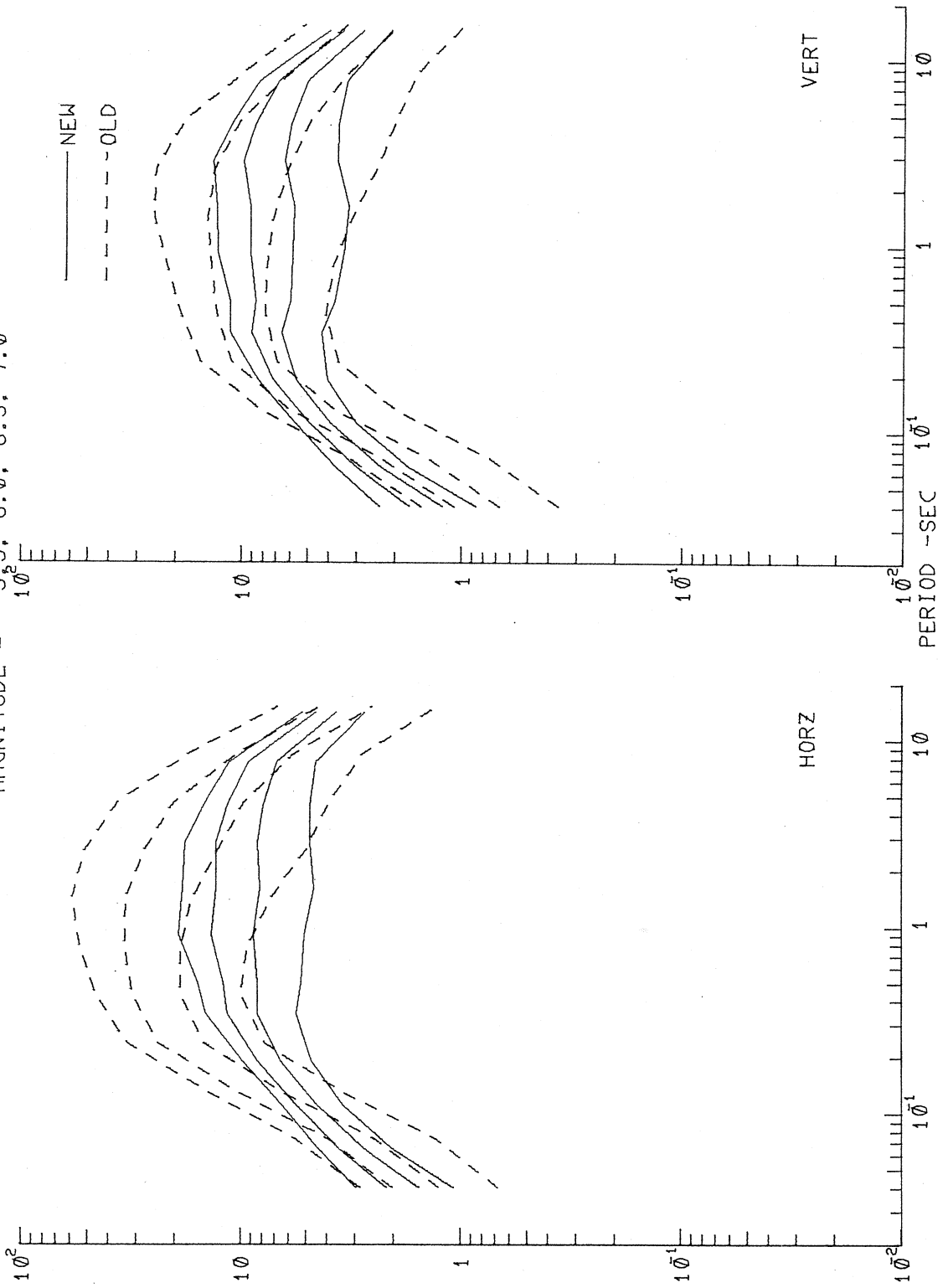


Figure 3.3.2

ESTIMATED PSV SPECTRA, 5% DAMPING  
FOCAL DEPTH(KM) = 5.0 ALLUV. DEPTH(KM) = 2.0 EPIC DIST(KM) = 100.0  
MAGNITUDE = 5.5, 6.0, 6.5, 7.0

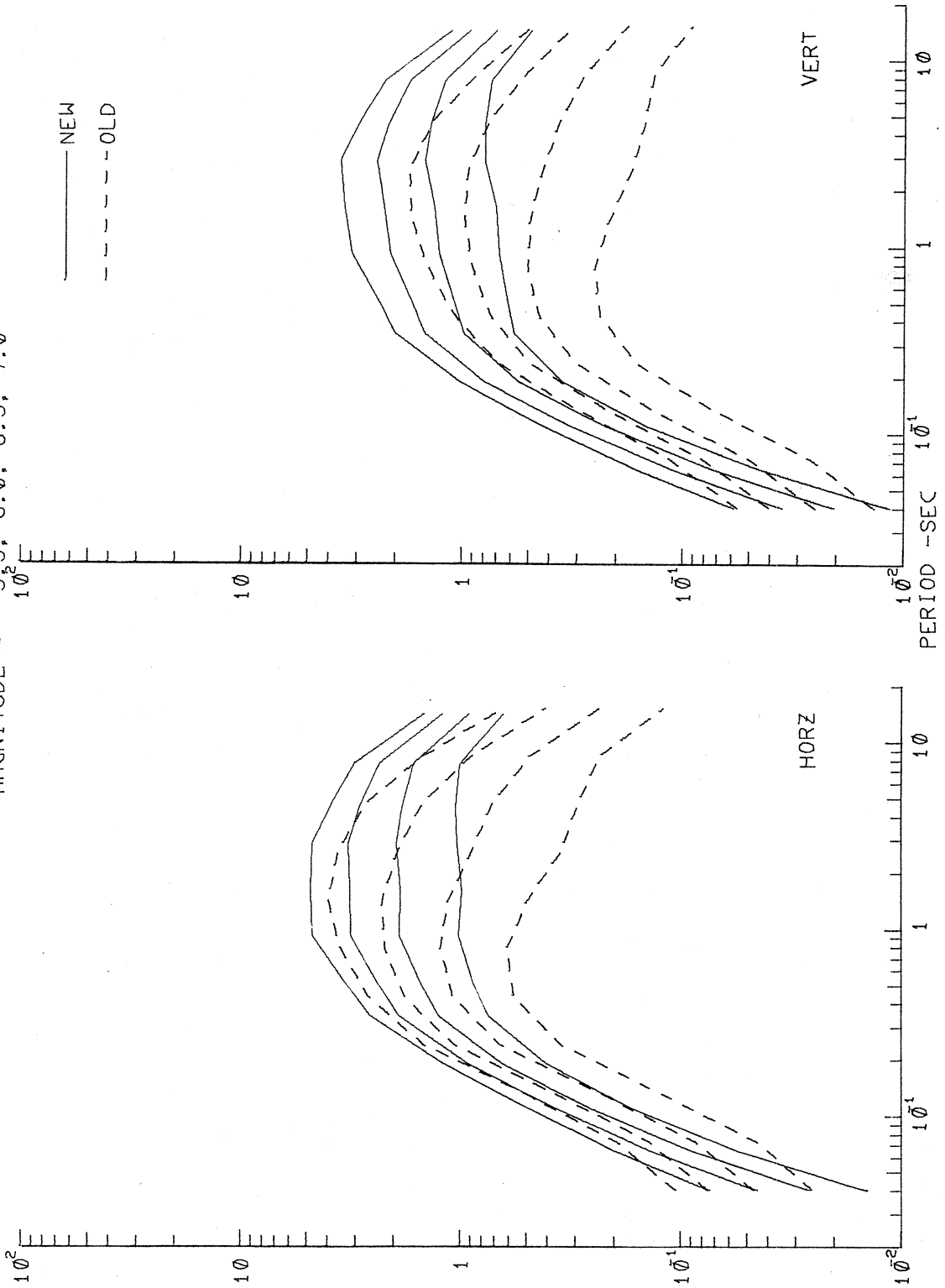


Figure 3.3.3

amplitudes than the corresponding solid lines for all magnitudes. At large epicentral distances, the new frequency dependent attenuation function attenuates more or less the same way as the old Richter's attenuation function.

### 3.4 Derivation of the Function $q_{ij}(S(\omega))$

The empirical scaling functions summarized in the previous sections for Fourier and response amplitude spectra can now be applied and inverted to obtain the function  $q_{ij}(S(\omega))$ . For a given functional  $S(\omega)$  of strong ground motion at frequency  $\omega$ ,  $q_{ij}(S(\omega))$  is defined to be the probability that  $S(\omega)$  will be exceeded at the site in an event of size  $M_j$  in the  $i$ -th source element. It implicitly assumes a scaling model of the attenuation of  $S(\omega)$  from the source (the  $i$ -th element) to the site. Examples of these scaling models are presented in the previous sections. For a given model, let  $\hat{S}_{ij}(\omega)$  be the estimated amplitude of the functional at the site from an event of size  $M_j$  in the  $i$ -th source element. Consider the residuals,  $\epsilon_{ij}$ , defined by

$$\epsilon_{ij} = \log_{10} S(\omega) - \log_{10} \hat{S}_{ij}(\omega) \quad . \quad (3.4.1)$$

In the scaling model, it is assumed that  $\epsilon_{ij}$  can be described by a probability distribution function,  $p(\epsilon)$ , from which  $p_{ij}$ , the probability that  $\log_{10} S(\omega) - \log_{10} \hat{S}_{ij}(\omega) \leq \epsilon_{ij}$ , can be determined directly. For Fourier amplitudes, for example, the normal distribution function is assumed, and for pseudo relative velocity spectral amplitudes, the distribution function is presented, as described in Section 3.1.

As an example, consider the scaling of PSV amplitudes at 5% of critical damping. Figure 3.4.1 shows the plot of the residual levels

PSV RESIDUE STATISTICS DAMPING=.05 MAG-DEPTH MODEL

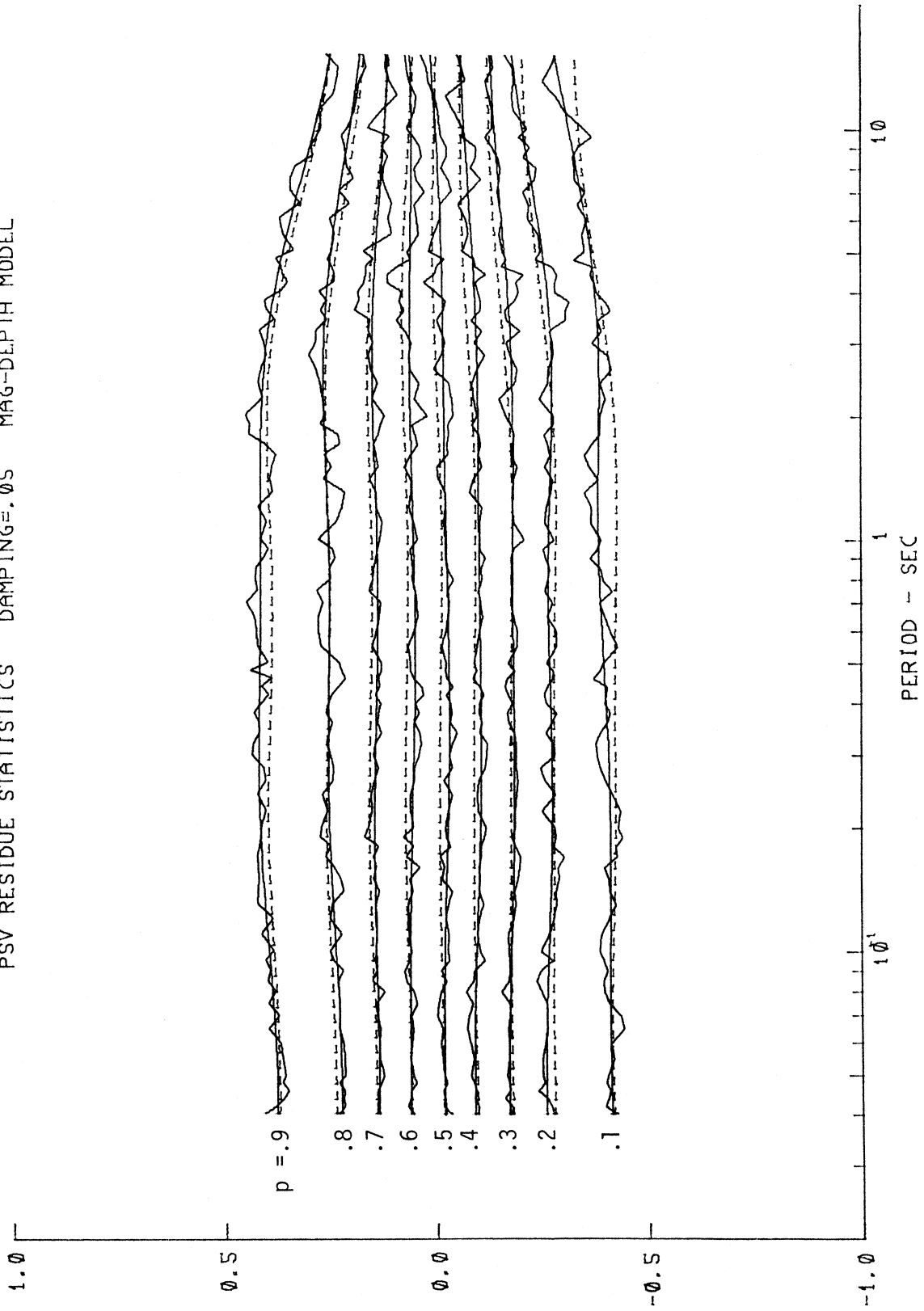


Figure 3.4.1

corresponding to  $p^*(\epsilon, T) = 0.1, 0.2, \dots, 0.8$  and  $0.9$ . The nine sets of curves, plotted versus period  $T$ , from the bottom to the top of the plot correspond to the residual levels at each of the probability levels,  $0.1$  through  $0.9$ . At each of the probability levels, the rough solid curve corresponds to the actual calculated residues at the particular level and the smooth solid curve is obtained by smoothing the rough solid curve along the  $T$ -axis. The corresponding dashed curve is the estimated residue,  $\epsilon(T)$ , at the particular level that is estimated by using the distribution function in (3.1.6). Both the calculated and estimated residue levels range from around  $\epsilon = -0.4$  at  $p^* = 0.1$  to around  $\epsilon = +0.4$  at  $p^* = 0.9$ . The range of these residue levels is a measure of the distribution of the observed  $PSV(T)$  about the estimated  $\hat{PSV}(T)$ .

Figure 3.4.2 shows a plot of the statistical parameters employed in the description of the residues from estimating PSV data of 5% damping.  $N(T)$  and the smooth amplitudes of  $\hat{\alpha}(T)$  and  $\hat{\beta}(T)$  of (3.1.6) together with their 95% confidence intervals are respectively given in the top 3 plots of the figure. The two full curves in the bottom of the figure show the smoothed amplitudes of the computed  $\chi^2$ ,  $\chi^2(T)$  and Komolgorov-Smirnov,  $KS(T)$ , statistics, respectively. They are used to measure the goodness of fit. The dashed lines are their corresponding 95% cutoff levels. The reader is referred to Trifunac and Lee (1985b,c) for a more complete description of these tests. It is seen from the figure that both the  $\chi^2$  and K-S tests fail to reject the hypothesis that the distribution is that given in (3.1.6). The density function  $p(\epsilon, T)$  thus represents an acceptable approximation to the actual  $p^*(\epsilon, T)$ .

Finally, the required function  $q_{ij}$  in the risk analysis is then defined by

PSV RESIDUE STATISTICS DAMPING=.05 MAG-DEPTH MODEL

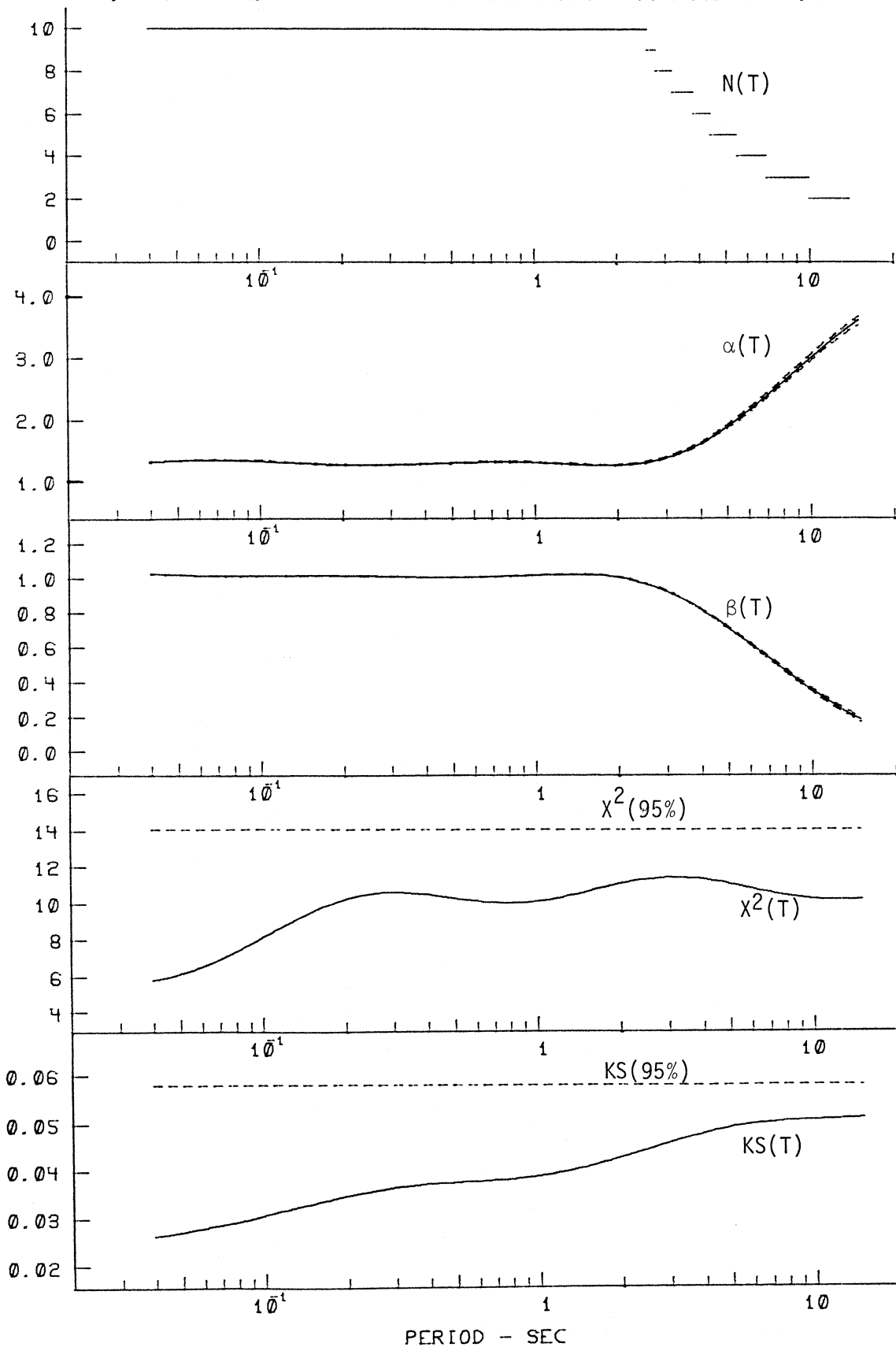


Figure 3.4.2



$$q_{ij} = 1 - p_{ij} \quad (3.4.2)$$

where  $p_{ij}$  is the estimated probability that  $\log_{10} S(\omega) - \log_{10} \hat{S}(\omega) \leq \epsilon_{ij}$ .

In summary, all the scaling relationships for Fourier and response spectral amplitudes that were derived by Trifunac (1976, 1979), Trifunac and Anderson (1978a,b), Trifunac and Lee (1978, 1979) and more recently by Trifunac and Lee (1985b,c) can also be used to find the function  $q_{ij}(S(\omega))$  needed in risk calculations. The recent scaling relationships are an improvement over the previous ones by the same authors through the use of the new larger database and the use of a new frequency dependent attenuation function, as described in Trifunac and Lee (1985a).

As pointed out by Anderson and Trifunac (1977), the incorporation of the detailed description of scatter of amplitudes about the mean trend in the scaling equation, as is done, here, is one of the most significant improvements of our risk analysis over much of the previous work in this area. Der-Kiureghian (1977) pointed out that the uncertainty associated with the scaling functions often far exceeds the uncertainties associated with the other aspects of the modeling of seismic risk. Thus, by using the probability distribution functions as proposed here, a major source of potential errors in seismic risk analysis has been described and quantified.

#### 4. MODEL OF SEISMIC RISK

##### 4.1 The Uniform Risk Spectra

Consider a given functional  $S(\omega)$  of strong ground motion and a given time interval of  $Y$  years at a given site. Following Anderson and Trifunac (1977), two functions of  $S(\omega)$  and  $Y$  are to be determined:

- (1) The expected number of times,  $N_E[S(\omega)]$ , that  $S(\omega)$  will be exceeded at the site in  $Y$  years, and
- (2)  $p[S(\omega)]$ , the probability that  $S(\omega)$  will be exceeded at least once in  $Y$  years.

Figure 4.1.1 shows an example of the function  $p[S(\omega)]$  at a particular frequency  $\omega$ . If  $p[S(\omega)]$  can be estimated at a chosen set of discrete frequencies, a uniform risk functional can be constructed as shown in Figures 4.1.2 and 4.1.3. Figure 4.1.2 shows the probability of exceeding  $S(\omega)$  at three selected frequencies,  $\omega_1$ ,  $\omega_2$  and  $\omega_3$  say. One can then construct a uniform risk spectra at a given probability level,  $p = .1$ , say, which at each frequency,  $\omega$ , gives the spectral amplitude  $S(\omega)$  that has the probability of 0.1 that it will be exceeded. To do this, one simply reads from these probability functions the spectral amplitudes  $S_i$  for each frequency  $\omega_i$  which has probability 0.1 as in Figure 4.1.2 and plots the amplitudes  $S_i$  vs  $\omega_i$ . Figure 4.1.3 is an example of such a plot, using only three frequencies for illustration purposes. In an actual calculation, one would use many frequencies and the resulting curve would have a much smoother appearance.

#### 4.2 Formulation of the Risk Model

Let there be  $I$  source elements in the region of a zone. For the  $i$ -th source element, let  $n_{ij}$  be the estimated number of earthquakes of size  $M_j$  in the  $i$ -th element as described in Section 2. For the functional  $S(\omega)$  at frequency  $\omega$ , let  $q_{ij}$  be the probability that  $S(\omega)$  will be exceeded at the site in an event of size  $M_j$  in the  $i$ -th element, as described in Section 3.

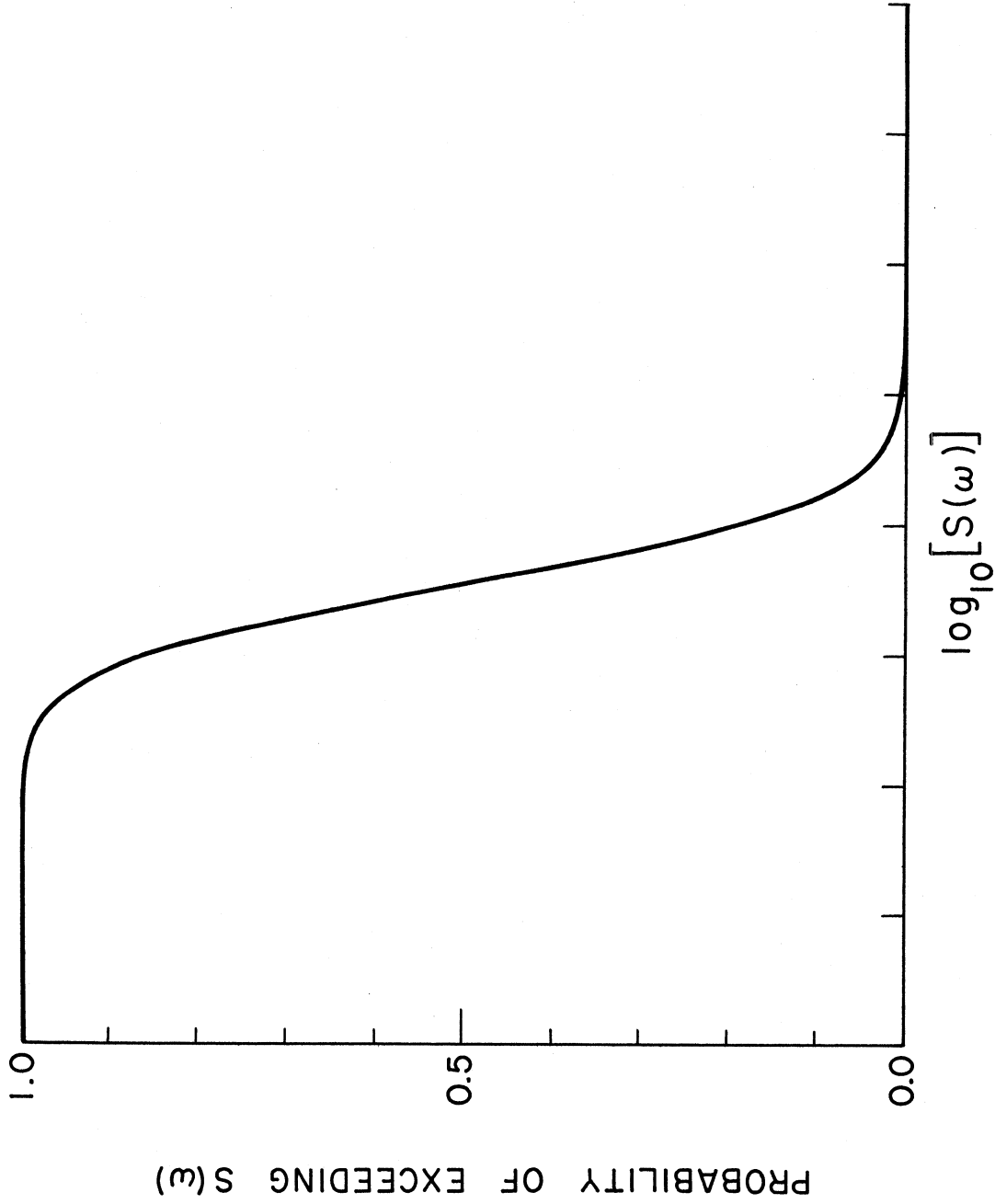


Figure 4.1.1 Example of the function  $p[S(\omega)]$ , the probability that  $S(\omega)$  will be exceeded at least once in  $Y$  years.

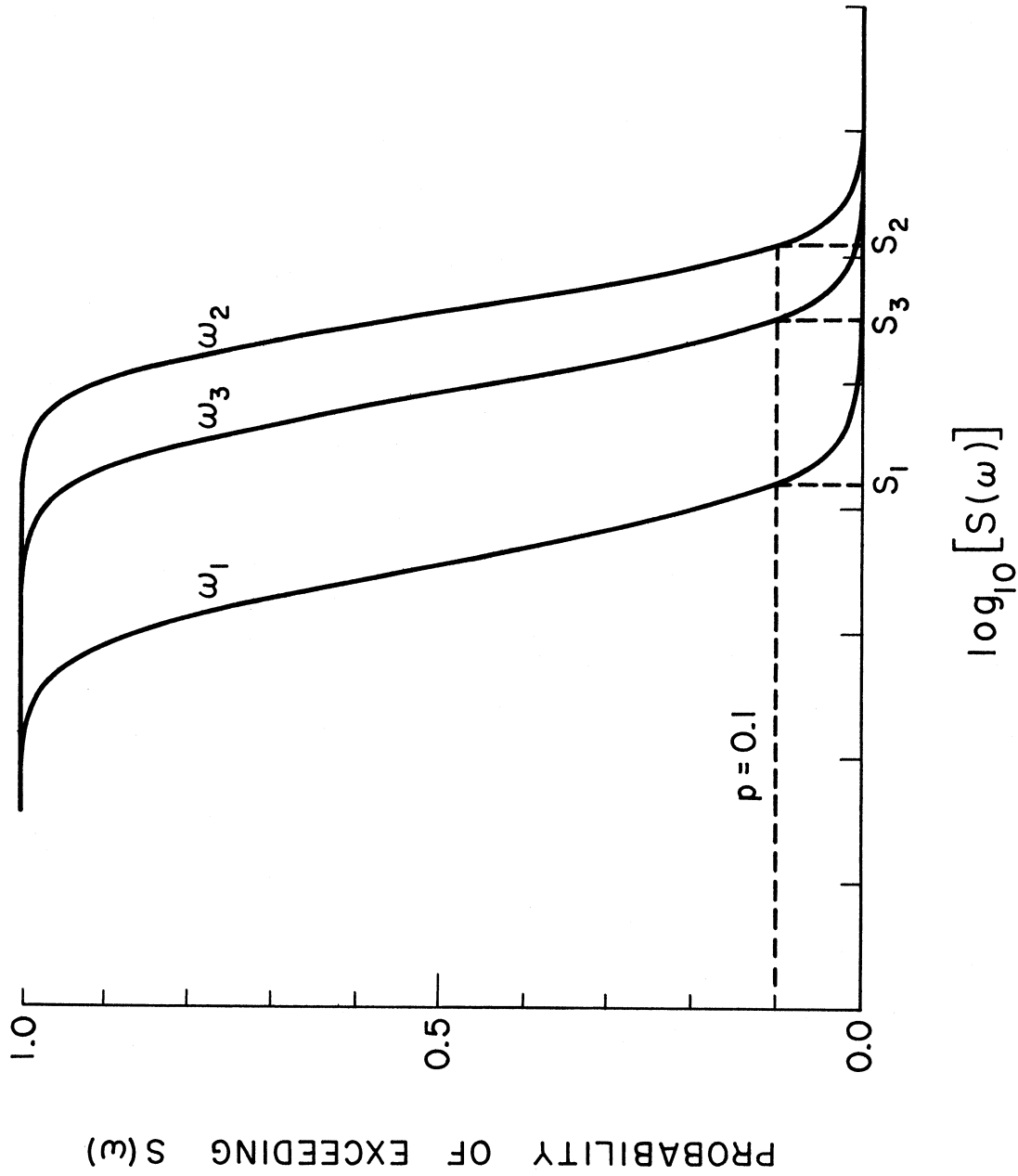


Figure 4.1.2 Example of the function  $p[S(\omega)]$  at three different frequencies:  $\omega_1$ ,  $\omega_2$  and  $\omega_3$ .

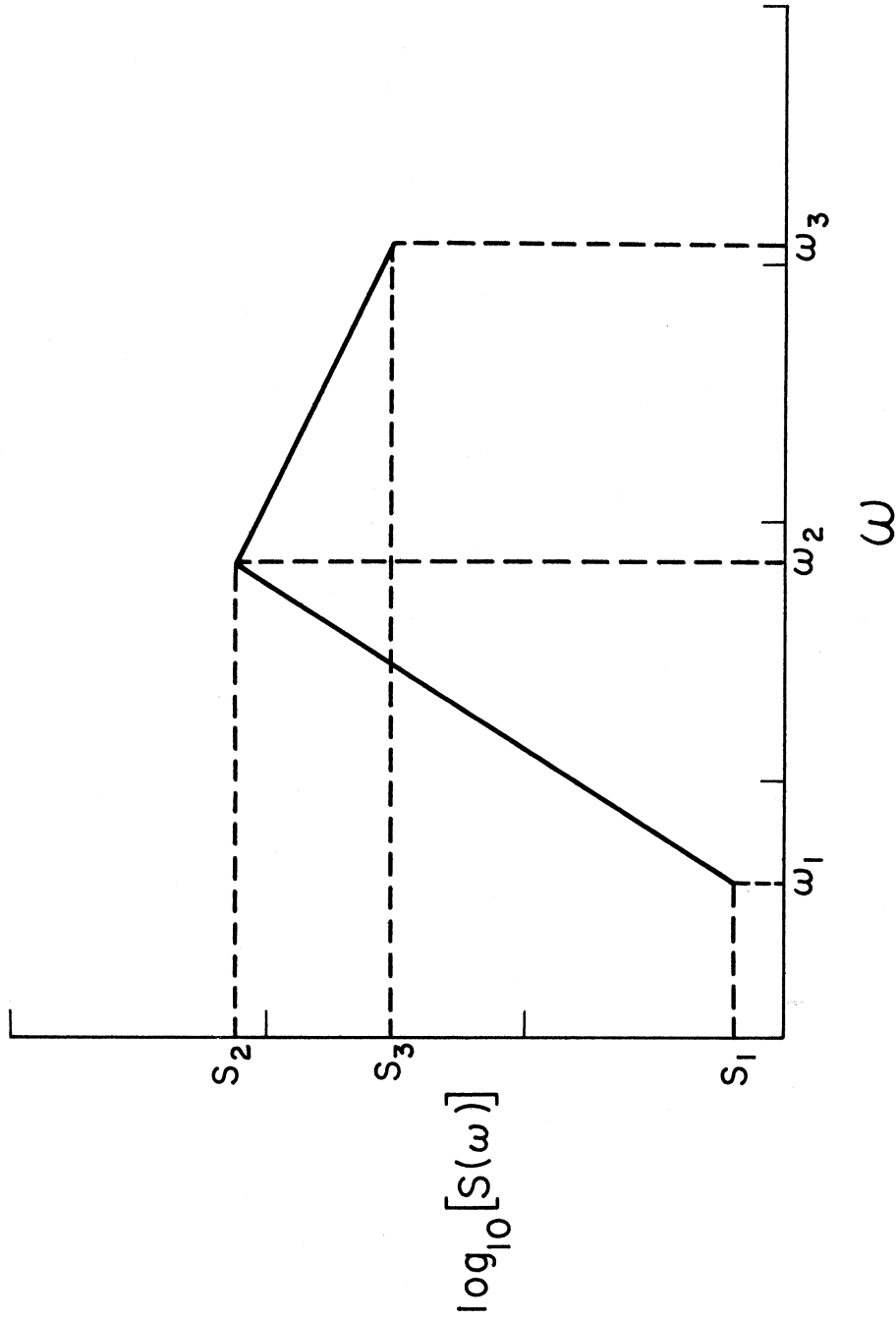


Figure 4.1.3 A uniform risk functional derived from the functions  $p[S(\omega)]$  shown in Figure 4.1.2. At each frequency, the probability is 0.1 that  $S(\omega)$  will be exceeded at least once in  $Y$  years. This figure uses only three frequencies for schematic purposes; in an actual calculation, one would use many frequencies and the resulting functional would have a smoother appearance.

Anderson and Trifunac (1977) derived  $N_E(S(\omega))$  as follows. Assume, following Cornell (1968) and others, that  $n_{ij}$  is the mean of a Poissonian distribution. Then the probability of exactly  $k$  events of size  $M_j$  in the  $i$ -th element is  $\exp(-n_{ij})n_{ij}^k/k!$ . For  $k$  such events in the  $i$ -th element, the expected number of times that  $S(\omega)$  will be exceeded at the site is  $kq_{ij}$ . Thus the expected number of times that  $S(\omega)$  will be exceeded at the site from at least one event of size  $M_j$  in the  $i$ -th element,  $E_{ij}$ , is given by

$$E_{ij} = \sum_{k=0}^{\infty} kq_{ij} e^{-n_{ij}} n_{ij}^k/k! = q_{ij}n_{ij} . \quad (4.2.1)$$

Then, the expected number of times  $S(\omega)$  will be exceeded at the site from all source elements,  $i = 1$  to  $I$ , and all earthquake sizes  $M_j$ ,  $j = 1$  to  $J$  is given by

$$N_E[S(\omega)] = \sum_{i=1}^I \sum_{j=1}^J q_{ij}n_{ij} . \quad (4.2.2)$$

The above derivation assumes no uncertainty in the estimation of the seismicity of the  $i$ -th source element. As pointed out in Section 2, uncertainties in the estimation should be included in the risk analysis. Two parameters of the  $i$ -th source element, namely  $n_{ij}$  and  $M_{\max}^i$ , the maximum allowed (upper bound) earthquake size for events in the  $i$ -th element, will be treated as random variables each described by an appropriate probability density function.

As before, the conditional probability of exactly  $k$  events of size  $M_j$  in the  $i$ -th element, given  $n_{ij}$ , is  $\exp(-n_{ij})n_{ij}^k/k!$ . Since  $n_{ij}$  is a random variable described by a probability density function  $p_n(n)$ , say, the true unconditional probability of exactly  $k$  such events is given by

$$\text{prob}(k \text{ events of size } M_j) = \int_0^{\infty} \frac{e^{-n_{ij}k}}{k!} p_n(n_{ij}) dn_{ij} \quad (4.2.3)$$

Again, the conditional probability that  $S(\omega)$  will be exceeded at the site given an event of size  $M_j$  in the  $i$ -th source element is  $q_{ij}$ , given that  $M_j \leq M_{\max}^i$ . Thus the unconditional probability that  $S(\omega)$  will thus be exceeded is  $\overline{q_{ij}} = q_{ij} \cdot \text{Prob}(M_j \leq M_{\max}^i)$ . For  $k$  such events, the expected number of times that  $S(\omega)$  will be exceeded at the site becomes  $k\overline{q_{ij}}$ . As before, the expected number of times that  $S(\omega)$  will be exceeded at the site from at least one event of size  $M_j$  in the  $i$ -th element,  $E_{ij}$ , is given by

$$\begin{aligned} E_{ij} &= \sum_{k=0}^{\infty} k\overline{q_{ij}} \int_0^{\infty} \frac{e^{-n_{ij}k}}{k!} p_n(n_{ij}) dn_{ij} \\ &= \overline{q_{ij}} \int_0^{\infty} \sum_{k=0}^{\infty} \frac{kn_{ij}^k}{k!} e^{-n_{ij}} p_n(n_{ij}) dn_{ij} \\ &= \overline{q_{ij}} \int_0^{\infty} n_{ij} p_n(n_{ij}) dn_{ij} \\ &= \overline{q_{ij}} E(n_{ij}) \end{aligned} \quad (4.2.4)$$

as in (4.2.1). (4.2.4) is more general than (4.2.1) in that it includes the uncertainties in the estimation of seismicity at each chosen discrete earthquake size and the uncertainty in the estimated maximum allowed earthquake size. When the uncertainty in the estimation of seismicity is not present,  $E(n_{ij})$  will be equal to  $n_{ij}$ . Similarly, when there is no uncertainty in the maximum allowed earthquake size,  $\overline{q_{ij}}$  reduces to  $q_{ij}$ . Thus when both uncertainties are absent, (4.2.4) reduces to (4.2.1).

As before, the expected number of times that  $S(\omega)$  will be exceeded at the site from all source elements and all allowed earthquake sizes is now given by

$$N_E[S(\omega)] = \sum_{i=1}^I \sum_{j=1}^J \overline{q_{ij}} E(n_{ij}) \quad , \quad (4.2.5)$$

where the summation  $i$  from 1 to  $I$  is over all source elements and the summation  $j$  from 1 to  $J$  is over all earthquake sizes.

Alternately, the same expressions for (4.2.4) and (4.2.5) can be derived by first assuming, as before, that the probability of exactly  $k$  events in the  $i$ -th element of size  $M_j$  is a Poissonian process. To include the uncertainties in the estimation of seismicity, the mean of the Poissonian distribution,  $n_{ij}$ , which is a random variable given by a probability density function  $p_n(n)$ , as described in the beginning of this section, can simply be taken as the expected value of  $n_{ij}$ ,  $E(n_{ij})$ . Then the probability of exactly  $k$  events of size  $M_j$  in the  $i$ -th element becomes  $\exp(-E(n_{ij}))E(n_{ij})^k/k!$ . Proceeding as before, for  $k$  such events in the  $i$ -th element, the expected number of times that  $S(\omega)$  will be exceeded at the site, including the uncertainty in the maximum allowed earthquake size is  $k\overline{q_{ij}}$ . Thus the expected number of times that  $S(\omega)$  will be exceeded at the site from at least one event of size  $M_j$  in the  $i$ -th element,  $E_{ij}$ , is now given by

$$E_{ij} = \sum_{k=0}^{\infty} k\overline{q_{ij}} e^{-E(n_{ij})} E(n_{ij})^k/k! = \overline{q_{ij}} E(n_{ij}) \quad , \quad (4.2.6)$$

which is identical to (4.2.4). The expected number of times that  $S(\omega)$  will be exceeded at the site from all source elements and all allowed



earthquake sizes,  $N_E[S(\omega)]$ , now follows from (4.2.6) the same way and is given in (4.2.5).

### 4.3 Characterizing Uncertainties of Seismicity

The previous section includes uncertainties in the estimation of seismicity and maximum allowed earthquake sizes in the calculation of the expected number of times that the spectral amplitude  $S(\omega)$  will be exceeded at the site. This section illustrates examples of how such uncertainties can be estimated and used in the description of seismicity. As stated in Section 4.2, it is assumed that  $n_{ij}$ , the estimated number of earthquakes of size  $M_j$  in the  $i$ -th element, and  $M_{\max}^i$ , the maximum allowed (upper bound) earthquake size for events in the  $i$ -th element, are both treated as random variables, each described by an appropriate probability density function.

For each earthquake size  $M_j$ , let  $n_{ij}$  be described by a probability density function  $p_n(n)$ . As shown in Section 2.3,  $n_{ij}$  is estimated from  $N(M_j)$  of the whole source zone of which the  $i$ -th element is a subelement.  $N(M_j)$  is the expected number of earthquakes of sizes in a specified interval around  $M_j$  in the source zone. It in turn is estimated from an empirical scaling formula of the form, for  $N_j = N(M_j)$ ,

$$\log N_j = a - bM_j, \quad (4.3.1)$$

where  $a$  and  $b$  are statistical parameters often estimated by regression. The uncertainties in the estimation of  $N(M_j)$  and hence  $n_{ij}$  are associated with those of  $a$  and  $b$ . For a given earthquake size  $M_j$ ,  $\log N_j$  and hence  $\log n_{ij}$  can first be described by a probability density function. The following are examples of such functions.

(a) Suppose that for a particular earthquake size  $M_j$  and at a particular zone,  $y = \log N_j$  is uniformly distributed with mean  $\mu$  in the range  $[\mu-\delta, \mu+\delta]$  (Figure 4.3.1a). The probability density function of  $y$ ,  $p_y(y)$ , is given by

$$p_y(y) = \begin{cases} \frac{1}{2\delta} & \mu-\delta \leq y \leq \mu+\delta \\ 0 & \text{otherwise} \end{cases} \quad (4.3.2)$$

The probability density function of  $N_j$ ,  $p_n(n)$ , is related to  $p_y(y)$  through the relation  $N_j = 10^y$ , and is given by

$$p_n(n) = \begin{cases} p_y(y)/\frac{dn}{dy} & n \geq 0 \\ 0 & \text{otherwise} \end{cases} \quad (4.3.3)$$

with  $dn/dy = d(10^y)/dy = c 10^y$ , where  $c = \ln 10$ .

The uncertainties in the estimation of  $N_j$  are then included in the analysis by calculating  $E(N_j)$  the expected value of  $N_j$ , which is to be used in (4.2.5). For this case,  $E(N_j)$  is given by

$$\begin{aligned} E(N_j) &= \int_0^{\infty} n p_n(n) dn = \int_0^{\infty} 10^y (p_y(y)/\frac{dn}{dy}) dn \\ &= \int_{-\infty}^{\infty} 10^y p_y(y) dy = \frac{1}{2\delta} \int_{\mu-\delta}^{\mu+\delta} 10^y dy \\ &= \frac{1}{2c\delta} (10^{\mu+\delta} - 10^{\mu-\delta}) \end{aligned} \quad (4.3.4)$$

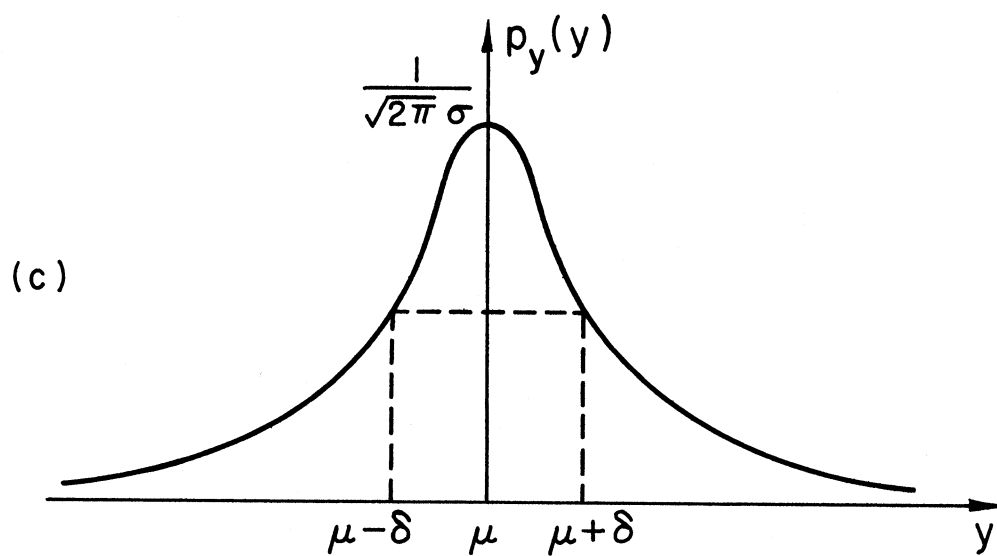
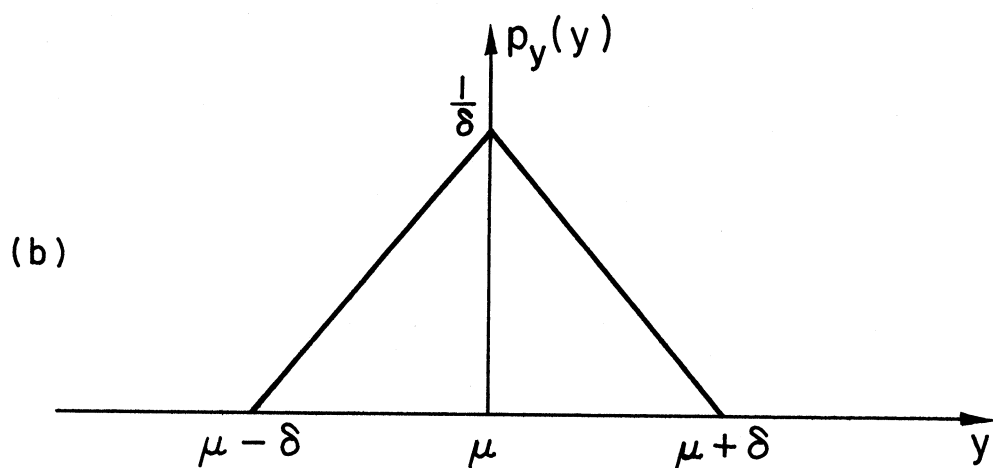
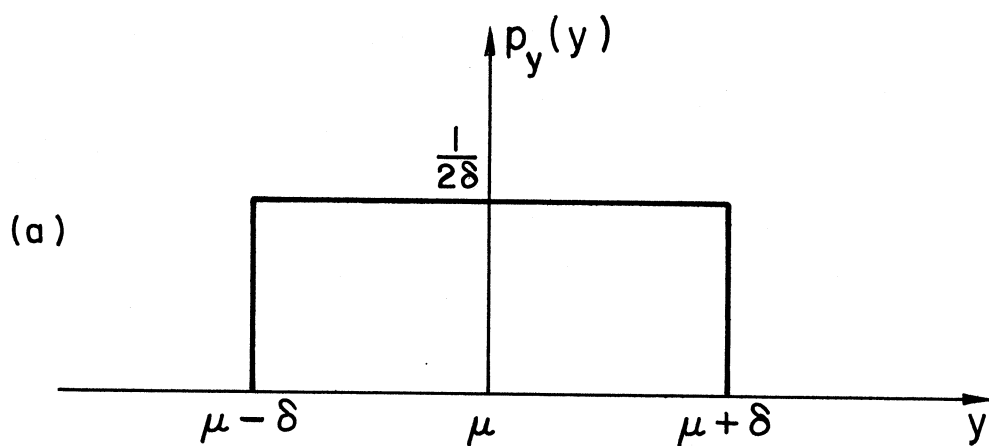


Figure 4.3.1

or

$$E(N_j) = 10^\mu \frac{\sinh c\delta}{c\delta}, \quad (4.3.5)$$

with  $c = \lambda n \log 10$ . Note that if  $\delta = 0$ , then  $\mu = \log N_j$ , and  $E(N_j) = N_j = 10^\mu$ .

(b) Suppose next that  $y = \log N_j$  is distributed according to a triangular distribution with mean  $\mu$  in the range  $[\mu - \delta, \mu + \delta]$  (Figure 4.3.1b), so that the probability density function  $p_y(y)$  is given by

$$p_y(y) = \begin{cases} (\delta + y - \mu) / \delta^2 & \mu - \delta \leq y \leq \mu \\ (\delta - (y - \mu)) / \delta^2 & \mu \leq y \leq \mu + \delta \\ 0 & \text{otherwise} \end{cases}. \quad (4.3.6)$$

The probability density function of  $N_j$ ,  $p_n(n)$ , is then given by

$$p_n(n) = \begin{cases} p_y(y) / \frac{dn}{dy} & n \geq 0 \\ 0 & \text{otherwise} \end{cases} \quad (4.3.7)$$

as in (4.3.3), with  $dn/dy = c10^y$ ,  $c = \lambda n \log 10$ .  $E(N_j)$  is now given by

$$\begin{aligned} E(N_j) &= \int_0^\infty n p_n(n) dn = \int_{-\infty}^\infty 10^y p_y(y) dy \\ &= \int_{\mu - \delta}^{\mu} \frac{e^{cy} (\delta + (y - \mu))}{\delta^2} dy + \int_{\mu}^{\mu + \delta} \frac{e^{cy} (\delta - (y - \mu))}{\delta^2} dy \\ &= \int_{\mu - \delta}^{\mu + \delta} \frac{e^{cy}}{\delta} dy + \int_{\mu - \delta}^{\mu} \frac{e^{cy} (y - \mu)}{\delta^2} dy - \int_{\mu}^{\mu + \delta} \frac{e^{cy} (y - \mu)}{\delta^2} dy \\ &= \frac{e^{cy}}{c\delta} \Big|_{\mu - \delta}^{\mu + \delta} + \int_{-\delta}^0 \frac{e^{c\mu} e^{cx} x}{\delta^2} dx - \int_0^{\delta} \frac{e^{c\mu} e^{cx} x}{\delta^2} dx, \quad (4.3.8) \end{aligned}$$

or substituting  $x = y - \mu$ ,

$$E(N_j) = \frac{e^{c\mu} 2 \sinh c\delta}{c\delta} - \frac{2e^{c\mu}}{\delta^2} \int_0^\delta x \cosh cx dx \quad .$$

Integrating once again by parts,

$$E(N_j) = \frac{e^{c\mu} 2 \sinh c\delta}{c\delta} - \frac{2e^{c\mu}}{c\delta^2} (\delta \sinh c\delta - (\frac{\cosh c\delta - 1}{c})) \quad . \quad (4.3.9)$$

The first two terms are identical and cancel. (4.3.9) becomes

$$\begin{aligned} E(N_j) &= \frac{2e^{c\mu} (\cosh c\delta - 1)}{c^2 \delta^2} \\ &= 10^\mu 2 \left( \frac{\cosh c\delta - 1}{c^2 \delta^2} \right) \quad . \end{aligned} \quad (4.3.10)$$

Again  $E(N_j) = 10^\mu$  if  $\delta = 0$ .

(c) As a third example, suppose  $y = \log N_j$  is normally distributed with mean  $\mu$  and standard deviation  $\sigma$ , so the distribution function of  $y$ ,  $p_y(y)$ , is (Fig. 4.3.1c)

$$p_y(y) = \frac{1}{\sqrt{2\pi}\sigma} \exp[-(\frac{y-\mu}{\sigma})^2 / 2] \quad . \quad (4.3.11)$$

$E(N_j)$  is now given by

$$\begin{aligned} E(N_j) &= \int_0^\infty n p_n(n) dn = \int_{-\infty}^\infty 10^y p_y(y) dy \\ &= \int_{-\infty}^\infty \frac{1}{\sqrt{2\pi}\sigma} \exp[cy - \frac{1}{2} (\frac{y^2 - 2\mu y + \mu^2}{\sigma^2})] dy \end{aligned}$$

$$\begin{aligned}
&= \int_{-\infty}^{\infty} \frac{1}{\sqrt{2\pi}\sigma} \exp\left[-\frac{1}{2} \left(\frac{y^2 - 2(\mu + c\sigma^2) + (\mu + c\sigma^2)^2}{\sigma^2}\right)\right] \exp\left(\mu + \frac{c\sigma^2}{2}\right) dy \\
&= \exp\left(\mu + \frac{c\sigma^2}{2}\right) \int_{-\infty}^{\infty} \frac{1}{\sqrt{2\pi}\sigma} \exp\left[-\frac{1}{2} \left(\frac{y - (\mu + c\sigma^2)}{\sigma}\right)^2\right] dy
\end{aligned}$$

or 
$$E(N_j) = 10^{\mu + c\sigma^2/2} \quad , \quad (4.3.12)$$

with the last integral in (4.3.12) being equal to 1. Again  $E(N_j) = 10^\mu$  when  $\sigma = 0$ .

In each of the above examples the uncertainties are characterized by two parameters, like the mean  $\mu$  and the range  $[\mu - \delta, \mu + \delta]$  in the first two examples of uniform and triangular distributions, or the mean  $\mu$  and the standard deviation  $\sigma$  in the last example with normal distribution of  $y = \log N_j$  at a particular earthquake magnitude or intensity. In each example, the mean of the distribution can be estimated, for example, by the regression equation as in (4.3.1), where for  $N_j = N(M_j)$  instead of  $\log N_j$ , the mean  $\mu = \mu(M_j)$  is estimated from the same empirical scaling formula

$$\mu(M_j) = a - bM_j \quad , \quad (4.3.14)$$

with  $a$  and  $b$  the same statistical parameters as in (4.3.1). The uncertainties in the estimation of  $a$  and  $b$  can now be characterized by additional parameters  $\delta a$  and  $\delta b$ . They in turn are used to characterize the uncertainties of seismicity,  $\delta = [\mu(M_j)]$ , where

$$\delta[\mu(M_j)] = \delta[a - bM_j] \quad . \quad (4.3.15)$$

$\mu(M_j)$  and  $\delta[\mu(M_j)]$  can now be used to estimate  $E(N(M_j))$ , the expected number of earthquakes of size  $M_j$ . Depending on the geometry of the zone,  $E(n_{ij})$  of the  $i$ -th element of the zone can now be estimated from  $E(N(M_j))$  as described in Section 2.3.

Figure 4.3.2 is an example of a plot of the seismicity at the Sierra Madre-Cucamonga fault in Los Angeles, California. It plots the number of earthquakes (on logarithmic scale) versus earthquake size in magnitude. The middle solid line represents the mean of the estimated number of earthquakes at each magnitude up to the maximum magnitude of 7.5. At each magnitude level, the estimated number of earthquakes is assumed to be triangularly distributed about the mean. The two outer solid lines represent the range of such distribution at each magnitude. The maximum magnitude  $M_{\max}$  is also assumed to be a random variable having triangular distribution centered at 7.5 and in the range from 6.5 to 8.5. The dashed line in Figure 4.3.1 represents  $E(N(M_j)) \cdot \text{prob}(M_j < M_{\max})$ , a term used to include the uncertainties in the estimation of seismicity in the following seismic risk calculations.

#### 4.4 The Probability of Exceedance $P[S(\omega)]$

In the previous sections we have discussed how the uncertainties in the estimation of seismicity and maximum allowed earthquake sizes could be included in the calculation of the expected number of times that the spectral amplitude  $S(\omega)$  will be exceeded at the site. The function,  $P[S(\omega)]$ , the probability that  $S(\omega)$  will be exceeded at least once in the given period, will next be derived. The following derivation is extended from that presented in Anderson and Trifunac (1977).

SIERRA MADRE - CUCAMONGA FAULT ZONE

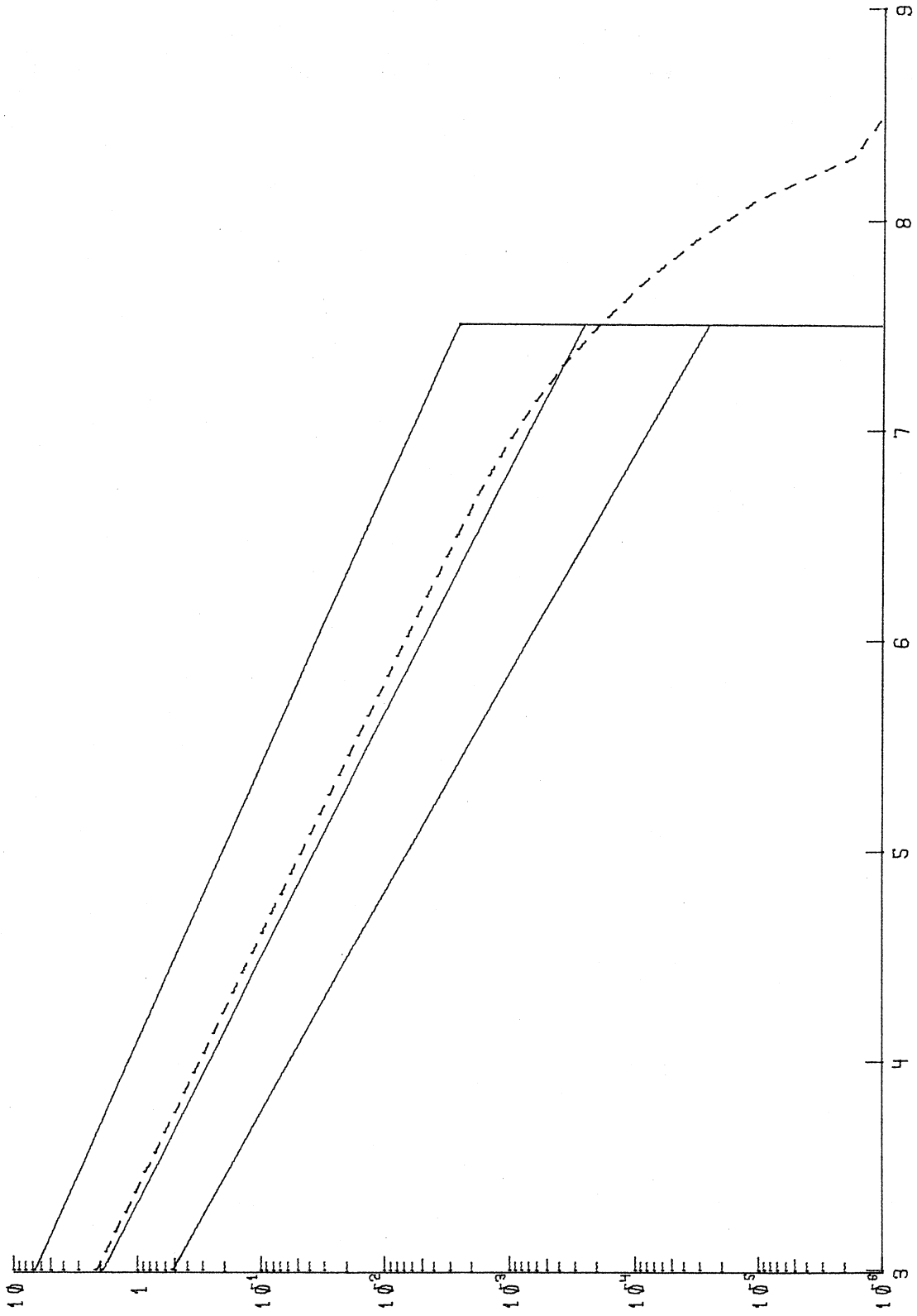


Figure 4.3.2



Given the functional  $S(\omega)$  at frequency  $\omega$ , let:

$p_{ij}$  = probability that at least one event of size  $M_j$  in the  $i$ -th element will cause  $S(\omega)$  to be exceeded.

To find  $p_{ij}$ , the Poisson assumption is used, and again treating  $n_{ij}$  as a random variable described by a probability density function  $p_n(n)$ .

With  $\bar{q}_{ij}$  defined as before,

$1 - \bar{q}_{ij}$  = probability of not exceeding  $S(\omega)$  for one event,

$(1 - \bar{q}_{ij})^k$  = probability of not exceeding for  $k$  events,

$1 - (1 - \bar{q}_{ij})^k$  = probability of exceeding at least once for  $k$  events.

Combining this with (4.2.3), the probability of exceeding at least once for all  $k$  events of size  $M_j$ , gives

$$\begin{aligned}
 p_{ij} &= \sum_{k=0}^{\infty} (1 - (1 - \bar{q}_{ij})^k) \int_0^{\infty} \frac{e^{-n_{ij}} n_{ij}^k}{k!} p_n(n_{ij}) dn_{ij} \\
 &= 1 - \int_0^{\infty} e^{-\bar{q}_{ij} n_{ij}} p_n(n_{ij}) dn_{ij} \\
 &= 1 - E(e^{-\bar{q}_{ij} n_{ij}}), \quad (4.4.1)
 \end{aligned}$$

where  $E(e^{-\bar{q}_{ij} n_{ij}})$  is the expected value of  $e^{-\bar{q}_{ij} n_{ij}}$  under the probability distribution function  $p_n(n_{ij})$ . (4.4.1) is of the same form as given in Anderson and Trifunac (1977), where no uncertainties in seismicity and maximum earthquake size are assumed, so that  $E(e^{-\bar{q}_{ij} n_{ij}}) = e^{-\bar{q}_{ij} n_{ij}}$ . To evaluate the probability of exceedance,  $P[S(\omega)]$ , we proceed as follows:

$1 - p_{ij}$  = probability that no earthquake of size  $M_j$  at the  $i$ -th element will cause  $S(\omega)$  to be exceeded,

$\prod_{j=1}^J (1-p_{ij})$  = probability that no earthquake of any size at the  $i$ -th element will cause  $S(\omega)$  to be exceeded,

$1-P[S(\omega)] = \prod_{i=1}^I \prod_{j=1}^J (1-p_{ij})$  = probability that no earthquake anywhere in the source region will cause  $S(\omega)$  to be exceeded.

Thus

$$\begin{aligned} P[S(\omega)] &= 1 - \prod_{i=1}^I \prod_{j=1}^J (1-p_{ij}) , \\ &= 1 - \prod_{i=1}^I \prod_{j=1}^J E(e^{-\bar{q}_{ij}n_{ij}}) , \end{aligned} \quad (4.4.2)$$

using (4.4.1). Assuming further that the earthquake events of all sizes in each element are independent, (4.4.2) simplifies to

$$\begin{aligned} P[S(\omega)] &= 1 - E\left(\prod_{i=1}^I \prod_{j=1}^J e^{-\bar{q}_{ij}n_{ij}}\right) \\ &= 1 - E\left(e^{-\sum_{i=1}^I \sum_{j=1}^J \bar{q}_{ij}n_{ij}}\right) . \end{aligned} \quad (4.4.3)$$

(4.4.3) is in a form similar to (1.2) in Anderson and Trifunac (1977).

When no uncertainty in seismicity is assumed,  $E(e^{-\bar{q}_{ij}n_{ij}}) = e^{-q_{ij}n_{ij}}$  and  $\sum_{i=1}^I \sum_{j=1}^J \bar{q}_{ij}n_{ij} = N_E[S(\omega)]$ , so that (4.4.3) reduces to

$$P[S(\omega)] = 1 - e^{-N_E[S(\omega)]} . \quad (4.4.4)$$

There is yet another way to derive  $P[S(\omega)]$  under the assumption that the probability of having exactly  $k$  events in the  $i$ -th element of size  $M_j$

is of Poisson type, and that both the uncertainties in the seismicity  $n_{ij}$  and maximum allowed earthquake size,  $M_{\max}^i$ , in the  $i$ -th element are also included. This is done by taking the mean of the Poisson distribution to be  $E(n_{ij})$ , the expected value of  $n_{ij}$ . The probability of exactly  $k$  events of size  $M_j$  occurring in the  $i$ -th element then becomes  $\exp(-E(n_{ij}))E(n_{ij})^k/k!$  and  $p_{ij}$  takes the form:

$$p_{ij} = \sum_{k=0}^{\infty} (1 - (1 - \bar{q}_{ij})^k) \frac{\exp(-E(n_{ij}))E(n_{ij})^k}{k!}$$

$$= 1 - \exp(-\bar{q}_{ij}E(n_{ij})) \quad , \quad (4.4.5)$$

and (4.4.2) for  $P[S(\omega)]$ , the probability of exceedance, now takes the form

$$P[S(\omega)] = 1 - \prod_{i=1}^I \prod_{j=1}^J (1 - p_{ij}) \quad ,$$

$$= 1 - \exp\left(-\sum_{i=1}^I \sum_{j=1}^J \bar{q}_{ij} E(n_{ij})\right) \quad ,$$

$$= 1 - \exp(-N_E[S(\omega)]) \quad , \quad (4.4.6)$$

using (4.2.5) as the expression for  $N_E[S(\omega)]$ . As before, (4.4.6) shows the close relationship between the expected number of exceedances  $N_E[S(\omega)]$ , and the probability of exceedance,  $P[S(\omega)]$ , when a Poisson assumption is used to describe the seismicity rate, and here, even when the uncertainties in seismicity are included. (4.4.6) is a more convenient expression for calculating  $P[S(\omega)]$  than (4.4.2) since it allows  $P[S(\omega)]$  to be estimated from  $N_E[S(\omega)]$  directly.

#### 4.5 Literal Seismicity

The previous sections discussed the calculations of the expected number of times the given spectral amplitude  $S(\omega)$  will be exceeded at the site and the probability that  $S(\omega)$  will be exceeded at least once in a given period. It showed how the uncertainties in the estimation of seismicity and maximum allowed earthquake sizes can be included in the calculations. This section considers a different hypothesis when one assumes that an earthquake and its aftershock sequence of known magnitudes will occur someplace within a specified fault or a diffused region. In this case, one again needs to know the risk at various sites. The two functions  $N_E^*[S(\omega)]$  and  $P^*[S(\omega)]$  will now be derived with the assumption that one knows how many earthquakes will occur within the source zone. This is referred to as a "literal" model because the seismicity is to be interpreted literally. The following derivations are those given in Anderson and Trifuanc (1977) and are included here for completeness only.

Given a source region, suppose it is known that  $N(M_j)$  events of size  $M_j$  for  $j = 1$  to  $J$  will occur somewhere in the region, but where exactly in the region is not known. As in Section 2.3, the source region is now divided into  $I$  subelements. Let  $\gamma_{ij}$  be the probability that an event of size  $M_j$  occurs in the  $i$ -th element. With  $n_{ij}$  the expected number of events of size  $M_j$  in the  $i$ -th element as defined in Section 2.3, it is clear that

$$n_{ij} = \gamma_{ij} N(M_j) \quad ,$$

and

$$\sum_{i=1}^I \gamma_{ij} = 1 \quad , \quad (4.5.1)$$

$$\sum_{i=1}^I n_{ij} = N(M_j) = N_j \quad .$$

There are many different ways in which the  $N(M_j)$  events can be distributed among the  $I$  elements. To determine  $N_E^*[S(\omega)]$ , we proceed as in Section 4.2 to determine  $E_{ij}^*$ , the expected number of times that  $S(\omega)$  will be exceeded at the site from at least one event of size  $M_j$  in the  $i$ -th element.  $E_{ij}^*$  is given by

$$E_{ij}^* = \sum_{n_{ij}=0}^{N_j} q_{ij} n_{ij} \cdot \text{prob} \left\{ \begin{array}{l} n_{ij} \text{ events of size } M_j \\ \text{occur in element } i \end{array} \right\}. \quad (4.3.2)$$

Considering the events as Bernoulli Trials, this is given by

$$\begin{aligned} E_{ij}^* &= \sum_{n_{ij}=0}^{N_j} q_{ij} n_{ij} \frac{N_j!}{n_{ij}!(N_j-n_{ij})!} \gamma_{ij}^{n_{ij}} (1-\gamma_{ij})^{N_j-n_{ij}}, \\ &= q_{ij} N_j \gamma_{ij} = q_{ij} n_{ij}. \end{aligned} \quad (4.5.3)$$

Thus

$$N_E^*[S(\omega)] = \sum_{j=1}^J \sum_{i=1}^I E_{ij}^* = \sum_{j=1}^J \sum_{i=1}^I q_{ij} n_{ij}. \quad (4.5.4)$$

It is clear that  $N_E^*[S(\omega)]$  is of the same form as  $N_E[S(\omega)]$  and that if no uncertainties of estimation of seismicity are included in  $N_E[S(\omega)]$ ,  $N_E^*[S(\omega)]$  is identical to  $N_E[S(\omega)]$ .

To find  $p^*[S(\omega)]$ , consider:

$(1-q_{ij})$  = probability that  $S(\omega)$  is not exceeded from one event of size  $M_j$  in the  $i$ -th element,

$(1-q_{ij})^{n_{ij}}$  = probability that  $S(\omega)$  is not exceeded from  $n_{ij}$  events of size  $M_j$  in the  $i$ -th element,

$\prod_{i=1}^I (i-q_{ij})^{n_{ij}}$  = probability that  $S(\omega)$  is not exceeded for a particular combination of events  $\{n_{ij} | i \in I\}$  of size  $M_j$ .

The probability of any one particular combination of events is given, by the multinomial theorem, as

$$\frac{N_j!}{n_{1j}! n_{2j}! \dots n_{Ij}!} \gamma_{1j}^{n_{1j}} \gamma_{2j}^{n_{2j}} \dots \gamma_{Ij}^{n_{Ij}}, \quad (4.5.5)$$

and the sum of the probabilities of all combinations is, by the multinomial theorem, unity,

$$\begin{aligned} & \sum \dots \sum \frac{N_j!}{n_{1j}! n_{2j}! \dots n_{Ij}!} \gamma_{1j}^{n_{1j}} \gamma_{2j}^{n_{2j}} \dots \gamma_{Ij}^{n_{Ij}} \\ & = (\gamma_{1j} + \gamma_{2j} + \dots + \gamma_{Ij})^{N_j} = 1, \end{aligned} \quad (4.5.6)$$

where the summation is over all combinations of  $\{n_{ij}, i=1 \text{ to } I\}$  such that  $\sum_{i=1}^I n_{ij} = N_j$ . Now the different combinations are mutually exclusive and exactly only one of them will occur, so the probability that  $S(\omega)$  is not exceeded by any one combination is

$$\begin{aligned} & \sum \dots \sum \left\{ \begin{array}{l} \text{probability that } S(\omega) \text{ is not} \\ \text{exceeded for a particular} \\ \text{combination} \end{array} \right\} \left\{ \begin{array}{l} \text{probability of that} \\ \text{particular combination} \end{array} \right\} \\ & = \sum \dots \sum \left\{ \prod_{i=1}^I (1-q_{ij})^{n_{ij}} \right\} \left\{ \frac{N_j!}{n_{1j}! n_{2j}! \dots n_{Ij}!} \gamma_{1j}^{n_{1j}} \gamma_{2j}^{n_{2j}} \dots \gamma_{Ij}^{n_{Ij}} \right\} \\ & = \sum \dots \sum \frac{N_j!}{n_{1j}! n_{2j}! \dots n_{Ij}!} [(1-q_{1j})\gamma_{1j}]^{n_{1j}} [(1-q_{2j})\gamma_{2j}]^{n_{2j}} \dots [(1-q_{Ij})\gamma_{Ij}]^{n_{Ij}} \end{aligned}$$

$$\begin{aligned}
&= \left\{ \sum_{i=1}^I [1-q_{ij}] \gamma_{ij} \right\}^{N_j} = \left\{ \sum_{i=1}^I \gamma_{ij} - \sum_{i=1}^I \gamma_{ij} q_{ij} \right\}^{N_j} \\
&= \left( 1 - \sum_{i=1}^I \gamma_{ij} q_{ij} \right)^{N_j}, \tag{4.5.7}
\end{aligned}$$

where the summation in (4.5.7) is again over all combinations of  $\{n_{ij} | i=1$  to  $I\}$  such that  $\sum_{i=1}^I n_{ij} = N_j$ . Since the different earthquake sizes  $M_j$ ,  $j=1$  to  $J$  are assumed to be independent,

$$\begin{aligned}
&\text{prob}\{S(\omega) \text{ is not exceeded by events of any size}\} = \\
&= \prod_{j=1}^J \text{prob}\{S(\omega) \text{ is not exceeded by events of size } M_j\} \\
&= 1 - p^*[S(\omega)], \tag{4.5.8}
\end{aligned}$$

so

$$p^*[S(\omega)] = 1 - \prod_{j=1}^J \left( 1 - \sum_{i=1}^I \gamma_{ij} q_{ij} \right)^{N_j},$$

or

$$p^*[S(\omega)] = 1 - \exp \left\{ \sum_{j=1}^J N(M_j) \ln \left( 1 - \sum_{i=1}^I \gamma_{ij} q_{ij} \right) \right\}. \tag{4.5.9}$$

Anderson and Trifuanc (1977) also derived an alternate set of expressions for  $N_E^+[S(\omega)]$  and  $p^+[S(\omega)]$ , denoted by  $N_E^+[S(\omega)]$  and  $P^+[S(\omega)]$  under the same assumption that the number of future earthquakes  $N(M_j)$  is to be taken literally. This is done by considering a very long time interval, say  $K$  times the base unit of  $Y$  years, or a duration of  $KY$  years in which  $KN(M_j)$  events of size  $M_j$  will occur in the source regions. Further, in

the  $i$ -th element, it is assumed that  $\gamma_{ij} \text{KN}(M_j) = \text{Kn}_{ij}$  events will occur, where  $\text{Kn}_{ij}$  is now an integer. For a sufficiently large number of events, this assumption will not introduce any significant error and is justifiable. Let

$N_E^\# [S(\omega)]$  = expected number of times that  $S(\omega)$  will be exceeded during  $KY$  years,

$P^\# [S(\omega)]$  = probability that  $S(\omega)$  will be exceeded at the site at least once in  $KY$  years.

These functions will first be derived from which  $N_E^+ [S(\omega)]$  and  $P^+ [S(\omega)]$  for  $Y$  years can be derived. Following the same logic, as in the derivation of  $N_E [S(\omega)]$  and  $N_E^* [S(\omega)]$ ,

$$N_E^\# [S(\omega)] = M \sum_{i=1}^I \sum_{j=1}^J n_{ij} q_{ij} \quad (4.5.10)$$

To derive  $P^\# [S(\omega)]$ , consider

$(1-q_{ij})$  = probability that  $S(\omega)$  is not exceeded from 1 event of size  $M_j$  in the  $i$ -th element,

since  $\text{Kn}_{ij}$  is the number of events of size  $M_j$  that will occur in the  $i$ -th element in the duration of  $KY$  years,

$(1-q_{ij})^{\text{Kn}_{ij}}$  = probability that  $S(\omega)$  is not exceeded from  $\text{Kn}_{ij}$  events of size  $M_j$  in the  $i$ -th element in  $KY$  years,

$\prod_{j=1}^J (1-q_{ij})^{\text{Kn}_{ij}}$  = probability that no earthquake of any size at the  $i$ -th element in  $KY$  years will cause  $S(\omega)$  to be exceeded,



$1 - P^{\#}[S(\omega)] = \prod_{i=1}^I \prod_{j=1}^J (1 - q_{ij})^{Kn_{ij}}$  = probability that no earthquake anywhere in the source region will cause  $S(\omega)$  to be exceeded in  $KY$  years.

Thus

$$\begin{aligned}
 P^{\#}[S(\omega)] &= 1 - \prod_{i=1}^I \prod_{j=1}^J (1 - q_{ij})^{Kn_{ij}} \\
 &= 1 - \exp\left\{ \sum_{i=1}^I \sum_{j=1}^J Kn_{ij} \ln(1 - q_{ij}) \right\} . \quad (4.5.11)
 \end{aligned}$$

Assuming that the  $K$  time intervals of  $Y$  years are independent, (4.5.10) and (4.5.11) give

$$N_E^+[S(\omega)] = \frac{1}{K} N_E^{\#}[S(\omega)] = \sum_{i=1}^I \sum_{j=1}^J n_{ij} q_{ij} = N_E^*[S(\omega)] , \quad (4.5.12)$$

and

$$1 - P^+[S(\omega)] = \{1 - P^{\#}[S(\omega)]\}^{1/K} ,$$

so that

$$P^+[S(\omega)] = 1 - \exp\left\{ \sum_{i=1}^I \sum_{j=1}^J n_{ij} \ln(1 - q_{ij}) \right\} . \quad (4.5.13)$$

It can be shown that (Anderson and Trifuanc (1977))

$$P^+[S(\omega)] \geq P^*[S(\omega)] \geq P[S(\omega)] . \quad (4.5.14)$$

Equality occurs between  $P^+$  and  $P^*$  only when there is just one source element, or when  $q_{ij}$  is identical for all source elements. Equality between  $P^*$  and  $P$  occurs only in the case where  $q_{ij} = 0$  for all source elements.

#### 4.6 Summary

The steps in the derivation of a uniform frequency dependent risk functional can be summarized as follows:

- (1) Specify the geometry of earthquake zones, by point, line, areal, dipping plane and volume sources. For each of these source zones, the estimated number of events of each earthquake size,  $N(M_j)$ , is defined. The uncertainties in the estimation of seismicity and maximum allowed earthquake size are also defined. This is done by studying previous seismicity, by insights obtained from geological studies and plate tectonics, and by statistical inference and scientific judgment.
- (2) Divide each source zone into small source elements, and assuming the epicenter of each event of size  $M_j$  is equally likely to occur any place in the source zone, distribute the seismicity to each element accordingly.
- (3) Specify a frequency-dependent description of the attenuation of strong-motion amplitudes in the region, plus a description of the distribution of the observed amplitudes  $S(\omega)$  about the mean estimated  $\hat{S}(\omega)$ . From this, define the function  $q_{ij}[S(\omega)]$  which gives the probability that  $S(\omega)$  will be exceeded at the site for an event of size  $M_j$  in the  $i$ -th element of the source zone.
- (4) Using (4.2.5), calculate  $N_E[S(\omega)]$ , the expected number of times that  $S(\omega)$  will be exceeded at the site from all source elements in all source zones and all allowed earthquake sizes. Then calculate  $P[S(\omega)]$ ,

the probability that  $S(\omega)$  will be exceeded at least once at the site in the given period, using (4.4.6), (4.5.9) or (4.5.13).

- (5) Using the method described in Section 4.1, derive the frequency dependent uniform risk functional from the functions  $P[S(\omega)]$ .

This completes the theoretical description of our Model of Seismic Risk.

## 5. THE COMPUTER PROGRAM

### 5.1 Introduction

A Fortran computer program, NEQRISK, has been written which evaluates the uniform risk spectra using the formulae developed in the previous sections. It has been written as a continuation of our effort to accurately describe seismic hazard. The original version of the program, EQRISK, was first written by Anderson (1978) using the theory and formulae developed by Anderson and Trifunac (1977).

EQRISK was first developed on a DEC computer with a TOPS10 operating system capable of running programs with large memory. Subsequently, it was modified to run on mini-computer Data General Eclipse S-130 with a program size of no more than 128 K-bytes. NEQRISK represents the most recent generation of this computer program currently also running on Data General Eclipse S-130 with an AOS operating system. It is able to use either the original scaling relations of FS, SV and PSV developed before 1980 and used by Anderson (1978), or the new scaling relations of FS and PSV developed recently (Trifunac and Lee, 1985b,c). NEQRISK is also able to include the uncertainties in the estimation of the seismicity of the various types of faults.

The program NEQRISK includes options to read in point, line, areal, dipping plane and volume sources. The original version of EQRISK in 1978 also had the option of reading in dipping plane sources, but there the program simply replaced each surface element by a corresponding dipping element and the epicentral distance by the corresponding hypocentral distance. It was mentioned then that this was done because of the lack of a more realistic method. The method outlined in Section 2.3 for dipping plane source is now used in NEQRISK. For a dipping plane source, option allows either the assumption that the epicentral distance should be used or the assumption that the closest point to the fault should be used to calculate the risk. Similarly, for the line source, the program automatically uses the closest point. For point, areal (diffused zones) and volume sources, however, the only option allowed is the use of epicentral distance.

Besides including the uncertainties in the estimation of seismicity to calculate the seismic risk spectra, one other major difference between "NEQRISK" and "EQRISK" is the use of efficient and accurate algorithms for interpolation and differentiation. Interpolation is used in constructing the seismic risk spectra of spectral amplitudes  $S(\omega)$  versus frequency  $\omega$  of a fixed probability level. It involves reading the probability of exceedance curves of  $P[S(\omega)]$  versus  $\log_{10}[S(\omega)]$  for various frequencies  $\omega$  and interpolating the spectral amplitudes at a fixed probability level. The original program "EQRISK" simply uses a straight line interpolation scheme between points. The current program "NEQRISK" uses an interpolation scheme involving the use of low pass digital filters (Lee and Trifunac, 1984), as was done in data processing of strong-motion earthquake accelerograms. Such interpolation filters can be described in a variety of ways,

as discussed in Chapter II of Lee and Trifunac (1984) for example, using window designs, equiripple designs, smooth designs, etc. The Finite Impulse Response (FIR) nonrecursive interpolation filter turns out to be the most efficient. The filter used here is one in this form, designed by Oetken et al (1975), in which the minimization of mean square criteria is used.

Differentiation is used to calculate the probability density function from the Poisson probability of exceedance. The original program "EQRISK" uses the forward central difference method to do the differentiation. A higher order differentiation formula as derived from the smooth low pass filter (Lee and Trifunac, 1984) is currently used in the updated program "NEQRISK." This gives more accurate end results.

## 5.2 Input Data

The input data can be divided into three main parts:

- (a) Input Part 1: Site Information and Model Parameters,
- (b) Input Part 2: Spectrum Scaling Data, and
- (c) Input Part 3: Seismicity Information.

The following computer listing is a description of these three parts of the input.



```

C           2           0.6       2.7       APPROX. PRESS
C           3           0.67      2.23      THATCHER & HANKS 1.7 BARS
C           4           0.67      1.41      THATCHER & HANKS 0.1 BARS
C           5           0.67      3.41      THATCHER & HANKS 100 BARS
C           6           0.53      1.47      WYSS & BRUNE
C           7           1.02      5.77      TOCHER
C           8           1.32      7.99      OKAMOTO
C           9           0.395     1.454     HOUSNER M. LT. 6. 4
C           0           0.900     4.673     HOUSNER M. GE. 6. 4
C          10           1.596     7.56      DER-KIUREGHIAN
C                                     USES EXP( ), NOT 10**( )
C
C IPPC = 0 NORMAL VALUE
C         1 PRINTS FINAL DISTANCE AND SEISMICITY ARRAY. THIS
C           CAN BE HELPFUL IN LEARNING THE SOURCE DISTRIBUTION,
C           AND THUS IN UNDERSTANDING THE RESULTS.
C
C LSSUP = 0 NORMAL VALUE
C         1 SUPPRESSES LISTING OF SEISMICITY MODEL.
C
C IDL1 = STTARTING PERIOD NUMBER FOR DO LOOPS OVER PERIODS
C         DEFAULT IDL1=1.
C
C IDL2 = ENDING PERIOD NUMBER FOR DO LOOPS OVER PERIODS
C         DEFAULT IDL2=11.
C
C IDL3 = SKIP PARAMETER FOR DO LOOPS OVER PERIODS.
C         DEFAULT IDL3=1.
C
C         BY DEFAULT, THE PROGRAM FINDS SPECTRA AT 11 PERIODS.
C         IF THESE ARE NOT ALL NEEDED, THEN IDL1, IDL2, IDL3 ALLOW
C         A FLEXIBLE WAY TO SELECT JUST THOSE THAT ARE NEEDED.
C
C ISTEP = 0 DEFAULT AND NORMAL VALUE
C         1 STOPS PROGRAM AFTER INTEGRATION IS SET UP.
C           DO NOT USE WITH ILTL=2.
C
C IMODE =0      DEFAULT, LONG & LAT INPUT IN DECIMALS
C         =1,    LONG & LAT INPUT IN DEG MIN & SEC
C
C YRS   = MULTIPLICATION FACTOR FOR SEISMICITY - DEFAULT = 1.0
C         ONLY USED FOR POISSONIAN SEISMICITY - LITERAL RATES
C         ARE ALWAYS EXACTLY AS INPUT
C
C
C LINE 2 904(2F10.5, I5, F5.0, 2I5, 20A2) SLONG, SLAT, IV, HIS, NPEX, MUST,
C *****
C           SLONG = WEST LONGITUDE OF SITE
C           SLAT  = NORTH LATITUDE OF SITE
C           IV    = 0 HORIZONTAL
C                 1 VERTICAL
C           HIS   = 0 SOFT, ALLUVIAL SITE, FOR MTY=1, 2, 3, 4
C                 1 INTERMEDIATE SITE, FOR MTY=1, 2, 3, 4
C                 2 HARD SITE, FFOR MTY=1, 2, 3, 4
C                 = DEPTH TO GEOLOGIC BASEMENT (KM.) FOR MTY=5, 6, 7, 8
C           NPEX  = NUMBER OF PROBABILITIES OF EXCEEDANCE FOR WHICH SPECTRA
C                 WILL BE CALCULATED (LIMIT 24)
C           MUST  = SITE NUMBER
C           NSITE = ALPHANUMERIC SITE NAME
C
C LINE 3 938(8F10.3) (PE(I), I=1, NPEX)
C *****
C           PE(I) = EXCEEDANCE PROBABILITIES FOR THE SPECTRA. USE ONLY AS
C                 MANY LINES AS NEEDED.
C
C LINE 4 (WHEN IMRAC=1) CONTROLS THE INTEGRATION OF DIFFUSE SOURCES.
C *****
C LINE 4 910(I1, F9.1, 7F10.1) NC, (RC(I), AC(I), I=1, NC)
C           NC = 1 TO 4
C           RC, AC ... NC PAIRS OF DISTANCE - AREA CRITERIA. MUST HAVE
C                 RC(I) LESS THAN RC(I-1) AND AC(I) LT AC(I-1).
C                 WITH A DIFFUSE SOURCE, NONE OF THE ELEMENTS OF
C                 AREA WITH A DISTANCE LESS THAN RC(I) FROM THE SITE
C                 WILL HAVE AN AREA GREATER THAN AC(I) IN THE

```



C  
C  
C  
C  
C

INTEGRATION.  
THIS LINE IS READ ONLY WHEN IMRAC=1.  
OTHERWISE, REASONABLE DEFAULT VALUES ARE ASSIGNED.





```

C      CONF = CONFIDENCE LEVEL FOR PREDICTED EARTHQUAKE.  USED ONLY
C              WHEN ILTL=2.  DEFAULT IS 0.0, WHICH MEANS THE
C              PREDICTION IS IGNORED UNLESS THIS PARAMETER IS SET.
C              THE PROCEEDURE ASSUMES THAT THERE IS ONLY ONE PREDICTED
C              EVENT, OR THAT THE CONFIDENCE IS THE SAME FOR ALL
C              PREDICTED EVENTS.
C              <CONF> NEGATIVE ALLOWS FINDING SPECTRA FOR MULTIPLE
C              CONFIDENCE LEVELS.  THE ENTRY <-K> GIVES K+1 CONFIDENCE
C              LEVELS EVENLY SPACED BETWEEN 0.0 AND 1.0.
C      JST = 0-10  DESCRIBES THE MAGNITUDE - RUPTURE LENGTH RELATION.
C              SAME CHOICE AS FOR <MRS> IN INPUT PART 1.
C      SL = STEP LENGTH (KM) FOR REPRESENTING THE LINE SOURCE.
C              DEFAULT = 5.0.
C      NL = NUMBER OF LINES TO INPUT SOURCE.
C      NAME = ALPHANUMERIC IDENTIFICATION OF FAULT.
C      LINE L2A (IF ISI=1,2,OR 3) (8F10.2) AAL,BBL,AMM,AMX,AZTM,AZTP
C      *****
C      AAL = COEFFICIENT 'A' IN LOG(N)=A-B*M (ISI=1,2)
C      BBL = COEFFICIENT 'B' IN LOG(N)=A-B*M (ISI=1,2,3)
C      AMM = MINIMUM MAGNITUDE (ISI=1,2,3) DEFAULT ALWAYS AVAILABLE)
C      AMX = MAXIMUM MAGNITUDE (ISI=1,2,3) DEFAULT ALWAYS AVAILABLE)
C      AZTM = USED TO DEFINE MOMENT RATE. (ISI=3)
C      AZTP = USED TO DEFINE MOMENT RATE. (ISI=3)
C              MOMENT RATE = AZTM * 10.0**AZTP
C      LINE L2B (IF ISI=4) (8F10.2) WS(12)
C      *****
C      WS(12)= SEISMICITY RATE ON THE FAULT.
C              REQUIRES TWO LINES WITH 12 VALUES.
C              BOTH MUST BE PRESENT EVEN IF ONE IS BLANK.
C              IF MAGNITUDE, RATE IS FOR M=3.0,3.5,4.0,...,8.0,8.5
C              IF INTENSITY, RATE IS FOR I=I,II,III,IV,...,X,XI,XII
C      LINES L3  S902 (2F10.5) XL(I),YL(I)  --NL LINES--
C      *****
C      XL(I) = WEST LONGITUDE (DECIMAL DEGREES)
C      YL(I) = NORTH LATITUDE (DECIMAL DEGREES)
C              XL(I),YL(I), FOR I FROM 1 TO NL, GIVE THE COORDINATES
C              OF SUCCESSIVE POINTS ON THE FAULT.
C
C      DIFFUSE SOURCE.  SUBROUTINE DSIN.
C      LINE D1 - SAME FORMAT AND VARIABLE NAMES AS L1 FOR LINE SOURCE.
C      *****
C              - USAGE OF FOLLOWING VARIABLES DIFFERS:
C      JST = 1 THE SOURCE RUPTURE LENGTHS ARE ZERO
C           = 2 THE SOURCES ARE ASSUMED TO BE UNILATERAL RUPTURE,
C               WITH THE EPICENTER HAVING EQUAL PROBABILITY TO BE
C               ANYPLACE IN THE ZONE.  THE DIRECTION OF RUPTURE
C               IS RANDOM.  THIS IS THE DEFAULT VALUE.
C               RUPTURE LENGTH GIVEN BY MRL IN BLOCK 1, LINE 1.
C      SL = NOT USED.
C      NL = NUMBER OF LONGITUDES USED TO DEFINE REGION.
C      LINE D2A OR D2B -- SAME AS L2A OR L2B FOR LINE SOURCE
C      *****
C      LINES D3  S902(3F10.5)  YC(I),XL(I),XR(I)  --NL LINES--
C      *****
C      ON EACH LINE, A NORTH LATITUDE <YC(I)>, AND THE
C      LONGITUDE AT WHICH IT INTERSECTS THE WEST <XL(I)> AND
C      EAST <XR(I)> BOUNDARY OF THE REGION.
C      <YC(I)> MUST INCREASE WITH SUCCESSIVE LINES.
C      THE FIRST VALUE OF <YC(I)> IS THE SOUTHERN BOUNDARY OF THE
C      REGION, AND THE LAST VALUE IS THE NOUTHERN BOUNDARY.
C
C      DIPPING PLANAR SOURCE.  SUBROUTINE DIPSIN.
C      SEE TEXT FOR THE CURRENT METHOD OF ASSIGNING PROBABILITY OF

```

```
C      OCCURRENCES IN THE SUB-REGIONS, DEPENDING OF THE MAGNITUDE
C      AND SIZE OF RUPTURE.
C      LINE DP1 - SAME AS LINE D1
C      *****
C      LINE DP2 - SAME AS LINE D2
C      *****
C      LINE DP3   S907(7F10.5)  PDPL(I), I=1,7
C      *****
C      PDPL(1),PDPL(2)  LONGITUDE AND LATITUDE OF A SURFACE POINT
C      TRACE OF THE DIPPING FAULT.
C      PDPL(3),PDPL(4)  LONGITUDE AND LATITUDE OF SECOND SURFACE POINT
C      ON THE SURFACE TRACE OF THE DIPPING PLANE.
C      PDPL(5),PDPL(6),PDPL(7)  LONGITUDE, LATITUDE, AND DEPTH(KM) OF
C      THIRD POINT ON THE DIPPING FAULT.
C      LINES DP4  --  SAME AS LINES D3
C      *****
C      VOLUME SOURCE SUBROUTINE VOLSIN
C      AT PRESENT, EXTENDED SOURCES CANNOT BE USED, ONLY POINT SOURCES ARE
C      TO BE USED.
C      INPUT FOR VOLUME SOURCE IS SAME AS THAT FOR DIFFUSE & DIPPING PLANE
C      SOURCE. THE SURFACE OF THE VOLUME IS DEFINED AS THAT OF THE
C      DIFFUSE SURFACE, AND ITS DEPTH DEFINED AS THAT IN LINE DP3 ABOVE.
C
C
C
```

### 5.3 The Flow Chart and Program Description

Figure 5.3.1 is a flow chart of the program NEQRISK. Each rectangular box corresponds to the calling of a subroutine whose name appears in the box. The subroutine usually will perform a specific task and subsequently return to the MAIN program. Figure 5.3.2 is an additional flow chart for the subroutine INSEIS. It involves calling 8 more subroutines which are not shown on the previous flow chart in Figure 5.3.1. For each of the subroutines whose names appear on these two figures, a brief description of its function will be presented.

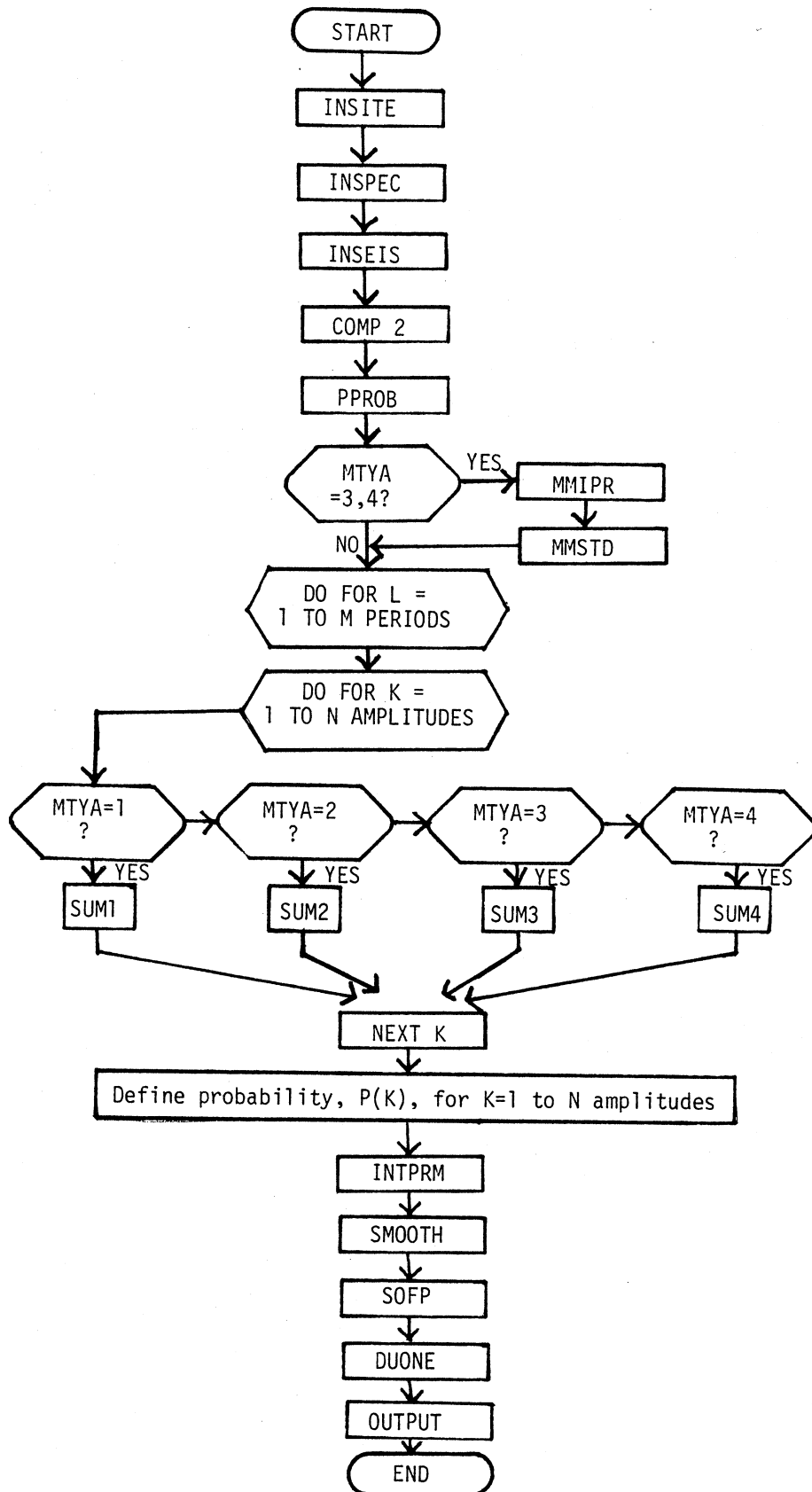


Figure 5.3.1 NEQRISK

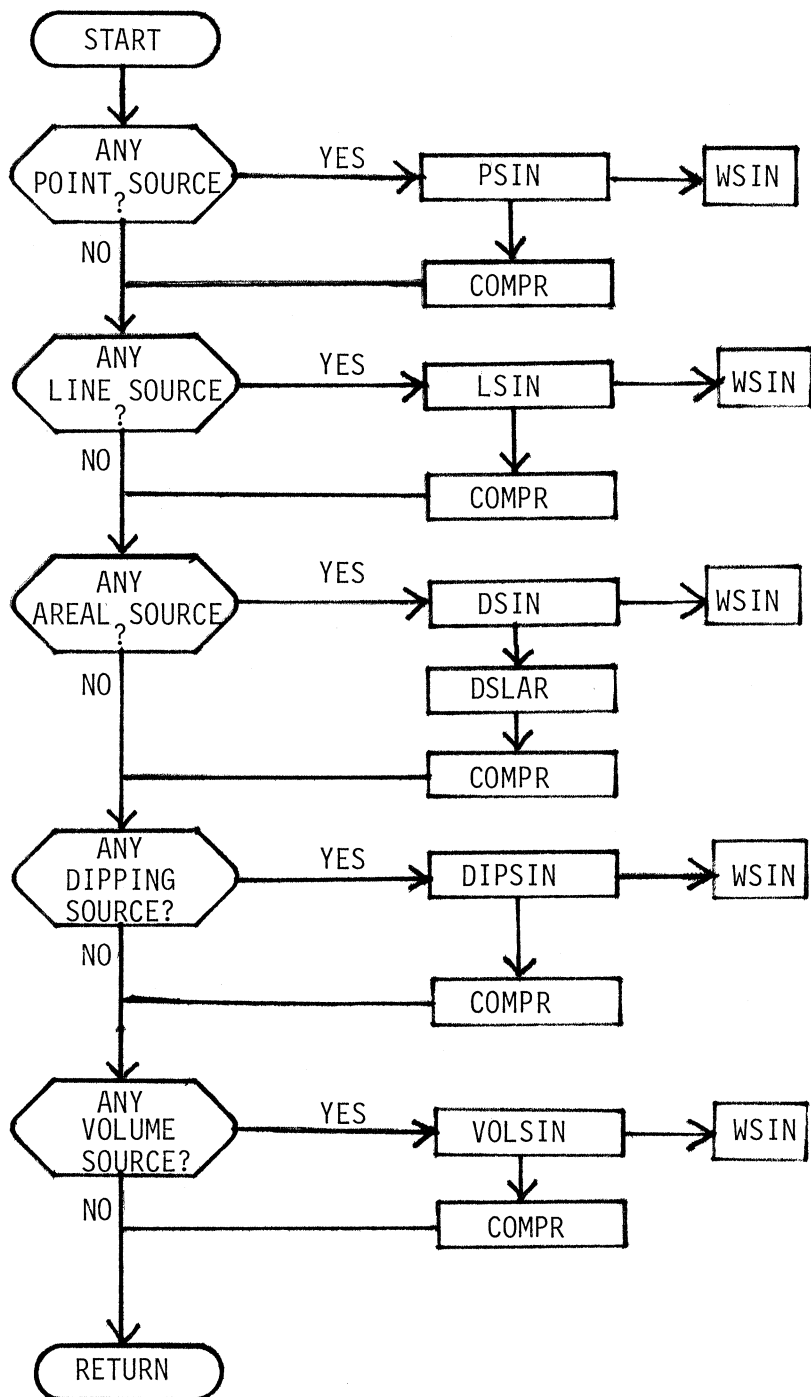


Figure 5.3.2 Subroutine INSEIS



### 5.3.1 INSITE

Subroutine INSITE reads in the model identification and site parameters from the data file SITE.DAT.

### 5.3.2 INSPEC

Subroutine INSPEC reads in the regression parameters for the particular scaling relations of the spectral amplitudes to be used in the analysis. For the old data base and the old scaling equations, this is stored in the data file SPEC.DAT. For the new data base and the updated scaling equations, this is stored in the data file ASPEC.DAT.

### 5.3.3 INSEIS

Subroutine INSEIS first reads in the number of various source types used. For each source type, through the corresponding subroutine, it reads in the necessary parameters for the calculation of seismicity at discrete earthquake sizes. It also reads in the maximum allowed earthquake size. In the new program NEQEISK, uncertainties associated with the estimation of seismicity parameters  $a$  and  $b$  and maximum allowed earthquake size are read in as confidence intervals of the corresponding parameters at a specified type of probability distribution. These are available in the file FSIN.DAT.

### 5.3.4 PSIN

This subroutine is called by subroutine INSEIS. It in turn calls WSIN to read in the parameters for the seismicity of a point source. It then calculates the expected number of earthquakes at each interval around discrete earthquake sizes.

### 5.3.5 WSIN

Subroutine WSIN is used to read in the seismicity parameters for all of the source types. It is called by PSIN, LSIN, DSIN and DPISIN. The seismicity parameters read in may include the uncertainties in the estimation and maximum allowed earthquake sizes. For each of the discrete earthquake sizes, WSIN computes the expected number of earthquakes of that size.

### 5.3.6 LSIN

Subroutine LSIN is called by subroutine INSEIS. It first calls WSIN to read in the parameters for the estimation of seismicity of line source. The line source is described by a set of straight lines, which are input as a consecutive sequence of coordinates as latitudes and longitudes. LSIN then represents the line source as a sequence of equally spaced points on the fault. The distances from these points to the observation point are calculated. The seismicity is then assigned to each point according to the probability of being the closest point that ruptures for each earthquake size.

### 5.3.7 DSIN

Subroutine DSIN is called by subroutine INSEIS. It first calls WSIN to read in the area boundaries and the parameters for the estimation of seismicity of the aeral source (diffuse zone). From the coordinates of the area boundary, DSIN generates a set of roughly square rectangles. Each of these squares may further be divided so that they are small enough, according to the criteria in the program, determined mainly by the epicentral distance between the site and the source elements. The seismicity is then divided among these areas in proportion to the area of each sub-element.

### 5.3.8 DIPSIN

Subroutine DIPSIN is called by INSEIS. It first calls WSIN to read in the area boundaries and the parameters necessary for the estimation of seismicity of the dipping plane source. As in subroutine DSIN, from the dimensions of the area boundary, DIPSIN generates a set of roughly square rectangles, which may further be divided so that they are small enough, according to the criteria of hypocentral distance and rupture area. Unlike DSIN, which divided the seismicity evenly among the elements, DIPSIN assigns the seismicity to each element according to the probability of being the closest element that ruptures for each earthquake size.

### 5.3.9 VOLSIN

Subroutine VOLSIN is called by INSEIS. It first calls WSIN to read in the volume boundaries and the parameters necessary for the estimation of seismicity of the volume source. VOLSIN then generates a set of roughly cubic elements, which may further be divided so that they are small enough, depending on the hypocentral distances to the site. As in DSIN, the seismicity is divided among the elements in proportion to the volume of each subelement. As pointed out earlier, this is only an approximate procedure for volume source representation and the procedure used here is only acceptable if the site is far enough. A criteria is set in the program which will automatically stop the program if the site is "too close" to the volume source.

### 5.3.10 COMPR

Subroutine COMPR is called by subroutines PSIN, LSIN, DSIN, DIPSIN and VOLSIN. Each time the seismicity is calculated and assigned to each of the source subelements of different source types, subroutine COMPR is

called to compress the seismicity and distance arrays so that all the points of equal distances are consolidated.

#### 5.3.11 COMP2

Subroutine COMP2 is called by the MAIN program to compress the seismicity and distance arrays to eliminate any distances that have no seismicity.

#### 5.3.12 PPROB

Subroutine PPROB is called by the MAIN program to compute the ratio  $\gamma_{ij} = n_{ij}/N(M_j)$  defined in Section 4.3 for the calculation of probability of exceedance  $P^+[S(\omega)]$  under the assumption that the number of earthquakes  $N(M_j)$  is known (literal assumption).

#### 5.3.13 MMIPR

Subroutine MMIPR is called by the MAIN program for the case of using the intensity (MMI) scaling functions to compute the intensity (MMI) at the site for a given magnitude and epicentral distance. An intensity attenuation scaling function for both eastern and western U.S. are available.

#### 5.3.14 MMSTD

Subroutine MMSTD is called by the MAIN program for the case of using the intensity (MMI) scaling functions. It computes and prints the expected number of occurrences of each Modified Mercalli Intensity (MMI) at the site. The calculation is based on the attenuation function model developed by Anderson (1979b).

### 5.3.15 SUM1

Subroutine SUM1 is called by the MAIN program. Given a value of period,  $PER(L)$ , and a spectral amplitude,  $SP(K)$ , SUM1 performs the summation  $i$  from 1 to  $I$  over all source elements and the summation  $j$  from 1 to  $J$  over all earthquake sizes of  $\bar{q}_{ij}E(n_{ij})$  to get  $N_E(SP(K))$ , the expected number of times that spectral amplitude  $SP(K)$  of period  $PER(L)$  will be exceeded at the site. The spectral amplitude assumed in the subroutine is the Fourier spectral amplitudes,  $FS$ , scaled in terms of magnitude, representative source-to-station distance and local site geology (Trifunac and Lee, 1985b).

### 5.3.16 SUM2

Subroutine SUM2 is called by the MAIN program. As in SUM1, given a value of period,  $PER(L)$ , and a spectral amplitude  $SP(K)$ , SUM2 performs the summation of  $\bar{q}_{ij}E(n_{ij})$  to get  $N_E(SP(K))$ . The spectral amplitude assumed is pseudo relative velocity spectral amplitude,  $PSV$ , scaled in terms of magnitude, representative source-to-station distance and local site geology (Trifunac and Lee, 1985c).

### 5.3.17 SUM3

Subroutine SUM3 is called by the MAIN program. As in SUM1 and SUM2, given a value of period,  $PER(L)$ , and a spectral amplitude,  $SP(K)$ , SUM3 performs the summation of  $\bar{q}_{ij}E(n_{ij})$  to get  $N_E(SP(K))$ . The spectral amplitude assumed is Fourier spectral amplitude,  $FS$ , scaled in terms of Modified Mercalli Intensity (MMI) and local site geology (using Trifunac and Lee, 1985b).

### 5.3.18 SUM4

Subroutine SUM4 is called by the MAIN program. As in SUM1, SUM2 and SUM3, given a value of period, PER(L), and a spectral amplitude, SP(K), SUM4 performs the summation of  $\bar{q}_{ij} \cdot E(n_{ij})$  to get  $N_E(SP(K))$ . The spectral amplitude assumed is pseudo relative velocity response spectral amplitude, PSV, scaled in terms of Modified Mercalli Intensity (MMI) and local site geology (Trifunac and Lee, 1985c).

### 5.3.19 INTPRM

Subroutine INTPRM is called by the MAIN program. Having calculated the Poisson probability of exceedance for N spectral amplitudes at a particular period, INTPRM is called to interpolate the Poisson probabilities at intermediate amplitudes to result in 4 times as many points. INTPRM uses a finite impulse response (FIR) nonrecursive interpolation filter designed by Oetken et al (1975).

### 5.3.20 SMOOTH

Subroutine SMOOTH is called by the MAIN program. Having interpolated the Poisson probability of exceedance from N points to  $4(N-1)+1$  points, SMOOTH is called to smooth the interpolated data using the 1/4, 1/2, 1/4 weights. This is repeated several times.

### 5.3.21 SOFP

Subroutine SOFP is called by the MAIN program. It is called to construct a uniform risk spectra. For a given probability level, and for each discrete frequency  $\omega$ , it calculates the spectral amplitude  $S(\omega)$  that has the given probability that it will be exceeded. The probability versus spectral amplitudes  $S(\omega)$  data to be used are the smoothed, interpolated set of data just calculated.

### 5.3.22 DUONE

Subroutine DUONE is called by the MAIN program. It is called to calculate the probability density function from the Poisson probability of exceedance. It uses a higher order differentiation formula derived from the smooth low-pass filter used in data processing of strong-motion accelerograms.

### 5.3.23 OUTPUT

Subroutine OUTPUT is called by the MAIN program. It prints out on a file the input site and model information, spectral information and seismicity information. For the logarithm of spectral amplitudes from -5 to +5, it prints out  $N_E[S(\omega)]$ , in the form of the logarithm of expected number of exceedances. In the same amplitude range, it prints out the probability of exceedances, the probability density function, and finally, the uniform risk spectra versus periods at a specified set of probability levels. It also plots out the expected number of exceedances versus periods and spectral amplitudes, the probabilities of exceedances, the probability density functions, both versus periods and spectral amplitudes, and finally the uniform risk spectra.

This completes the brief outline of the flow chart of the "NEQRISK" computer program.

## 5.4 Listing of Sample Inputs

### 5.4.1 Listing of Input Part 1



\*\*\*\*\*

DIRECTORY : UDD:EQRISK:WORKING:PEQRISK

SITES.DAT                   TXT   12-JUL-85   8:42:30   351

\*\*\*\*\*

6 3 1 011 0 6 0 0 111 1 0	1.								
117.90000	34.10000	0 2.3	17 1001	L. A. VICINITY 01					
0.9	0.5	0.35	0.2	0.1	0.05	0.035	0.02		
0.01	0.005	0.0035	0.0020	0.0010	0.00050	0.00035	0.00020		
0.000100									

#### 5.4.2 Listing of Input Part 2

\*\*\*\*\*

DIRECTORY : UDD:EQRISK:WORKING:PEQRISK

SPEC. DAT                    UDF 12-JUL-85    8:44:24    17324

\*\*\*\*\*

```

0 0 1 3 FREQUENCY DEPENDENT ATTENUATION FUNCTION
12PER .040 .065 .11 .19 .34 .50 .90 1.6 2.8 4.4 7.5 14.0
AOR-2.174-1.830-1.510-1.236-1.010 -.896 -.781 -.734 -.732 -.732 -.732 -.732
SZM 29.27 29.39 29.51 29.65 29.78 29.87 30.01 30.14 30.28 30.38 30.51 30.66
0 0 1 2 WESTERN USA
12RMU 1.15 1.48 1.78 2.04 2.25 2.42 2.56 2.67 2.77 2.85 2.92 2.99
RSG 0.3 0.3 0.3 0.3 0.3 0.3 0.3 0.3 0.3 0.3 0.3 0.3
0 0 2 2 EASTERN USA
12RMU 1.18 1.54 1.90 2.23 2.53 2.79 3.01 3.18 3.32 3.44 3.54 3.62
RSG 0.3 0.3 0.3 0.3 0.3 0.3 0.3 0.3 0.3 0.3 0.3 0.3
1 0 0 8 FS AMPLITUDE MAG-SITE MODEL
12PER .040 .065 .11 .19 .34 .50 .90 1.60 2.80 4.40 7.50 14.00
A -.258 -.019 .222 .433 .610 .706 .820 .883 .869 .712 .184 -.933
B .041 .042 .033 -.003 -.057 -.084 -.102 -.110 -.122 -.121 -.086 .002
C .086 .015 -.092 -.216 -.309 -.329 -.294 -.223 -.191 -.201 -.183 -.044
D -1.373-1.681-2.207-2.965-3.844-4.394-5.100-5.487-5.395-4.741-2.924 .580
E -.030 -.052 -.072 -.086 -.094 -.098 -.103 -.107 -.109 -.102 -.069 .012
MU -.005 -.001 .002 .002 -.001 -.003 -.004 -.004 -.003 -.003 -.002 -.001
ST .471 .460 .438 .402 .363 .351 .361 .388 .400 .388 .358 .331
2 1 0 9 PSV .00 DAMPING MAG-SITE MODEL
12PER .040 .065 .11 .19 .34 .50 .90 1.60 2.80 4.40 7.50 14.00
A .010 -.008 .075 .271 .515 .666 .867 1.018 1.099 1.047 .712 -.083
B -.004 .004 -.003 -.040 -.092 -.118 -.137 -.148 -.160 -.164 -.141 -.079
C -.072 -.019 .002 -.026 -.092 -.136 -.166 -.139 -.107 -.104 -.108 -.077
D -1.669-1.510-1.768-2.526-3.543-4.206-5.098-5.694-5.868-5.551-4.371-1.912
E -.041 -.045 -.053 -.068 -.084 -.094 -.108 -.119 -.129 -.129 -.110 -.054
ALP 1.247 1.252 1.220 1.211 1.256 1.290 1.268 1.166 1.211 1.530 2.225 3.086
BET 1.026 1.006 1.005 1.007 1.000 .998 1.014 1.019 .935 .767 .492 .198
N 10 10 10 10 10 10 10 10 9 6 3 2
2 2 0 9 PSV .02 DAMPING MAG-SITE MODEL
12PER .040 .065 .11 .19 .34 .50 .90 1.60 2.80 4.40 7.50 14.00
A .002 .006 .123 .350 .577 .690 .832 .974 1.081 1.052 .758 .059
B -.018 -.004 .000 -.025 -.069 -.093 -.115 -.131 -.150 -.158 -.138 -.075
C -.099 -.056 -.033 -.046 -.100 -.140 -.171 -.145 -.112 -.110 -.115 -.087
D -1.719-1.622-1.973-2.815-3.797-4.351-5.062-5.609-5.842-5.589-4.550-2.423
E -.041 -.049 -.063 -.080 -.094 -.100 -.108 -.118 -.129 -.132 -.115 -.065
ALP 1.314 1.328 1.281 1.239 1.263 1.299 1.287 1.185 1.220 1.543 2.271 3.209
BET 1.026 1.007 1.007 1.009 1.002 1.000 1.016 1.022 .936 .767 .492 .200
N 10 10 10 10 10 10 10 10 9 6 3 2
2 3 0 9 PSV .05 DAMPING MAG-SITE MODEL
12PER .040 .065 .11 .19 .34 .50 .90 1.60 2.80 4.40 7.50 14.00
A .011 .018 .134 .363 .596 .699 .802 .906 1.013 1.020 .813 .260
B -.021 -.009 -.007 -.026 -.063 -.085 -.105 -.121 -.142 -.151 -.135 -.074
C -.101 -.069 -.051 -.059 -.104 -.144 -.178 -.154 -.118 -.112 -.118 -.102
D -1.811-1.731-2.078-2.919-3.904-4.427-5.020-5.453-5.674-5.526-4.754-3.115
E -.040 -.048 -.063 -.082 -.098 -.103 -.107 -.114 -.125 -.131 -.120 -.080
ALP 1.316 1.350 1.313 1.263 1.267 1.292 1.276 1.187 1.245 1.586 2.327 3.262
BET 1.026 1.007 1.008 1.010 1.002 1.001 1.017 1.023 .936 .768 .494 .203
N 10 10 10 10 10 10 10 10 9 6 3 2
2 4 0 9 PSV .10 DAMPING MAG-SITE MODEL
12PER .040 .065 .11 .19 .34 .50 .90 1.60 2.80 4.40 7.50 14.00
A .056 .039 .136 .355 .579 .674 .767 .878 1.002 1.029 .864 .410
B -.027 -.016 -.012 -.028 -.061 -.080 -.100 -.117 -.140 -.150 -.135 -.075
C -.103 -.076 -.059 -.066 -.108 -.146 -.182 -.163 -.127 -.117 -.123 -.118

```

D	-1.974	-1.870	-2.186	-2.993	-3.934	-4.419	-4.966	-5.407	-5.674	-5.583	-4.954	-3.632
E	-.043	-.049	-.063	-.081	-.097	-.102	-.106	-.113	-.126	-.132	-.124	-.092
ALP	1.319	1.368	1.341	1.289	1.280	1.295	1.274	1.196	1.276	1.632	2.376	3.299
BET	1.026	1.007	1.008	1.010	1.003	1.002	1.018	1.023	.936	.768	.497	.212
N	10	10	10	10	10	10	10	10	9	6	3	2
2 5 0 9 PSV .20 DAMPING MMI-SITE MODEL												
12PER	.040	.065	.11	.19	.34	.50	.90	1.60	2.80	4.40	7.50	14.00
A	.123	.092	.165	.348	.537	.616	.704	.820	.948	.986	.866	.512
B	-.031	-.022	-.018	-.030	-.058	-.075	-.095	-.113	-.137	-.149	-.135	-.073
C	-.096	-.084	-.076	-.081	-.111	-.142	-.176	-.165	-.130	-.114	-.118	-.135
D	-2.218	-2.116	-2.389	-3.098	-3.922	-4.354	-4.864	-5.297	-5.567	-5.511	-5.017	-3.982
E	-.048	-.053	-.064	-.080	-.094	-.098	-.101	-.110	-.123	-.131	-.126	-.101
ALP	1.305	1.363	1.348	1.303	1.286	1.293	1.273	1.220	1.321	1.673	2.398	3.324
BET	1.026	1.008	1.009	1.010	1.003	1.002	1.019	1.024	.937	.769	.500	.219
N	10	10	10	10	10	10	10	10	9	6	3	2
3 0 0 7 FS AMPLITUDE MMI-SITE MODEL												
12PER	.040	.065	.11	.19	.34	.50	.90	1.60	2.80	4.40	7.50	14.00
A	.184	.209	.253	.306	.352	.368	.369	.347	.310	.263	.179	.045
B	.121	.101	.065	.019	-.021	-.036	-.044	-.056	-.079	-.081	-.029	.109
C	.091	.028	-.090	-.227	-.323	-.334	-.277	-.200	-.157	-.148	-.144	-.143
D	-2.118	-1.774	-1.476	-1.397	-1.540	-1.659	-1.709	-1.542	-1.225	-.911	-.519	-.061
MU	-.003	.002	.006	.006	.004	.003	.005	.009	.010	.008	.002	-.006
ST	.565	.516	.448	.394	.385	.405	.450	.467	.439	.397	.353	.329
4 1 0 8 PSV .00 DAMPING MMI-SITE MODEL												
12PER	.040	.065	.11	.19	.34	.50	.90	1.60	2.80	4.40	7.50	14.00
A	.220	.229	.258	.305	.349	.364	.362	.337	.297	.257	.209	.155
B	.093	.085	.060	.013	-.037	-.057	-.069	-.078	-.094	-.097	-.063	.029
C	-.056	-.024	-.011	-.042	-.106	-.137	-.132	-.089	-.062	-.067	-.090	-.105
D	-1.811	-1.555	-1.350	-1.318	-1.437	-1.515	-1.518	-1.340	-1.034	-.779	-.593	-.587
ALP	1.066	1.102	1.129	1.155	1.157	1.127	1.028	.945	1.078	1.457	2.168	2.999
BET	1.007	.988	.988	.990	.984	.982	.998	1.002	.917	.750	.483	.203
N	10	10	10	10	10	10	10	10	9	6	3	2
4 2 0 8 PSV .02 DAMPING MMI-SITE MODEL												
12PER	.040	.065	.11	.19	.34	.50	.90	1.60	2.80	4.40	7.50	14.00
A	.207	.210	.239	.292	.347	.368	.372	.348	.309	.269	.220	.167
B	.082	.085	.071	.036	-.008	-.029	-.044	-.058	-.079	-.087	-.059	.029
C	-.090	-.062	-.044	-.063	-.118	-.149	-.147	-.105	-.074	-.078	-.104	-.122
D	-1.854	-1.625	-1.465	-1.488	-1.650	-1.744	-1.752	-1.562	-1.235	-.957	-.746	-.715
ALP	1.141	1.163	1.169	1.188	1.206	1.193	1.107	1.012	1.118	1.490	2.231	3.139
BET	1.007	.989	.989	.990	.982	.981	.998	1.003	.916	.749	.482	.204
N	10	10	10	10	10	10	10	10	9	6	3	2
4 3 0 8 PSV .05 DAMPING MMI-SITE MODEL												
12PER	.040	.065	.11	.19	.34	.50	.90	1.60	2.80	4.40	7.50	14.00
A	.209	.212	.236	.287	.341	.365	.372	.353	.316	.279	.231	.179
B	.080	.081	.070	.040	.001	-.017	-.033	-.048	-.072	-.081	-.055	.028
C	-.095	-.074	-.058	-.073	-.123	-.154	-.158	-.117	-.085	-.088	-.115	-.136
D	-1.903	-1.688	-1.538	-1.566	-1.734	-1.834	-1.858	-1.687	-1.372	-1.098	-.884	-.846
ALP	1.177	1.200	1.194	1.201	1.219	1.213	1.138	1.046	1.153	1.528	2.275	3.196
BET	1.006	.989	.989	.990	.982	.982	.999	1.004	.917	.749	.481	.203
N	10	10	10	10	10	10	10	10	9	6	3	2
4 4 0 8 PSV .10 DAMPING MMI-SITE MODEL												
12PER	.040	.065	.11	.19	.34	.50	.90	1.60	2.80	4.40	7.50	14.00
A	.214	.216	.239	.285	.337	.360	.370	.354	.321	.287	.243	.195
B	.076	.076	.065	.039	.005	-.012	-.027	-.043	-.066	-.075	-.052	.028
C	-.096	-.083	-.070	-.083	-.128	-.156	-.163	-.127	-.092	-.094	-.122	-.148
D	-1.958	-1.760	-1.621	-1.649	-1.809	-1.906	-1.936	-1.784	-1.495	-1.240	-1.040	-1.000
ALP	1.212	1.236	1.223	1.218	1.232	1.227	1.158	1.079	1.201	1.580	2.309	3.188
BET	1.006	.989	.990	.991	.983	.983	1.001	1.006	.917	.748	.479	.199
N	10	10	10	10	10	10	10	10	9	6	3	2
4 5 0 8 PSV .20 DAMPING MMI-SITE MODEL												
12PER	.040	.065	.11	.19	.34	.50	.90	1.60	2.80	4.40	7.50	14.00
A	.222	.224	.243	.284	.332	.354	.364	.350	.321	.292	.254	.211
B	.068	.068	.059	.037	.006	-.010	-.025	-.040	-.061	-.069	-.048	.026

C	-.099	-.089	-.081	-.093	-.131	-.158	-.166	-.134	-.101	-.099	-.124	-.150
D	-2.027	-1.856	-1.735	-1.758	-1.902	-1.991	-2.015	-1.871	-1.611	-1.389	-1.214	-1.171
ALP	1.253	1.280	1.265	1.248	1.250	1.240	1.172	1.114	1.271	1.662	2.359	3.148
BET	1.006	.990	.991	.992	.984	.983	1.002	1.006	.918	.748	.477	.195
N	10	10	10	10	10	10	10	10	9	6	3	2
5 0 0 8 FS AMPLITUDE MAG-DEPTH MODEL												
12PER	.040	.065	.11	.19	.34	.50	.90	1.60	2.80	4.40	7.50	14.00
A	-.228	.014	.251	.432	.545	.594	.668	.734	.718	.549	.048	-.933
B	.018	.014	.012	.017	.033	.045	.063	.082	.093	.089	.063	.013
C	.077	.007	-.098	-.219	-.308	-.325	-.287	-.219	-.196	-.214	-.196	-.050
D	-1.401	-1.714	-2.241	-2.967	-3.724	-4.164	-4.766	-5.187	-5.141	-4.477	-2.698	.556
E	-.034	-.056	-.076	-.086	-.089	-.090	-.092	-.096	-.098	-.090	-.058	.011
MU	-.004	.000	.003	.002	.001	.003	.003	.004	.004	.004	.003	.000
ST	.473	.462	.438	.401	.364	.351	.353	.366	.367	.356	.338	.328
6 1 0 9 PSV .00 DAMPING MAG-DEPTH MODEL												
12PER	.040	.065	.11	.19	.34	.50	.90	1.60	2.80	4.40	7.50	14.00
A	-.021	-.018	.070	.237	.408	.505	.651	.786	.839	.747	.407	-.276
B	.039	.030	.027	.035	.052	.063	.076	.088	.097	.095	.079	.046
C	-.076	-.024	-.002	-.029	-.090	-.130	-.153	-.125	-.100	-.108	-.121	-.091
D	-1.580	-1.465	-1.747	-2.470	-3.345	-3.877	-4.627	-5.205	-5.341	-4.924	-3.693	-1.442
E	-.041	-.045	-.054	-.066	-.076	-.082	-.091	-.101	-.108	-.106	-.086	-.038
ALP	1.258	1.259	1.224	1.212	1.258	1.297	1.296	1.235	1.327	1.673	2.373	3.216
BET	1.027	1.006	1.006	1.007	1.000	.998	1.013	1.018	.935	.767	.492	.197
N	10	10	10	10	10	10	10	10	9	6	3	2
6 2 0 9 PSV .02 DAMPING MAG-DEPTH MODEL												
12PER	.040	.065	.11	.19	.34	.50	.90	1.60	2.80	4.40	7.50	14.00
A	-.036	-.009	.121	.331	.497	.555	.638	.768	.852	.780	.479	-.097
B	.039	.032	.028	.034	.047	.055	.066	.079	.093	.095	.083	.051
C	-.104	-.061	-.037	-.049	-.097	-.134	-.160	-.135	-.110	-.115	-.127	-.102
D	-1.630	-1.571	-1.954	-2.786	-3.645	-4.067	-4.632	-5.186	-5.400	-5.046	-3.951	-2.066
E	-.040	-.049	-.064	-.079	-.089	-.090	-.094	-.102	-.112	-.110	-.092	-.052
ALP	1.316	1.334	1.290	1.252	1.279	1.316	1.317	1.253	1.340	1.696	2.441	3.377
BET	1.027	1.008	1.008	1.010	1.002	.999	1.014	1.019	.935	.767	.492	.197
N	10	10	10	10	10	10	10	10	9	6	3	2
6 3 0 9 PSV .05 DAMPING MAG-DEPTH MODEL												
12PER	.040	.065	.11	.19	.34	.50	.90	1.60	2.80	4.40	7.50	14.00
A	-.040	-.003	.131	.344	.517	.571	.628	.728	.807	.764	.538	.092
B	.042	.037	.032	.034	.044	.052	.065	.078	.090	.091	.080	.053
C	-.101	-.072	-.054	-.062	-.103	-.140	-.168	-.143	-.114	-.117	-.131	-.113
D	-1.697	-1.672	-2.060	-2.889	-3.750	-4.154	-4.638	-5.099	-5.296	-5.026	-4.167	-2.723
E	-.038	-.049	-.065	-.082	-.092	-.094	-.094	-.101	-.109	-.110	-.097	-.068
ALP	1.320	1.360	1.324	1.273	1.282	1.315	1.321	1.263	1.358	1.731	2.520	3.526
BET	1.028	1.008	1.008	1.010	1.003	1.000	1.014	1.018	.934	.767	.494	.200
N	10	10	10	10	10	10	10	10	9	6	3	2
6 4 0 9 PSV .10 DAMPING MAG-DEPTH MODEL												
12PER	.040	.065	.11	.19	.34	.50	.90	1.60	2.80	4.40	7.50	14.00
A	.007	.016	.128	.334	.508	.558	.603	.700	.787	.762	.581	.241
B	.043	.038	.033	.035	.044	.052	.064	.076	.087	.089	.079	.049
C	-.105	-.080	-.062	-.067	-.107	-.144	-.175	-.153	-.123	-.124	-.138	-.132
D	-1.867	-1.809	-2.160	-2.960	-3.795	-4.171	-4.605	-5.047	-5.265	-5.044	-4.336	-3.229
E	-.041	-.049	-.064	-.081	-.092	-.094	-.094	-.100	-.109	-.111	-.102	-.079
ALP	1.326	1.382	1.356	1.302	1.296	1.318	1.312	1.258	1.376	1.772	2.573	3.558
BET	1.028	1.009	1.009	1.011	1.003	1.001	1.015	1.018	.932	.766	.496	.210
N	10	10	10	10	10	10	10	10	9	6	3	2
6 5 0 9 PSV .20 DAMPING MAG-DEPTH MODEL												
12PER	.040	.065	.11	.19	.34	.50	.90	1.60	2.80	4.40	7.50	14.00
A	.092	.063	.136	.315	.473	.520	.555	.637	.732	.739	.616	.338
B	.046	.042	.038	.039	.046	.053	.063	.074	.087	.091	.081	.049
C	-.094	-.085	-.078	-.082	-.110	-.139	-.170	-.157	-.128	-.120	-.131	-.150
D	-2.151	-2.044	-2.322	-3.035	-3.803	-4.150	-4.528	-4.906	-5.144	-5.036	-4.511	-3.575
E	-.048	-.052	-.063	-.079	-.089	-.091	-.091	-.096	-.106	-.111	-.105	-.088
ALP	1.307	1.377	1.368	1.325	1.312	1.321	1.307	1.277	1.432	1.848	2.646	3.618
BET	1.028	1.010	1.010	1.011	1.003	1.001	1.016	1.019	.933	.767	.500	.218

N	10	10	10	10	10	10	10	10	10	9	6	3	2
7 0 0 7	FS AMPLITUDE MMI-DEPTH MODEL												
12PER	.040	.065	.11	.19	.34	.50	.90	1.60	2.80	4.40	7.50	14.00	
A	.189	.209	.247	.296	.334	.345	.339	.320	.290	.249	.170	.040	
B	-.038	-.024	-.003	.022	.047	.063	.081	.095	.099	.091	.058	-.009	
C	.084	.022	-.095	-.231	-.326	-.335	-.279	-.209	-.177	-.170	-.163	-.156	
D	-1.993	-1.657	-1.388	-1.352	-1.522	-1.637	-1.687	-1.579	-1.357	-1.081	-.626	.039	
MU	-.003	.003	.006	.005	.003	.003	.004	.006	.008	.006	.001	-.005	
ST	.566	.518	.450	.392	.378	.393	.427	.433	.401	.365	.336	.331	
8 1 0 8	PSV .00 DAMPING MMI-DEPTH MODEL												
12PER	.040	.065	.11	.19	.34	.50	.90	1.60	2.80	4.40	7.50	14.00	
A	.223	.231	.257	.297	.332	.341	.335	.315	.283	.248	.201	.145	
B	-.027	-.023	-.009	.017	.050	.069	.088	.096	.097	.089	.070	.036	
C	-.061	-.029	-.015	-.045	-.109	-.139	-.135	-.099	-.082	-.089	-.107	-.115	
D	-1.715	-1.464	-1.278	-1.284	-1.435	-1.524	-1.551	-1.434	-1.207	-.983	-.757	-.612	
ALP	1.061	1.096	1.126	1.167	1.194	1.181	1.105	1.055	1.219	1.605	2.288	3.066	
BET	1.006	.987	.988	.991	.984	.982	.998	1.004	.919	.752	.484	.204	
N	10	10	10	10	10	10	10	10	9	6	3	2	
8 2 0 8	PSV .02 DAMPING MMI-DEPTH MODEL												
12PER	.040	.065	.11	.19	.34	.50	.90	1.60	2.80	4.40	7.50	14.00	
A	.208	.213	.241	.289	.333	.348	.347	.328	.294	.259	.211	.158	
B	-.023	-.026	-.020	.001	.033	.054	.076	.086	.090	.086	.070	.036	
C	-.093	-.066	-.048	-.067	-.122	-.152	-.153	-.117	-.093	-.099	-.120	-.132	
D	-1.766	-1.540	-1.393	-1.441	-1.625	-1.726	-1.756	-1.630	-1.383	-1.142	-.900	-.747	
ALP	1.139	1.159	1.165	1.193	1.236	1.241	1.183	1.121	1.267	1.653	2.359	3.176	
BET	1.006	.988	.988	.990	.983	.981	.998	1.004	.918	.751	.482	.201	
N	10	10	10	10	10	10	10	10	9	6	3	2	
8 3 0 8	PSV .05 DAMPING MMI-DEPTH MODEL												
12PER	.040	.065	.11	.19	.34	.50	.90	1.60	2.80	4.40	7.50	14.00	
A	.213	.215	.238	.283	.328	.344	.347	.333	.305	.271	.223	.168	
B	-.024	-.025	-.019	.000	.031	.050	.071	.083	.088	.086	.072	.041	
C	-.101	-.080	-.064	-.077	-.126	-.155	-.163	-.134	-.112	-.116	-.135	-.148	
D	-1.824	-1.607	-1.466	-1.513	-1.694	-1.798	-1.845	-1.746	-1.521	-1.286	-1.040	-.876	
ALP	1.176	1.194	1.186	1.202	1.249	1.264	1.217	1.152	1.295	1.688	2.413	3.249	
BET	1.005	.988	.989	.990	.982	.981	.999	1.005	.918	.750	.480	.199	
N	10	10	10	10	10	10	10	10	9	6	3	2	
8 4 0 8	PSV .10 DAMPING MMI-DEPTH MODEL												
12PER	.040	.065	.11	.19	.34	.50	.90	1.60	2.80	4.40	7.50	14.00	
A	.219	.219	.239	.281	.324	.340	.345	.333	.308	.278	.235	.185	
B	-.025	-.023	-.017	-.001	.027	.046	.069	.082	.086	.083	.070	.043	
C	-.102	-.087	-.075	-.086	-.129	-.157	-.165	-.137	-.114	-.117	-.139	-.158	
D	-1.882	-1.682	-1.551	-1.597	-1.769	-1.869	-1.921	-1.838	-1.634	-1.417	-1.190	-1.039	
ALP	1.211	1.231	1.215	1.216	1.256	1.276	1.244	1.195	1.341	1.725	2.425	3.231	
BET	1.004	.988	.989	.991	.983	.982	1.000	1.006	.919	.749	.477	.192	
N	10	10	10	10	10	10	10	10	9	6	3	2	
8 5 0 8	PSV .20 DAMPING MMI-DEPTH MODEL												
12PER	.040	.065	.11	.19	.34	.50	.90	1.60	2.80	4.40	7.50	14.00	
A	.226	.228	.245	.280	.319	.335	.343	.331	.308	.282	.245	.199	
B	-.022	-.024	-.018	-.000	.027	.043	.062	.073	.079	.079	.068	.043	
C	-.102	-.093	-.086	-.096	-.132	-.157	-.168	-.143	-.117	-.117	-.140	-.161	
D	-1.960	-1.791	-1.675	-1.708	-1.862	-1.956	-2.004	-1.920	-1.735	-1.550	-1.355	-1.205	
ALP	1.251	1.277	1.259	1.250	1.277	1.290	1.254	1.220	1.394	1.787	2.458	3.190	
BET	1.004	.988	.990	.991	.983	.982	1.000	1.006	.918	.748	.473	.185	
N	10	10	10	10	10	10	10	10	9	6	3	2	

### 5.4.3 Listing of Input Part 3

\*\*\*\*\*

DIRECTORY :UDD:EQRISK:WORKING:PEQRISK

FSIN.DAT                   TXT 12-JUL-85   8:46:56   1638

\*\*\*\*\*

0	2	1	0	8					
5	0	2	511	SIERRA MADRE - CUCAMONGA FAULT ZONE					
			3.1482	0.86	2.75	7.5	3.8	24.0	2 2
			.25	0.1	1.				
			118.480	34.281	WEST END - 1971 BREAK				
			118.420	34.293	CENTER, 1971 BREAK				
			118.294	34.266	EAST END, 1971 BREAK				
			118.128	34.185	ALTADENA				
			118.000	34.158	RAYMOND FAULT				
			117.910	34.144	AZUSA				
			117.844	34.152	GLENDDORA				
			117.735	34.118	CLAREMONT				
			117.645	34.163	ALTA LOMA				
			117.488	34.165	RIALTO-COLTON FAULT				
			117.425	34.196	SAN JACINTO FAULT - EAST END				
5	0	2	517	SAN ANDREAS FAULT - CAJON PASS TO SAN LUIS OBISPO					
			4.4660	0.86	2.75	8.5	7.9	25.0	2 2
			.25	0.1	1.				
			117.482	34.277	CAJON JCT.				
			117.627	34.345	WRIGHTWOOD				
			117.844	34.438	VALLERMO				
			118.285	34.612	LEONA VALLEY				
			118.713	34.759	SANDBERG				
			118.946	34.818	FRAZIER PARK				
			119.008	34.816	BIG PINE FLT. JCT				
			119.251	34.871	BIG BEND				
			119.364	34.911	BIG BEND				
			119.443	34.963	RT. 166 & 33				
			119.675	35.136	SOUTH CARRIZO PLAIN				
			119.885	35.329	HWY. 58				
			120.296	35.718	CHOLAME				
			120.337	35.806					
			120.424	35.889	PARKFIELD				
			121.248	36.647	"ABOVE S"				
			121.533	36.843	SAN JUAN BAUTISTA - S.END, 1906				
4	0	2	0 2	TRANSVERSE RANGES					
			0.0	9.6	2.8	0.84	0.25	0.073	0.022 .0064
			0.0	0.0	0.0	0.0	2 2		
			.25	0.1	1.				
			33.0	121.0	117.5				
			35.5	121.0	117.5				



### 5.5 Listing of Printer Output

The following is a sample of a listing of the output data file from running "NEQRISK": RISK.OUTPUT.DAT. The data file consists of 5 parts:

(1) Listing of input site and model parameters, spectral data and seismicity information, as read in respectively from input data files "SITES.DAT," "SPEC.DAT" and "FSIN.DAT," which were listed in the previous Section 5.4.

(2) Listing of the output data,  $N_E[S(\omega)]$ , the expected number of exceedances on logarithmic scale, as a function of periods and spectral amplitudes. The discrete periods range from .04 sec. to about 2 sec., while the spectral amplitudes, in the form of  $\log_{10}[S(\omega)]$ , range from -5.00 to +5.00 in steps of .2.

(3) Listing of the output data,  $P[S(\omega)]$ , the probability of exceeding  $S(\omega)$  at the site, again as a function of periods and spectral amplitudes in the same range.

(4) Listing of the output data  $dP[S(\omega)/S(\omega)]$ , the probability density function in the same range of periods and spectram amplitudes.

(5) Listing of the output uniform risk spectrum, which gives the  $\log_{10}[S(\omega)]$  amplitudes in the same period range for a discrete set of probability levels.

Alternatively, the user can choose to have NEQRISK output only the the expected M.M.I. values, to be exceeded at specified probability levels. In such a case, only part (1) followed by a listing of such M.M.I. values will be the output data.

\*\*\*\*\*

DIRECTORY :UDD:EGRISK:WORKING:PEORISK

RISK\_OUTPUT.DAT      TXT    12-JUL-85    16:30:06    48593

\*\*\*\*\*

\*\*\*\*\*  
 THE FREQUENCY DEPENDENT SEISMIC RISK  
 \*\*\*\*\*

THIS PROGRAM WAS ORIGINALLY DEVELOPED BY J. G. ANDERSON & M. D. TRIFUNAC,  
 SUBSEQUENTLY IT WAS UPDATED BY V. W. LEE & M. D. TRIFUNAC,  
 AND CURRENTLY RUNNING ON AOS ECLIPSE S-130

CONTROL PARAMETERS

MTY	MRS	MAL	ILTL	IPPL	IMRAC	MRL	IPPC	LSSUP	IDL1	IDL2	IDL3	ISTP
6	3	1	0	11	0	6	0	0	1	11	1	0

SEE PROGRAM LISTING FOR EXPLANATION

YRS =      1.000

INPUT SEISMICITY RATES ARE MULTIPLIED BY YRS FOR RISK CALCULATIONS

12PER	.040	.065	.110	.190	.340	.500	.900	1.600	2.800	4.400	7.500	14.000
0A0R-2.	1.74	-1.830	-1.510	-1.236	-1.010	-.896	-.781	-.734	-.732	-.732	-.732	-.732
0SZM29.	27029.	39029.	51029.	65029.	78029.	87030.	01030.	14030.	28030.	38030.	51030.	660
12PER	.040	.065	.110	.190	.340	.500	.900	1.600	2.800	4.400	7.500	14.000
0 A	-.040	-.003	.131	.344	.517	.571	.628	.728	.807	.764	.538	.092
0 B	.042	.037	.032	.034	.044	.052	.065	.078	.090	.091	.080	.053
0 C	-.101	-.072	-.054	-.062	-.103	-.140	-.168	-.143	-.114	-.117	-.131	-.113
0 D	-1.697	-1.672	-2.060	-2.889	-3.750	-4.154	-4.638	-5.099	-5.296	-5.026	-4.167	-2.723
0 E	-.038	-.049	-.065	-.082	-.092	-.094	-.094	-.101	-.109	-.110	-.097	-.068
0ALP	1.320	1.360	1.324	1.273	1.282	1.315	1.321	1.263	1.358	1.731	2.520	3.526
0BET	1.028	1.008	1.008	1.010	1.003	1.000	1.014	1.018	.934	.767	.494	.200
0 N	10	10	10	10	10	10	10	10	9	6	3	2

THE RISK IS FOUND FOR THE SITE

L. A. VICINITY 01

SITE NO. 1001

117.90000 DEG WEST LONGITUDE

34.10001 DEG NORTH LATITUDE

IV =      0

HIS =      2.300

RISK FOUND FOR    17    PROBABILITIES OF EXCEEDANCE --

.90000	.50000	.35000	.20000	.10000
.05000	.03500	.02000	.01000	.00500
.00350	.00200	.00100	.00050	.00035
.00020	.00010			

1    THE FOLLOWING SOURCES TREATED AS POISSON

MODEL OF SEISMICITY NO. (MOSN)...    8

THE SEISMICITY IS REGARDED AS A SUPERPOSITION OF

- 0 POINT SOURCES
- 2 LINE SOURCES (FAULTS)
- 1 REGIONS OF DIFFUSE SEISMICITY
- 0 DIPPING PLANES
- 0 DIPPING VOLUMES

LINE SOURCE    SIERRA MADRE - CUCAMONGA FAULT ZONE  
 SEISMICITY INPUT BY MOMENT RATE (PER YEAR), B, MMAX

A, B, M-MIN, M-MAX, MOMENT/YR

314820 01 .860000 00 2.750 7.500 .380000 25

SCALED UP BY 1 YEARS.

LPTYPE, MPTYPE, DAAL, DBBL, DMXM 2 2 .25 .10 1.00

LOCATIONS OF ENDS ARE

118.48000 WEST LONGITUDE 34.28101 NORTH LATITUDE

117.42500 WEST LONGITUDE 34.19600 NORTH LATITUDE

FAULT IS REPRESENTED BY 11 - 1 STRAIGHT LINE SEGMENTS

ISI= 3

SEISMICITY # OF ASSUMED

MAG EARTHQUAKES FAULT LENGTH

3.0 2.1980240 .1259

3.5 .8370583 .2512

4.0 .3194134 .5012

4.5 .1221269 1.0000

5.0 .0467860 1.9953

5.5 .0179578 3.9811

6.0 .0069057 7.9432

6.5 .0026605 15.8489

7.0 .0008985 31.6226

7.5 .0001985 63.0954

8.0 .0000192 105.0000

8.5 .0000000 105.0000

THE FAULT IS REPRESENTED BY 22 POINTS AT SPACING OF 5.00 KILOMETER

THIS GIVES A LENGTH OF 105.00 KILOMETER

INSERTED IN DISTANCE AND SEISMICITY ARRAYS IN POSITIONS 1 TO 22

LINE SOURCE SAN ANDREAS FAULT - CAJON PASS TO SAN LUIS OBISPO

SEISMICITY INPUT BY MOMENT RATE (PER YEAR), B, MMAX

A, B, M-MIN, M-MAX, MOMENT/YR

446600 01 .860000 00 2.750 8.500 .790000 26

SCALED UP BY 1 YEARS.

LPTYPE, MPTYPE, DAAL, DBBL, DMXM 2 2 .25 .10 1.00

LOCATIONS OF ENDS ARE

117.48200 WEST LONGITUDE 34.27699 NORTH LATITUDE

121.53300 WEST LONGITUDE 36.84300 NORTH LATITUDE

FAULT IS REPRESENTED BY 17 - 1 STRAIGHT LINE SEGMENTS

ISI= 3

SEISMICITY # OF ASSUMED

MAG EARTHQUAKES FAULT LENGTH

3.0 45.6957600 .1259

3.5 17.4019900 .2512

4.0 6.6404380 .5012

4.5 2.5389540 1.0000

5.0 .9726570 1.9953

5.5 .3733327 3.9811

6.0 .1435649 7.9432

6.5 .0553097 15.8489

7.0 .0213471 31.6226

7.5 .0082536 63.0954

8.0 .0027971 125.8919

8.5 .0006201 251.1867

THE FAULT IS REPRESENTED BY 96 POINTS AT SPACING OF 5.00 KILOMETER

THIS GIVES A LENGTH OF 475.00 KILOMETER

INSERTED IN DISTANCE AND SEISMICITY ARRAYS IN POSITIONS 1 TO 96

DIFFUSE SEISMICITY REGION TRANSVERSE RANGES

N(M) READ DIRECTLY

SEISMICITY # OF

```

MAG    EARTHQUAKES
3.0    .0000000
3.5    11.2274700
4.0    3.3633060
4.5    1.0383550
5.0    .3186481
5.5    .0961237
6.0    .0299835
6.5    .0090447
7.0    .0000000
7.5    .0000000
8.0    .0000000
8.5    .0000000

EVENTS ARE ASSUMED TO BE UNILATERAL RUPTURES
INPUT GIVES LONGITUDE OF EAST AND WEST BOUNDARY AT 2 LATITUDES
INITIALLY 4 RECTANGLES
REGION HAS AREA      89388.1
BEGINNING AREA-DISTANCE CHECKS
AREA, CORNER DISTANCE, CENTER DISTANCE
10000.000      220.000      339.052
NOW 16 RECTANGLES
REGION HAS AREA      89388.1
AREA, CORNER DISTANCE, CENTER DISTANCE
1140.000      75.000      154.057
NOW 80 RECTANGLES
REGION HAS AREA      89388.1
AREA, CORNER DISTANCE, CENTER DISTANCE
130.000      25.000      51.693
NOW 184 RECTANGLES
REGION HAS AREA      89388.1
AREA, CORNER DISTANCE, CENTER DISTANCE
15.000      9.000      18.014
NOW 304 RECTANGLES
REGION HAS AREA      89388.1
INSERTED INTO RA, SA ARRAYS IN ELEMENTS      1 TO 304

ML, MX      1      12
MAGNITUDE-RUPTURE LENGTH NO. . .      6
3.0    .1259
3.5    .2512
4.0    .5012
4.5    1.0000
5.0    1.9953
5.5    3.9811
6.0    7.9432
6.5    15.8489
7.0    31.6226
7.5    63.0954
8.0    125.8919
8.5    251.1867
DATA COMPRESSED TO 144 DISTANCES FOR INTEGRATION

```

LOG10(EXPECTED NUMBER OF EXCEEDANCES) --- IV = 0 HIS = 2.300

LOG(SL)	PERIOD							
	.04000	.06500	.11000	.19000	.34000	.50000	.90000	1.60000
-5.00	1.93383	1.97000	1.97075	1.97076	1.97076	1.97076	1.97076	1.97076
-4.80	1.91010	1.96794	1.97070	1.97075	1.97076	1.97076	1.97075	1.97073
-4.60	1.88051	1.96260	1.97045	1.97068	1.97071	1.97072	1.97070	1.97059
-4.40	1.84516	1.95188	1.96945	1.97037	1.97051	1.97052	1.97046	1.97004
-4.20	1.80329	1.93456	1.96648	1.96926	1.96971	1.96973	1.96950	1.96829
-4.00	1.75383	1.91066	1.95960	1.96615	1.96733	1.96730	1.96666	1.96389
-3.80	1.69631	1.88077	1.94702	1.95930	1.96171	1.96152	1.96015	1.95514
-3.60	1.63126	1.84493	1.92795	1.94714	1.95122	1.95074	1.94838	1.94089
-3.40	1.55978	1.80206	1.90264	1.92903	1.93504	1.93423	1.93078	1.92098
-3.20	1.48252	1.75044	1.87151	1.90514	1.91325	1.91220	1.90768	1.89580
-3.00	1.39791	1.68890	1.83421	1.87577	1.88623	1.88508	1.87951	1.86554
-2.80	1.30097	1.61729	1.78923	1.84059	1.85393	1.85278	1.84607	1.82950
-2.60	1.18486	1.53587	1.73447	1.79817	1.81523	1.81412	1.80591	1.78571
-2.40	1.04609	1.44360	1.66811	1.74615	1.76786	1.76666	1.75632	1.73107
-2.20	.88875	1.33615	1.58859	1.68181	1.70868	1.70696	1.69360	1.66149
-2.00	.72223	1.20698	1.49356	1.60202	1.63387	1.63078	1.61309	1.57232
-1.80	.55500	1.05285	1.37880	1.50293	1.53916	1.53352	1.51001	1.46006
-1.60	.39093	.87830	1.23971	1.38086	1.42139	1.41255	1.38236	1.32483
-1.40	.22922	.69268	1.07560	1.23497	1.28089	1.26937	1.23261	1.17018
-1.20	.06581	.50350	.89121	1.06816	1.12089	1.10760	1.06509	1.00043
-1.00	-.10617	.31301	.69284	.88395	.94387	.92922	.88316	.81908
-.80	-.29710	.11830	.48390	.68338	.75031	.73499	.68925	.62830
-.60	-.51968	-.08798	.26351	.46564	.54046	.52607	.48467	.42849
-.40	-.78377	-.31722	.02711	.22945	.31485	.30326	.26936	.21896
-.20	-1.09142	-.58188	-.23235	-.02678	.07313	.06597	.04234	-.00153
-.00	-1.43522	-.89028	-.52218	-.30579	-.18668	-.18771	-.19794	-.23471
.20	-1.80106	-1.24381	-.84828	-.61183	-.46768	-.46038	-.45360	-.48281
.40	-2.17800	-1.63717	-1.21497	-.95016	-.77368	-.75555	-.72756	-.74881
.60	-2.57238	-2.06316	-1.62533	-1.32626	-1.10938	-1.07794	-1.02377	-1.03668
.80	-3.01145	-2.52411	-2.08316	-1.74542	-1.48078	-1.43415	-1.34780	-1.35199
1.00	-3.53084	-3.04149	-2.59708	-2.21301	-1.89558	-1.83318	-1.70767	-1.70265
1.20	-4.16350	-3.65104	-3.18425	-2.73633	-2.36311	-2.28662	-2.11475	-2.09963
1.40	-4.93866	-4.39232	-3.87006	-3.32786	-2.89470	-2.80833	-2.58398	-2.55694
1.60	-5.88234	-5.30592	-4.68569	-4.00812	-3.50477	-3.41425	-3.13294	-3.09091
1.80	-7.01540	-6.43307	-5.66700	-4.80757	-4.21279	-4.12322	-3.78114	-3.71961
2.00	-8.36159	-7.81581	-6.85652	-5.76756	-5.04622	-4.95951	-4.55034	-4.46329
2.20	-10.00000	-9.51042	-8.31011	-6.94019	-6.04479	-5.95784	-5.46651	-5.34574
2.40	-10.00000	-10.00000	-10.00000	-8.38869	-7.26378	-7.17018	-6.56423	-6.39682
2.60	-10.00000	-10.00000	-10.00000	-10.00000	-8.77574	-8.67077	-7.99578	-7.65851
2.80	-10.00000	-10.00000	-10.00000	-10.00000	-10.00000	-10.00000	-9.54095	-9.19443
3.00	-10.00000	-10.00000	-10.00000	-10.00000	-10.00000	-10.00000	-10.00000	-10.00000
3.20	-10.00000	-10.00000	-10.00000	-10.00000	-10.00000	-10.00000	-10.00000	-10.00000
3.40	-10.00000	-10.00000	-10.00000	-10.00000	-10.00000	-10.00000	-10.00000	-10.00000
3.60	-10.00000	-10.00000	-10.00000	-10.00000	-10.00000	-10.00000	-10.00000	-10.00000
3.80	-10.00000	-10.00000	-10.00000	-10.00000	-10.00000	-10.00000	-10.00000	-10.00000
4.00	-10.00000	-10.00000	-10.00000	-10.00000	-10.00000	-10.00000	-10.00000	-10.00000
4.20	-10.00000	-10.00000	-10.00000	-10.00000	-10.00000	-10.00000	-10.00000	-10.00000
4.40	-10.00000	-10.00000	-10.00000	-10.00000	-10.00000	-10.00000	-10.00000	-10.00000
4.60	-10.00000	-10.00000	-10.00000	-10.00000	-10.00000	-10.00000	-10.00000	-10.00000
4.80	-10.00000	-10.00000	-10.00000	-10.00000	-10.00000	-10.00000	-10.00000	-10.00000
5.00	-10.00000	-10.00000	-10.00000	-10.00000	-10.00000	-10.00000	-10.00000	-10.00000

LOG(SL)	POISSON PROBABILITY OF EXCEEDANCE --- IV= 0 HIS= 2.300							
	PERIOD							
	.04000	.06500	.11000	.19000	.34000	.50000	.90000	1.60000
-5.00	1.00000	1.00000	1.00000	1.00000	1.00000	1.00000	1.00000	1.00000
-4.80	1.00000	1.00000	1.00000	1.00000	1.00000	1.00000	1.00000	1.00000
-4.60	1.00000	1.00000	1.00000	1.00000	1.00000	1.00000	1.00000	1.00000
-4.40	1.00000	1.00000	1.00000	1.00000	1.00000	1.00000	1.00000	1.00000
-4.20	1.00000	1.00000	1.00000	1.00000	1.00000	1.00000	1.00000	1.00000
-4.00	1.00000	1.00000	1.00000	1.00000	1.00000	1.00000	1.00000	1.00000
-3.80	1.00000	1.00000	1.00000	1.00000	1.00000	1.00000	1.00000	1.00000
-3.60	1.00000	1.00000	1.00000	1.00000	1.00000	1.00000	1.00000	1.00000
-3.40	1.00000	1.00000	1.00000	1.00000	1.00000	1.00000	1.00000	1.00000
-3.20	1.00000	1.00000	1.00000	1.00000	1.00000	1.00000	1.00000	1.00000
-3.00	1.00000	1.00000	1.00000	1.00000	1.00000	1.00000	1.00000	1.00000
-2.80	1.00000	1.00000	1.00000	1.00000	1.00000	1.00000	1.00000	1.00000
-2.60	1.00000	1.00000	1.00000	1.00000	1.00000	1.00000	1.00000	1.00000
-2.40	.99999	1.00000	1.00000	1.00000	1.00000	1.00000	1.00000	1.00000
-2.20	.99957	1.00000	1.00000	1.00000	1.00000	1.00000	1.00000	1.00000
-2.00	.99488	1.00000	1.00000	1.00000	1.00000	1.00000	1.00000	1.00000
-1.80	.97238	.99999	1.00000	1.00000	1.00000	1.00000	1.00000	1.00000
-1.60	.91456	.99948	1.00000	1.00000	1.00000	1.00000	1.00000	1.00000
-1.40	.81644	.99276	.99999	1.00000	1.00000	1.00000	1.00000	1.00000
-1.20	.68765	.95874	.99958	.99999	1.00000	1.00000	1.00000	1.00000
-1.00	.54302	.87203	.99277	.99953	.99985	.99980	.99999	.99996
-.80	.39622	.73101	.95251	.99196	.99640	.99563	.99247	.98572
-.60	.26082	.55808	.84030	.94616	.96892	.96519	.95276	.93159
-.40	.15170	.38227	.65507	.81660	.87314	.86605	.84422	.80903
-.20	.07782	.23040	.44327	.60945	.69376	.68777	.66793	.63082
-.00	.03604	.12080	.25954	.39016	.47827	.47747	.46951	.44149
.20	.01569	.05545	.13222	.21685	.28870	.29279	.29663	.28036
.40	.00662	.02279	.05914	.10610	.15498	.16102	.17077	.16332
.60	.00267	.00861	.02342	.04608	.07479	.08017	.09033	.08780
.80	.00097	.00299	.00822	.01781	.03251	.03613	.04390	.04349
1.00	.00029	.00091	.00253	.00610	.01264	.01458	.01941	.01963
1.20	.00007	.00022	.00065	.00183	.00433	.00516	.00765	.00792
1.40	.00001	.00004	.00013	.00047	.00127	.00155	.00260	.00277
1.60	.00000	.00000	.00002	.00010	.00031	.00039	.00074	.00081
1.80	.00000	.00000	.00000	.00002	.00006	.00008	.00017	.00019
2.00	.00000	.00000	.00000	.00000	.00001	.00001	.00003	.00003
2.20	.00000	.00000	.00000	.00000	.00000	.00000	.00000	.00000
2.40	.00000	.00000	.00000	.00000	.00000	.00000	.00000	.00000
2.60	.00000	.00000	.00000	.00000	.00000	.00000	.00000	.00000
2.80	.00000	.00000	.00000	.00000	.00000	.00000	.00000	.00000
3.00	.00000	.00000	.00000	.00000	.00000	.00000	.00000	.00000
3.20	.00000	.00000	.00000	.00000	.00000	.00000	.00000	.00000
3.40	.00000	.00000	.00000	.00000	.00000	.00000	.00000	.00000
3.60	.00000	.00000	.00000	.00000	.00000	.00000	.00000	.00000
3.80	.00000	.00000	.00000	.00000	.00000	.00000	.00000	.00000
4.00	.00000	.00000	.00000	.00000	.00000	.00000	.00000	.00000
4.20	.00000	.00000	.00000	.00000	.00000	.00000	.00000	.00000
4.40	.00000	.00000	.00000	.00000	.00000	.00000	.00000	.00000
4.60	.00000	.00000	.00000	.00000	.00000	.00000	.00000	.00000
4.80	.00000	.00000	.00000	.00000	.00000	.00000	.00000	.00000
5.00	.00000	.00000	.00000	.00000	.00000	.00000	.00000	.00000

ABOVE DATA ARE THEN INTERPOLATED AND SMOOTHED.

FOLLOWING SPECTRA ASSUME EARTHQUAKES ARE POISSON, WITH MEAN AS INPUT  
 ROBABILITY DENSITY FUNCTION  
 LOG(SL)

	PERIOD							
	.04000	.06500	.11000	.19000	.34000	.50000	.90000	1.60000
-5.00	.00000	.00000	.00000	.00000	.00000	.00000	.00000	.00000
-4.80	.00000	.00000	.00000	.00000	.00000	.00000	.00000	.00000
-4.60	.00000	.00000	.00000	.00000	.00000	.00000	.00000	.00000
-4.40	.00000	.00000	.00000	.00000	.00000	.00000	.00000	.00000
-4.20	.00000	.00000	.00000	.00000	.00000	.00000	.00000	.00000
-4.00	.00000	.00000	.00000	.00000	.00000	.00000	.00000	.00000
-3.80	.00000	.00000	.00000	.00000	.00000	.00000	.00000	.00000
-3.60	.00000	.00000	.00000	.00000	.00000	.00000	.00000	.00000
-3.40	.00000	.00000	.00000	.00000	.00000	.00000	.00000	.00000
-3.20	.00000	.00000	.00000	.00000	.00000	.00000	.00000	.00000
-3.00	.00000	.00000	.00000	.00000	.00000	.00000	.00000	.00000
-2.80	.00001	.00000	.00000	.00000	.00000	.00000	.00000	.00000
-2.60	.00008	.00000	.00000	.00000	.00000	.00000	.00000	.00000
-2.40	.00186	.00000	.00000	.00000	.00000	.00000	.00000	.00000
-2.20	.01888	.00001	.00000	.00000	.00000	.00000	.00000	.00000
-2.00	.09255	.00009	.00000	.00000	.00000	.00000	.00000	.00000
-1.80	.25660	.00233	.00000	.00000	.00000	.00000	.00000	.00000
-1.60	.47311	.02702	.00007	.00000	.00000	.00000	.00000	.00000
-1.40	.66191	.13908	.00198	.00008	.00003	.00003	.00007	.00001
-1.20	.77573	.38505	.02761	.00223	.00080	.00103	.00222	.00026
-1.00	.81069	.68668	.16285	.03078	.01443	.01727	.02851	.00571
-.80	.77070	.90587	.49044	.18500	.11003	.12206	.16117	.22500
-.60	.65141	.97233	.89816	.56423	.40530	.42330	.47579	.55535
-.40	.47119	.88555	1.13369	1.01209	.84447	.84710	.85816	.89192
-.20	.28610	.68233	1.07401	1.20373	1.13796	1.11633	1.06750	1.03598
.00	.14786	.43834	.80625	1.04800	1.10421	1.07584	1.00856	.94666
.20	.06810	.23518	.49734	.72298	.84088	.82454	.78075	.72598
.40	.02979	.10810	.25928	.41738	.53528	.53452	.52294	.48888
.60	.01291	.04443	.11690	.20816	.29672	.30485	.31370	.29738
.80	.00538	.01695	.04634	.09111	.14628	.15590	.17154	.16569
1.00	.00196	.00594	.01621	.03519	.06440	.07158	.08572	.08458
1.20	.00057	.00177	.00491	.01197	.02510	.02910	.03868	.03905
1.40	.00012	.00041	.00122	.00354	.00851	.01021	.01534	.01588
1.60	.00002	.00007	.00023	.00088	.00244	.00300	.00514	.00549
1.80	.00000	.00001	.00003	.00018	.00058	.00071	.00140	.00155
2.00	.00000	.00000	.00001	.00002	.00011	.00013	.00030	.00034
2.20	.00000	.00000	.00000	.00000	.00001	.00002	.00004	.00006
2.40	.00000	.00000	.00000	.00000	.00000	.00000	.00000	.00001
2.60	.00000	.00000	.00000	.00000	.00000	.00000	.00000	.00000
2.80	.00000	.00000	.00000	.00000	.00000	.00000	.00000	.00000
3.00	.00000	.00000	.00000	.00000	.00000	.00000	.00000	.00000
3.20	.00000	.00000	.00000	.00000	.00000	.00000	.00000	.00000
3.40	.00000	.00000	.00000	.00000	.00000	.00000	.00000	.00000
3.60	.00000	.00000	.00000	.00000	.00000	.00000	.00000	.00000
3.80	.00000	.00000	.00000	.00000	.00000	.00000	.00000	.00000
4.00	.00000	.00000	.00000	.00000	.00000	.00000	.00000	.00000
4.20	.00000	.00000	.00000	.00000	.00000	.00000	.00000	.00000
4.40	.00000	.00000	.00000	.00000	.00000	.00000	.00000	.00000
4.60	.00000	.00000	.00000	.00000	.00000	.00000	.00000	.00000
4.80	.00000	.00000	.00000	.00000	.00000	.00000	.00000	.00000
5.00	.00000	.00000	.00000	.00000	.00000	.00000	.00000	.00000

MOSN=		8		SITE #= 1001		SPECTRUM # 1 TO		17		
PROBABILITY OF EXCEEDENCE		PERIOD								
	.04000	.06500	.11000	.19000	.34000	.50000	.90000	1.60000		
.90000	-1.5863	-1.0764	-.7166	-.5403	-.4698	-.4804	-.5129	-.5624		
.50000	-.9525	-.5450	-.2632	-.1110	-.0285	-.0298	-.0396	-.0720		
.35000	-.7427	-.3674	-.1099	.0369	.1249	.1278	.1279	.1021		
.20000	-.5000	-.1543	.0815	.2244	.3214	.3302	.3441	.3264		
.10000	-.2707	.0535	.2758	.4181	.5256	.5411	.5705	.5604		
.05000	-.0789	.2292	.4436	.5866	.7040	.7251	.7683	.7643		
.03500	.0121	.3119	.5225	.6667	.7884	.8122	.8618	.8604		
.02000	.1483	.4351	.6396	.7844	.9125	.9392	.9980	1.0001		
.01000	.3116	.5785	.7736	.9199	1.0543	1.0837	1.1517	1.1572		
.00500	.4701	.7143	.8984	1.0458	1.1843	1.2152	1.2910	1.2993		
.00350	.5489	.7810	.9588	1.1071	1.2476	1.2786	1.3573	1.3669		
.00200	.6679	.8816	1.0499	1.1992	1.3414	1.3723	1.4556	1.4670		
.00100	.8039	.9974	1.1550	1.3069	1.4507	1.4808	1.5673	1.5806		
.00050	.9270	1.1043	1.2533	1.4077	1.5521	1.5808	1.6705	1.6855		
.00035	.9854	1.1555	1.3012	1.4573	1.6018	1.6298	1.7203	1.7360		
.00020	1.0714	1.2317	1.3725	1.5317	1.6768	1.7032	1.7946	1.8115		
.00010	1.1685	1.3194	1.4563	1.6186	1.7642	1.7884	1.8816	1.8995		



## 6. CASE STUDIES AND AN APPLICATION

### 6.1 Introduction: Models I, II, III and IV

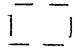
To study the selected properties of the proposed uniform risk spectra, the spectral amplitudes at six sites were calculated. Fig. 6.1.1 is a map showing the coordinates of the six sites and the two faults. The seismic sources consist of two line faults and of a diffused region. The first line fault is the Sierra Madre-Cucamonga fault of about 100 km in length. The second line fault is a portion of the San Andreas fault from Cajon Pass to the vicinity of San Luis Obispo. The diffused region is a rectangular region running from  $117^{\circ} 30' W$  to  $121^{\circ} W$  and from  $33^{\circ} N$  to  $35^{\circ} 30' N$ . For a detailed description of the seismicity of the faults and of the diffused region, the reader is referred to the data file "SEISMIC.INPUT" presented in Section 5.4. The six sites lie in a North-South direction through the center of the Sierra Madre-Cucamonga fault at distances of roughly 10, 25, 50, 100, 150 and 200 km south of the fault. Table 6.1.1 gives the coordinates of the locations of the six sites.

Four models of seismic risk have been studied. Model I is the original model of seismic risk (Anderson and Trifunac, 1977). It uses the original scaling functions for scaling Fourier and pseudo relative velocity spectra as was done in the original program "EQRISK." The original (old) scaling functions use the Richter's attenuation function. Model II uses the same (old) scaling functions but includes in the calculation the uncertainties in the estimation of seismicity and of maximum allowed earthquake sizes. Model III uses the new frequency dependent attenuation functions which replace the old Richter's attenuation functions in the scaling of Fourier and response spectral amplitudes. Like Model I, Model III does not include uncertainties in estimation of seismicity in the calculations. Finally, Model IV uses new frequency attenuation functions and includes in the

\* L.A. VICINITY SITES # 1, 2, 3, 4, 5, 6

FAULT #1 SIERRA MADRE - CUCAMONGA FAULT ZONE

FAULT #2 SAN ANDREAS FAULT - CAJON PASS TO SAN LUIS OBISPO

DIFFUSE REGION: 

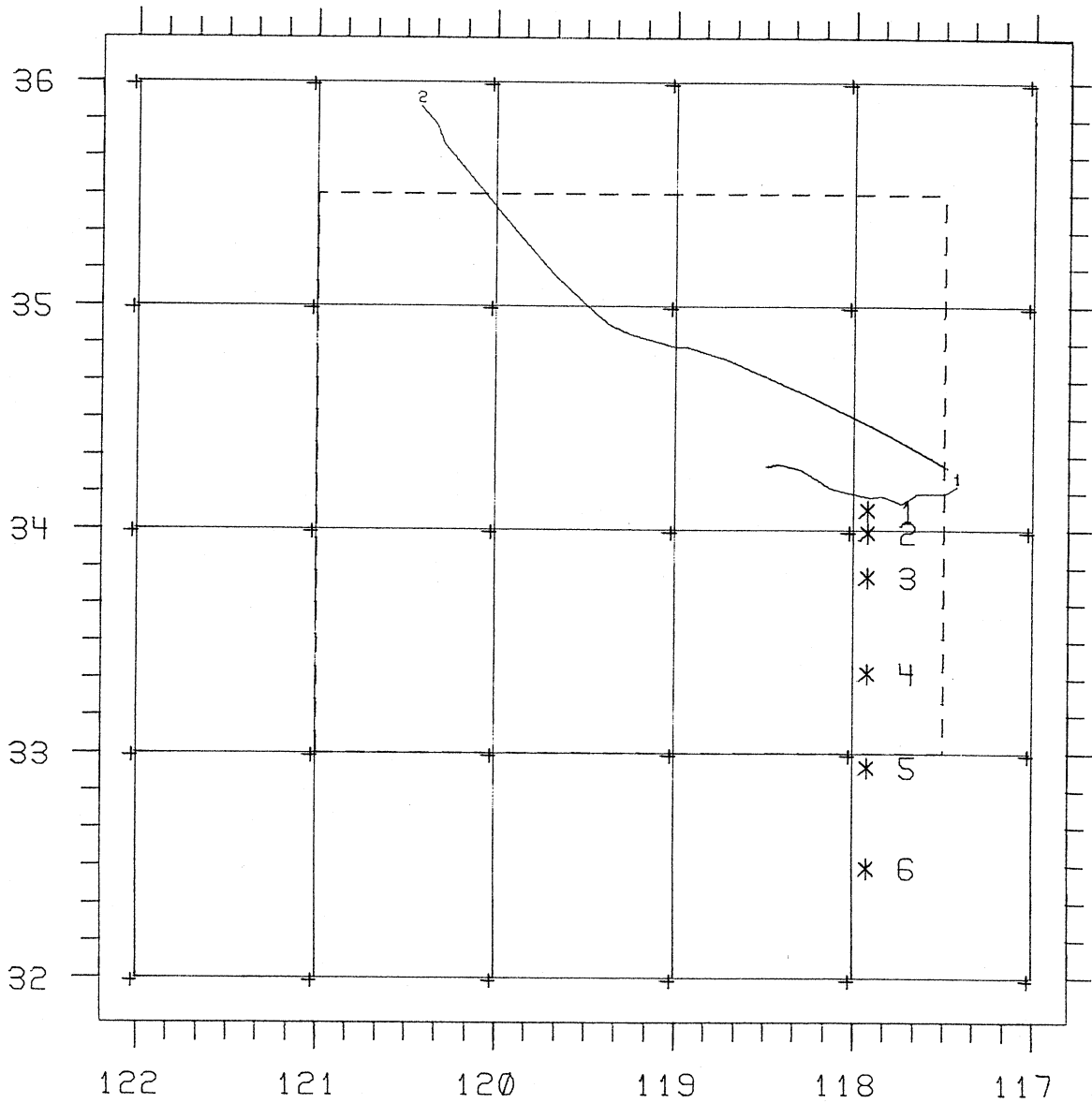


Figure 6.1.1

Table 6.1.1

SITE #	LATITUDE (N)	LONGITUDE (W)
1	34.1°	117.9°
2	34.0°	117.9°
3	33.8°	117.9°
4	33.367°	117.9°
5	32.95°	117.9°
6	32.50°	117.9°

Table 6.1.2

Model	Scaling Functions	Includes Uncertainties Seismicity
I	OLD	NO
II	OLD	YES
III	NEW	NO
IV	NEW	YES

calculations the uncertainties in the estimation of seismicity and of maximum allowed earthquake sizes. Table 6.1.2 is a summary of these characteristics of the four models.

## 6.2 Seismic Risk Spectra at 6 Sites

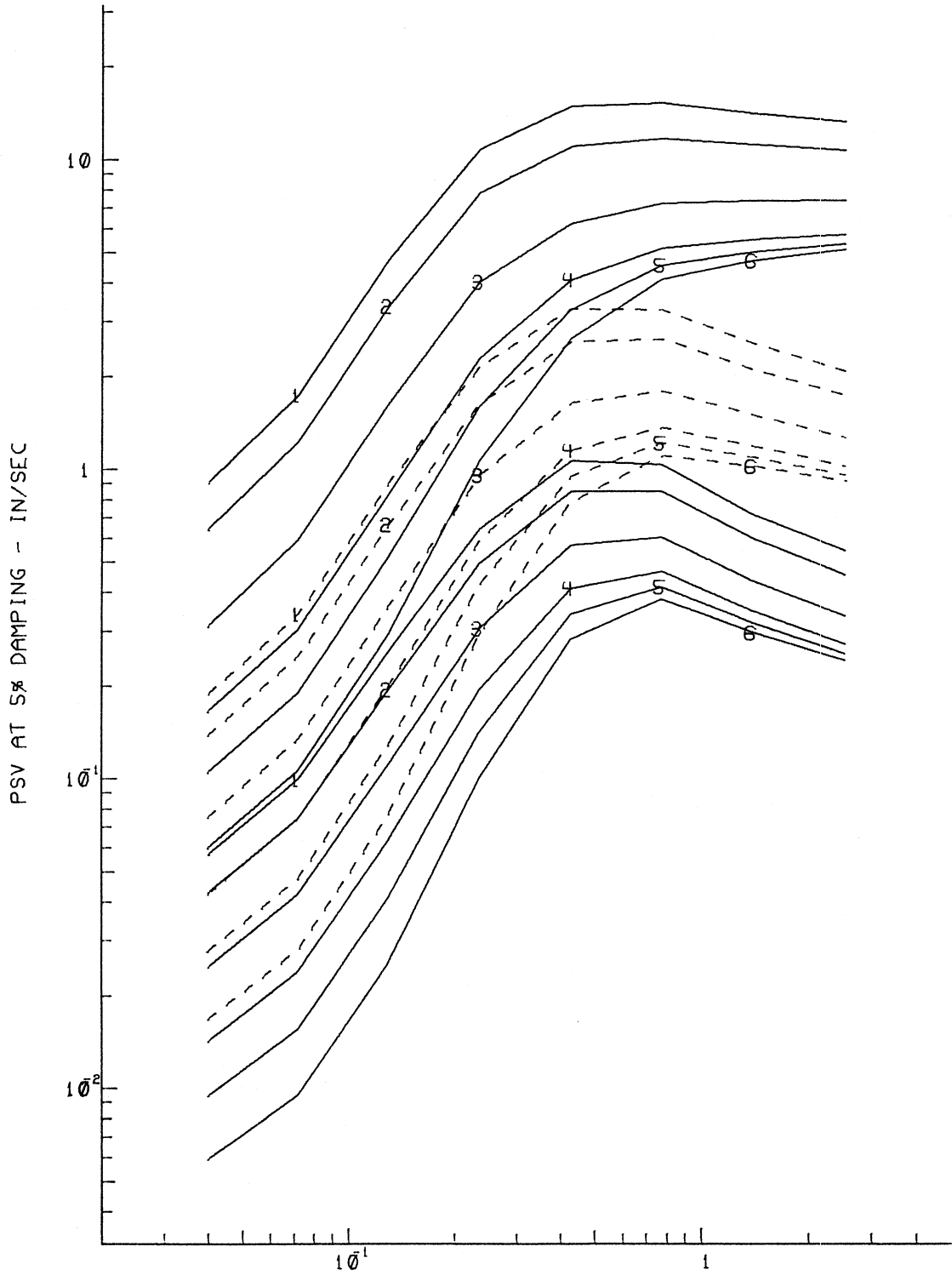
Figures 6.2.1 through Figure 6.2.4 show the seismic risk spectra of the four models at the six sites. Each figure gives the expected pseudo relative velocity amplitudes  $PSV(T)$ , at 8 periods  $T$  between .04 sec. and 2 sec., that will be exceeded at the 6 sites for the given probability levels of  $P = 0.1, 0.5$  and  $0.9$ . Each curve in the figure is associated with the corresponding site number (1 to 6) it represents. Thus the top six solid curves represent the  $PSV$  amplitudes that will be exceeded at the six sites with the probability level of  $P = 0.1$ . The next six dashed curves in the middle correspond to the corresponding amplitudes at  $P = 0.5$ . The bottom six solid curves correspond to  $P = 0.9$ .

Sites #1 through #6 are at 10, 25, 50, 100, 150 and 200 km from the nearest fault, the Sierra Madre-Cucamonga fault. All four models show that, at the same probability level, the expected  $PSV$  amplitudes are of decreasing amplitudes from site #1 down to site #6. The  $PSV$  amplitudes in all four figures are presented to periods of only up to 2 seconds, because for periods longer than 2 seconds, the  $PSV$  amplitudes may be distorted by noise, especially at low probability levels of exceedance.

## 6.3 Comparison of Different Models

It is interesting to compare the results of the different models at various sites. Figure 6.3.1 shows a comparison of the  $PSV$  spectra at site #1 for 5 probability levels  $P = 0.1, 0.2, 0.35, 0.5$  and  $0.9$ . The five dashed lines correspond to the  $PSV$  amplitudes (for  $p = 0.1$  to  $0.9$ )

PSV SEISMIC RISK SPECTRA AT 6 SITES  
 FOR P = 0.1, 0.5 & 0.9  
 MODEL I: ORIGINAL SCALING FUNCTIONS



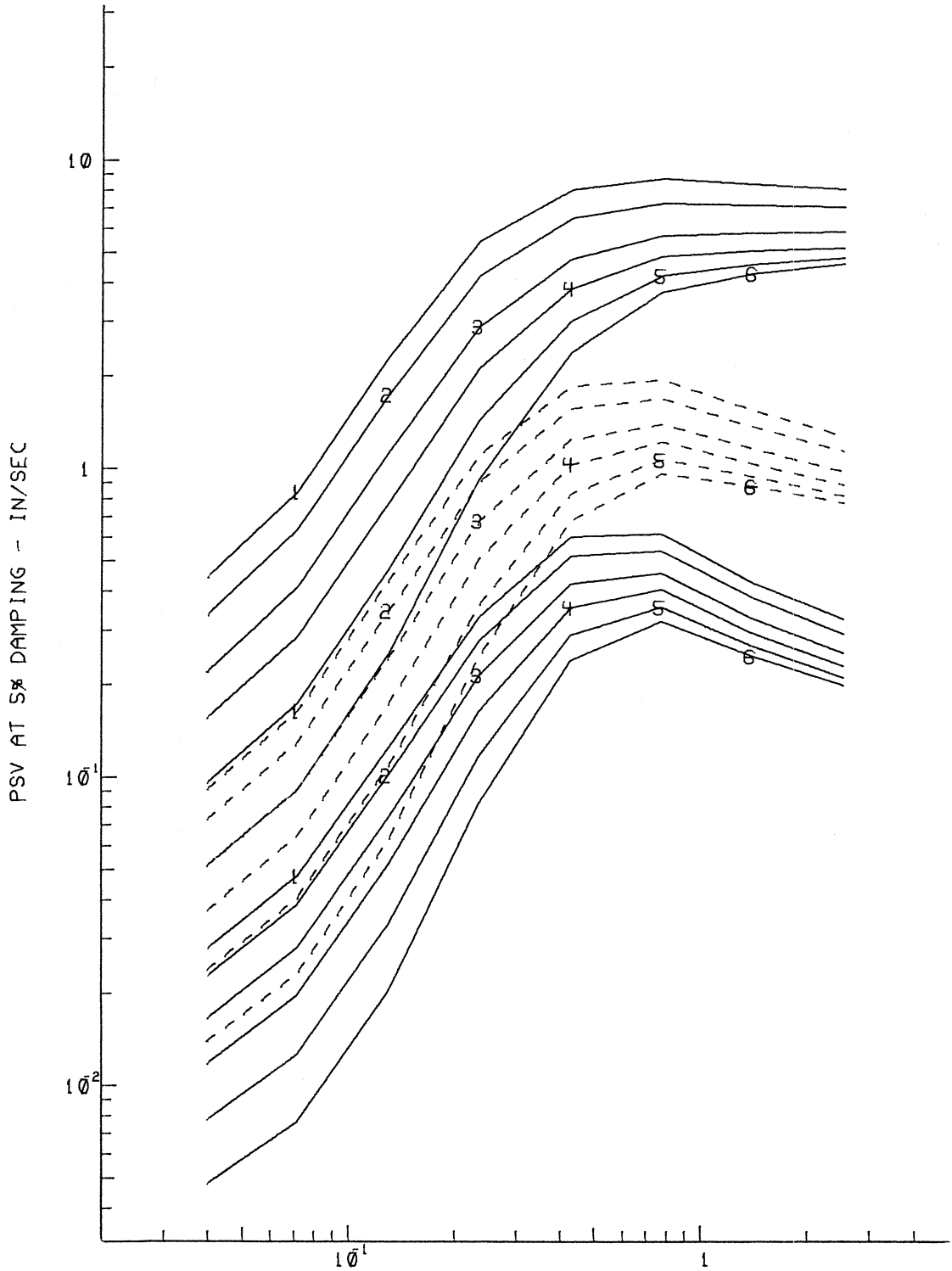
PERIOD - SEC  
 Figure 6.2.1

PSV SEISMIC RISK SPECTRA AT 6 SITES

FOR  $P = 0.1, 0.5 \text{ \& } 0.9$

MODEL II: ORIGINAL SCALING FUNCTIONS

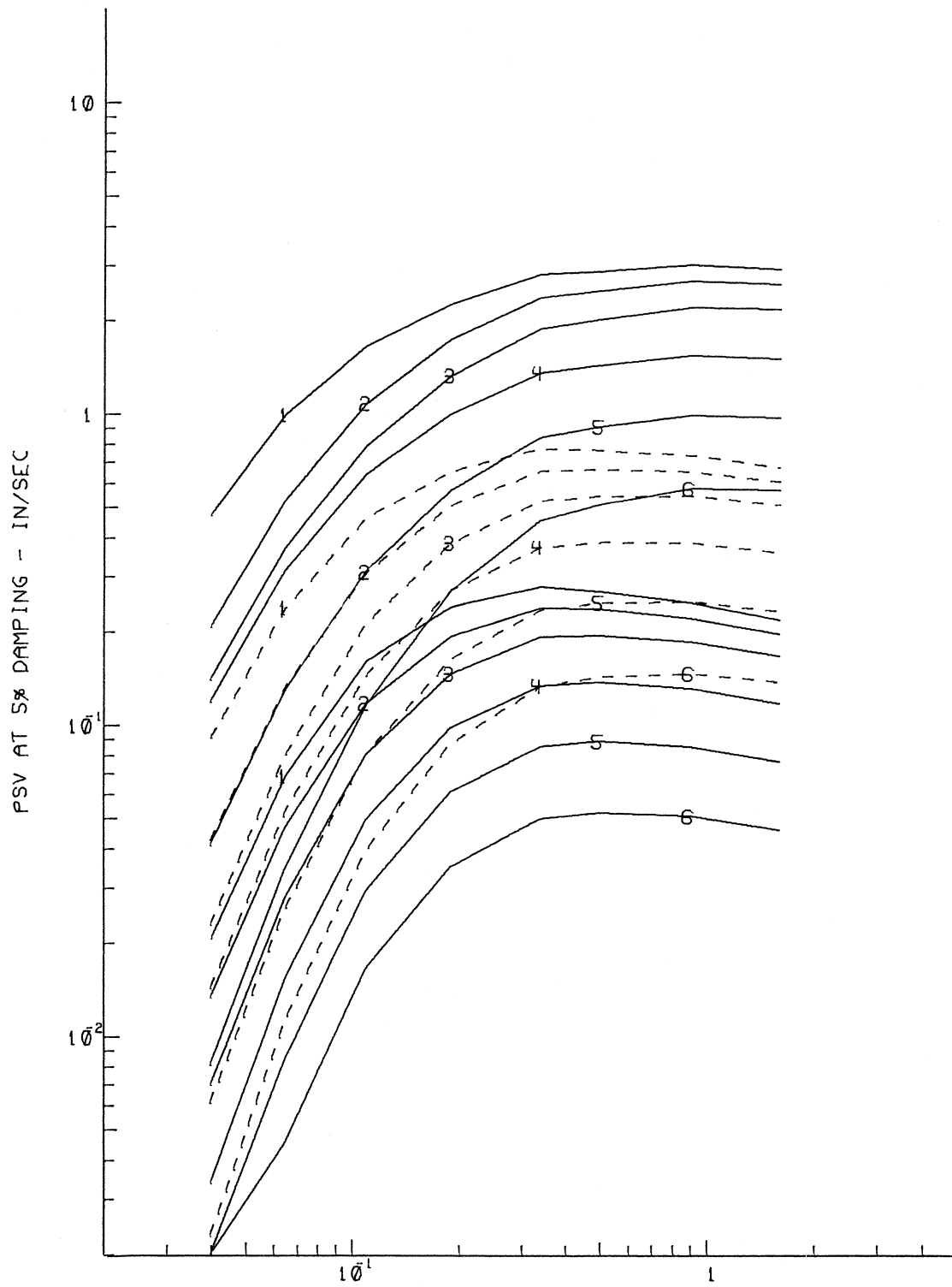
UNCERTAINTIES IN SEISMICITY INCLUDED



PERIOD - SEC

Figure 6.2.2

## PSV SEISMIC RISK SPECTRA AT 6 SITES

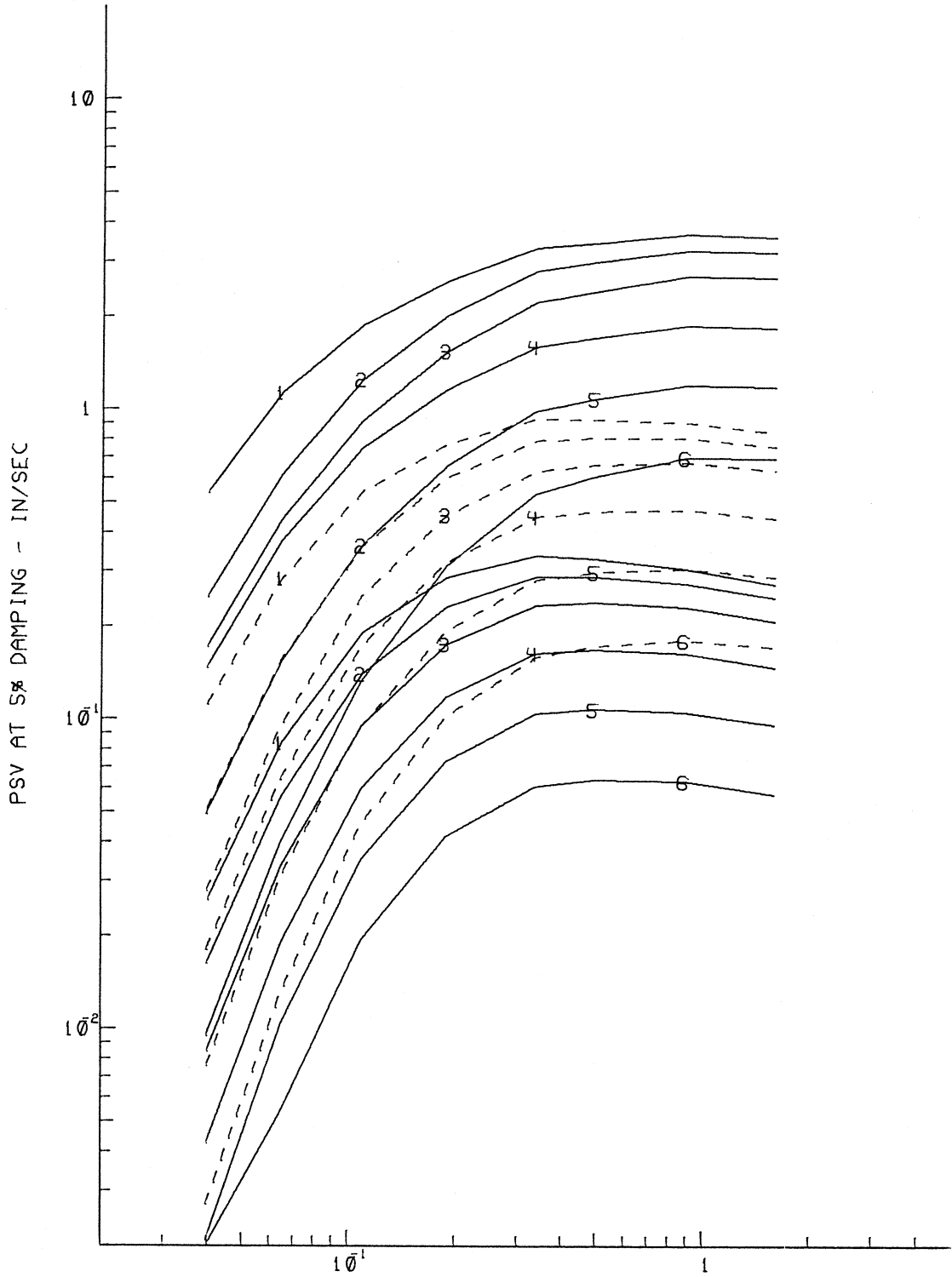
FOR  $P = 0.1, 0.5 \text{ \& } 0.9$   
MODEL III: NEW SCALING FUNCTIONS

PERIOD - SEC

Figure 6.2.3



PSV SEISMIC RISK SPECTRA AT 6 SITES  
FOR P = 0.1, 0.5 & 0.9  
MODEL IV: NEW SCALING FUNCTIONS  
UNCERTAINTIES IN SEISMICITY INCLUDED



PERIOD - SEC  
Figure 6.2.4

## PSV SEISMIC RISK SPECTRA AT SITE #1

FOR  $P = 0.1, 0.2, 0.35, 0.5 \text{ \& } 0.9$ 

ORIGINAL SCALING FUNCTIONS

UNCERTAINTIES IN SEISMICITY

MODEL I (-----): NOT INCLUDED

MODEL II (SOLID): INCLUDED

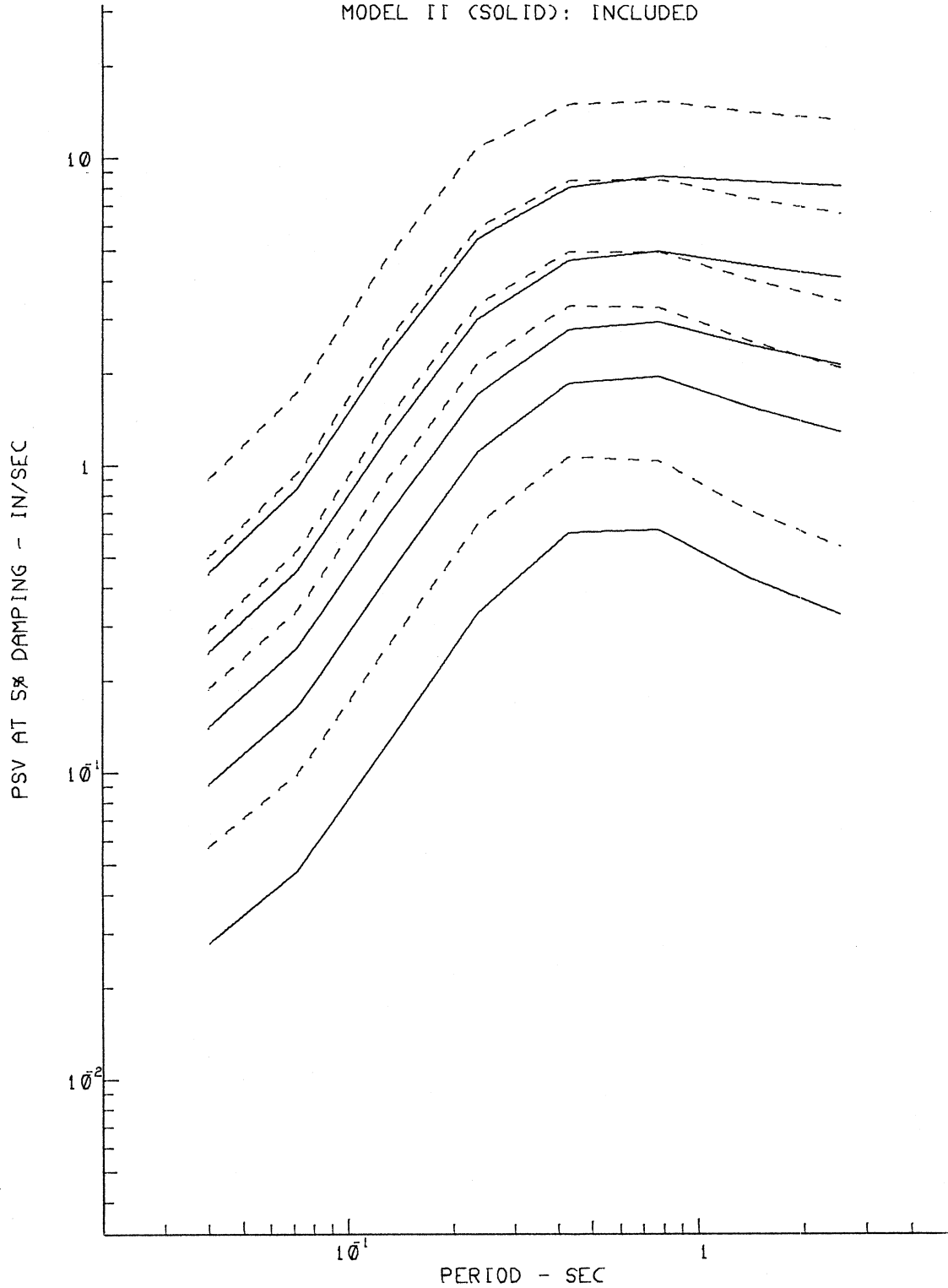


Figure 6.3.1

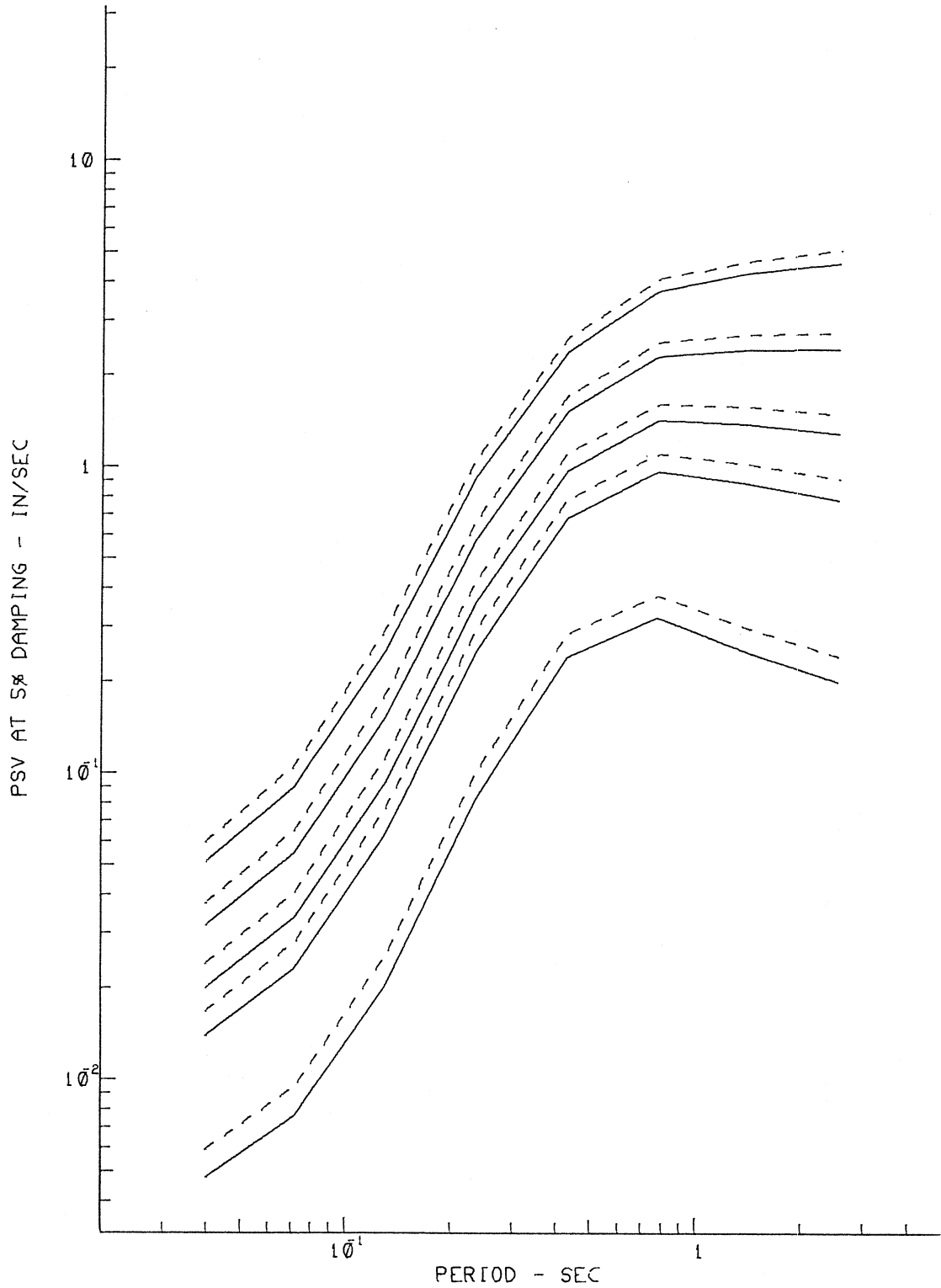
## PSV SEISMIC RISK SPECTRA AT SITE #6

FOR  $P = 0.1, 0.2, 0.35, 0.5$  &  $0.9$ 

UNCERTAINTIES IN SEISMICITY:

MODEL I (-----): NOT INCLUDED

MODEL II (SOLID): INCLUDED



PERIOD - SEC

Figure 6.3.2

## PSV SEISMIC RISK SPECTRA AT SITE #1

FOR  $P = 0.1, 0.2, 0.35, 0.5 \text{ \& } 0.9$ 

NEW SCALING FUNCTIONS

UNCERTAINTIES IN SEISMICITY

MODEL III (-----): NOT INCLUDED

MODEL IV (SOLID): INCLUDED

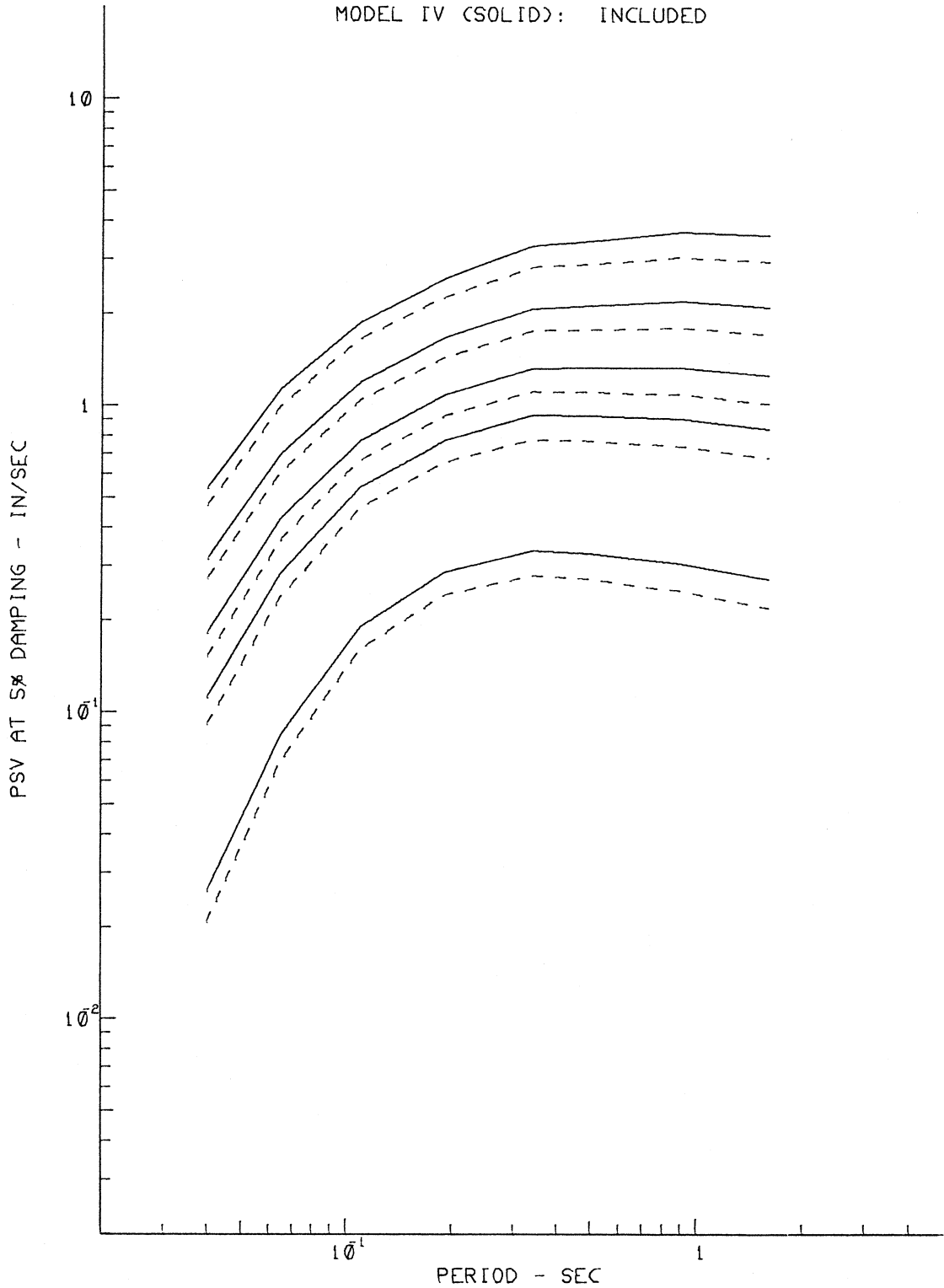


Figure 6.3.3

PSV SEISMIC RISK SPECTRA AT SITE #6

FOR P = 0.1, 0.2, 0.35, 0.5 & 0.9

NEW SCALING FUNCTIONS

UNCERTAINTIES IN SEISMICITY:

MODEL III (-----): NOT INCLUDED

MODEL IV (SOLID): INCLUDED

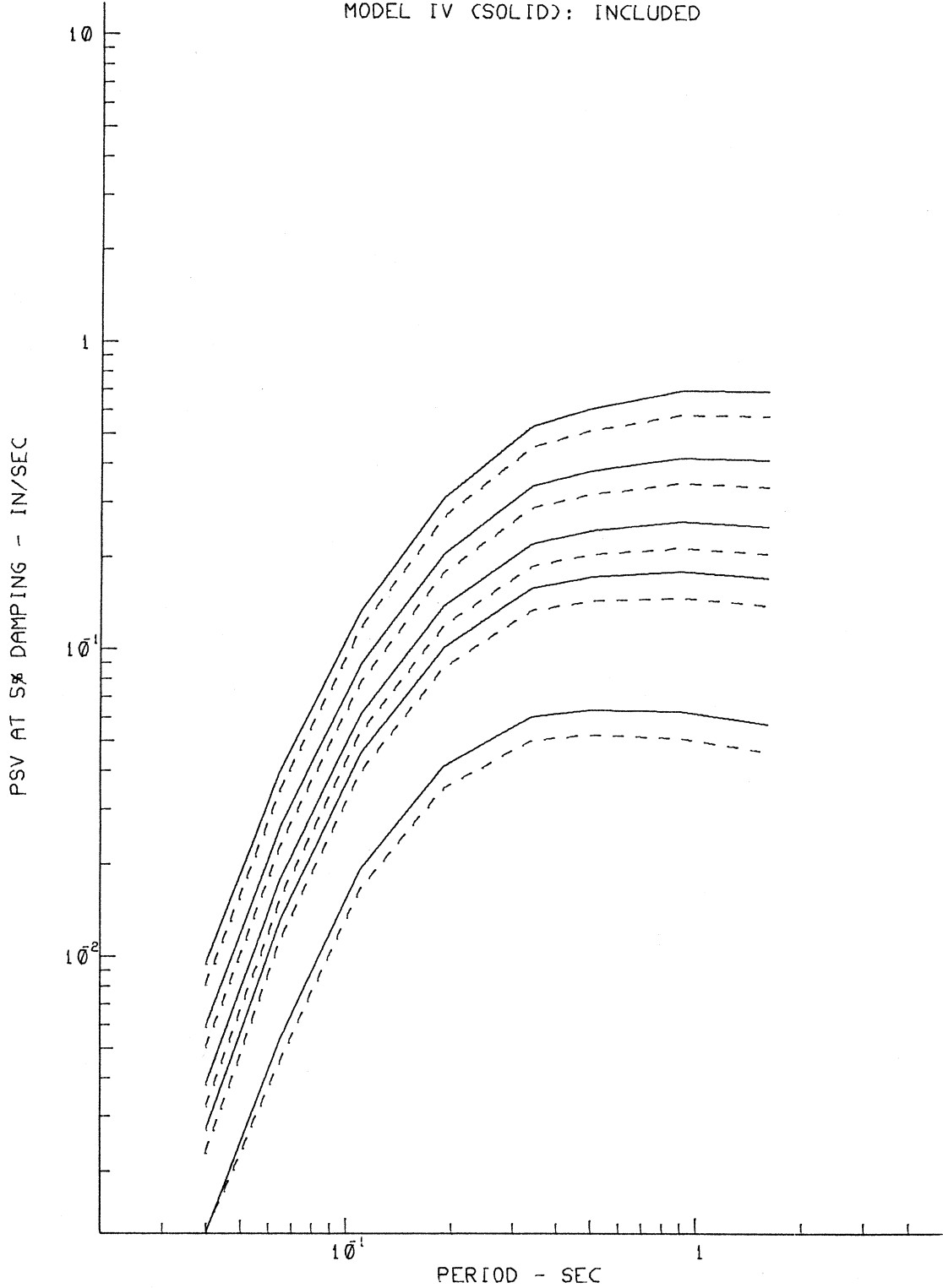
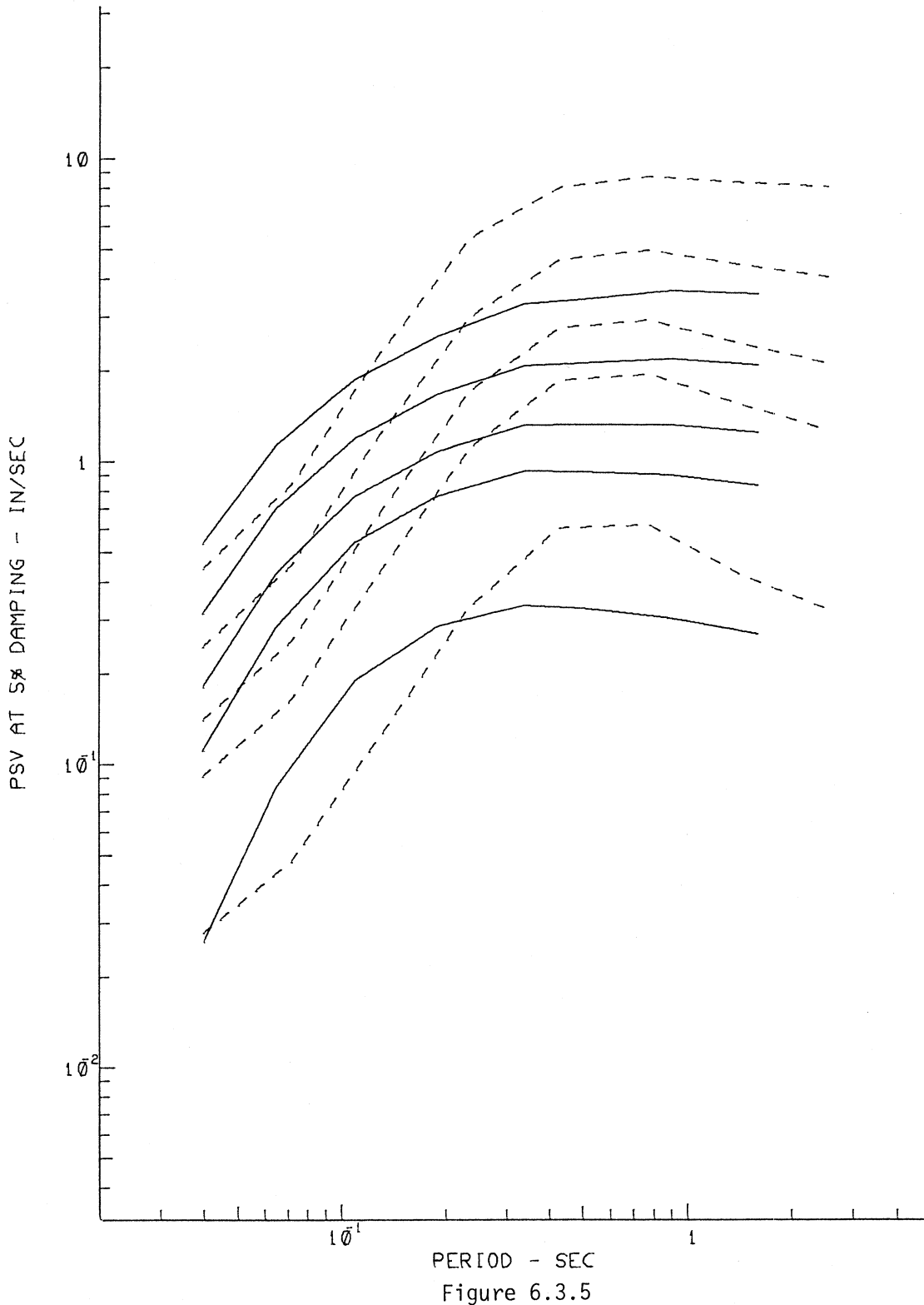


Figure 6.3.4

## PSV SEISMIC RISK SPECTRA AT SITE #1

FOR  $P = 0.1, 0.2, 0.35, 0.5$  &  $0.9$   
UNCERTAINTIES IN SEISMICITY INCLUDED  
MODEL II (-----): OLD SCALING FUNCTIONS  
MODEL IV (SOLID): NEW SCALING FUNCTIONS



## PSV SEISMIC RISK SPECTRA AT SITE #6

FOR  $P = 0.1, 0.2, 0.35, 0.5 \text{ \& } 0.9$   
UNCERTAINTIES IN SEISMICITY INCLUDED  
MODEL II (-----): OLD SCALING FUNCTIONS  
MODEL IV (SOLID): NEW SCALING FUNCTIONS

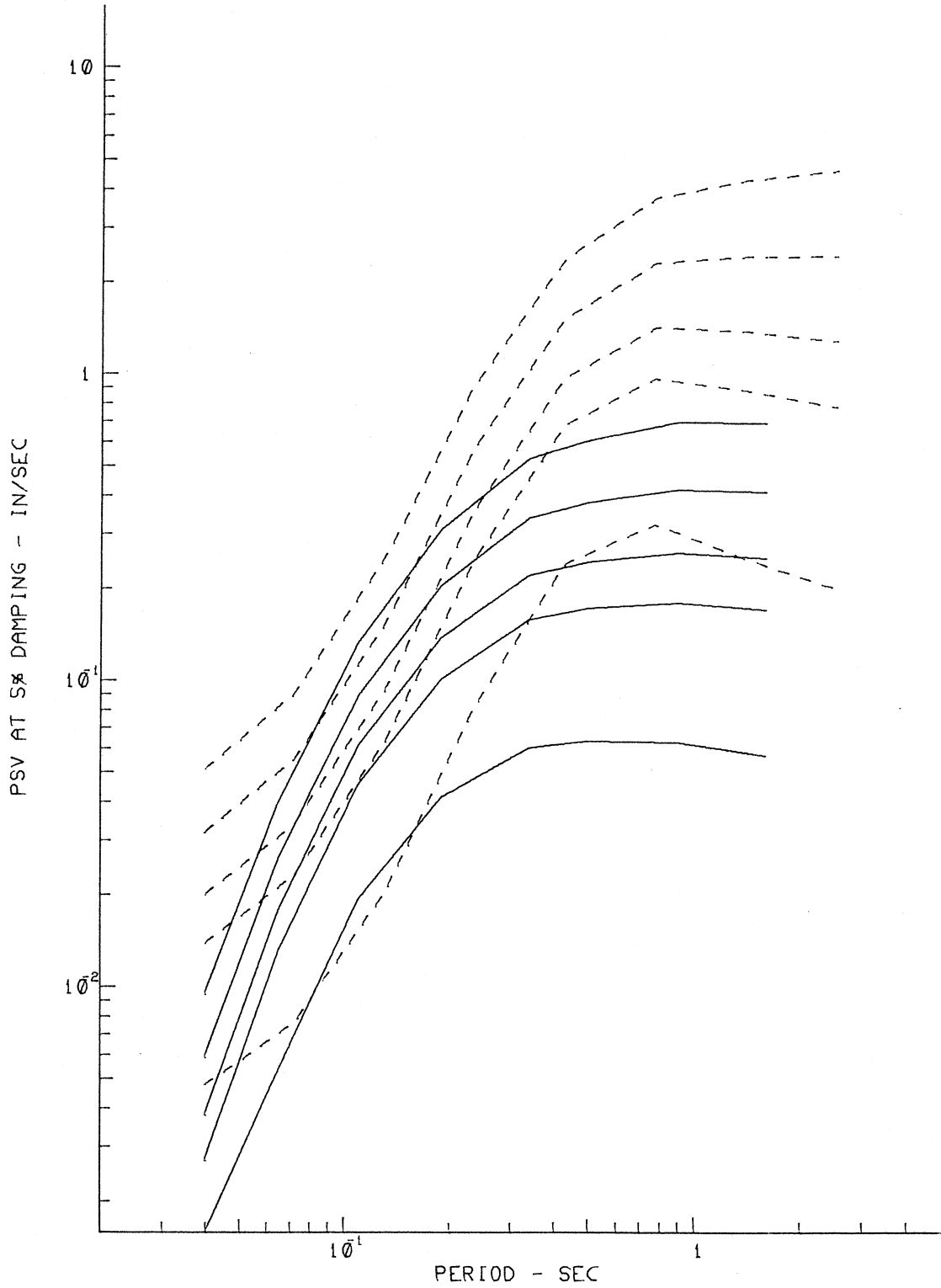


Figure 6.3.6

at the five probability levels for Model I, while the five solid lines correspond to those for Model II. Both Models I and II use the old scaling functions with Richter's attenuation function and the old database. The Model II differs from Model I in that Model II includes the uncertainties in the estimation of seismicity and of maximum allowed earthquake size in the calculation of the risk spectra. Figure 6.3.1 shows that for each of the five probability levels shown, the estimated PSV levels from Model I are higher than those from Model II in the entire period range. Figure 6.3.2 shows the same comparison of the two models but at site #6. The PSV spectra from Model I again are higher than the corresponding spectra from Model II, but this time to a smaller degree.

These two figures might lead one to conclude that, by including the uncertainties in the estimation of seismicity and in maximum allowed earthquake size into the calculation of risk spectra, the resulting amplitudes (Model II) at each level of probability may actually be lower than the corresponding spectra (Model I) computed without consideration of such uncertainties. Also the two figures might suggest that the differences may be larger for sites closer to the fault (site #1) than those further away (site #6).

#### 6.4 An Application

The following example is presented to illustrate the properties of the proposed model in a realistic practical setting. As in Anderson and Trifunac (1977), an application is made to evaluate the seismic risk for a site on the north coast of Puerto Rico, a site which has been studied by Kelleher et al. (1973), and by Der-Kiureghian and Ang (1975). To allow for comparison of the present model with that presented in Anderson and Trifunac (1977), the seismicity of the area will be described using the data available then



to Der-Kiureghian and Ang (1975), rather than obtaining a more current listing of events and their epicenters. The data used consists of a list of all events in the magnitude range from 3.0 to 8.5 that are known to have occurred in the area between 1915 and 1971. The area is within the rectangle bounded by latitudes  $17^{\circ}\text{N}$  to  $21^{\circ}\text{N}$  and longitudes  $63^{\circ}\text{W}$  to  $70^{\circ}\text{W}$ .

On the basis of the available events and using additional information in Kelleher et al. (1973), four models of the region have been constructed, each describing the seismicity to be expected in the region in the next 50 years. These four models, labeled A, B, C and D, are reconstructed here following Trifunac and Anderson (1977), where the models have been described independently by four experts, each describing the seismicity they expected in the same region during the next 50 years. The models are shown in Figure 6.4.1 and are identical to those in Figure 2.1.4 of Anderson and Trifunac (1977). The following is a brief summary of how the four models have been constructed:

Model A assumes that the seismicity during the next 50 years will essentially be the same as that which has occurred in the past. The map is divided into five zones: I, II, III, IV and V. Zones I through IV are subregions while zone V is the whole region ( $17^{\circ}$  to  $21^{\circ}\text{N}$ ,  $63^{\circ}$  to  $70^{\circ}\text{W}$ ) overlapping with the four subregions. The overall seismicity is first assigned to the whole region (zone V), and additional seismicity is then assigned to the four subregions (zones I, II, III and IV). The seismicity in each zone is scaled to account for the differences in the time periods for which the data is available and the period for which the risk is to be estimated (50 years). This model will not consider the incomplete coverage of small earthquakes for much of the historical record.

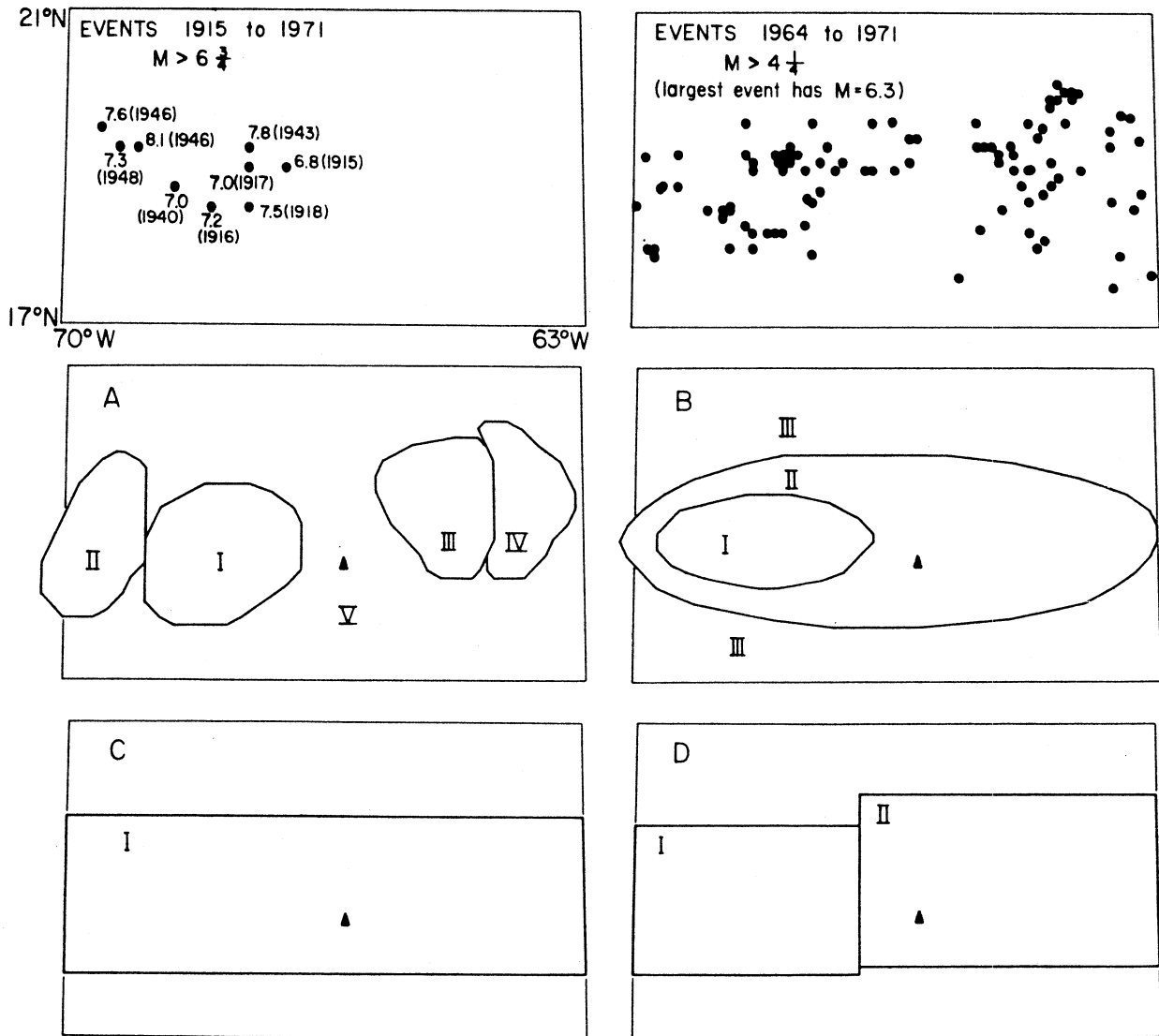


Figure 6.4.1 Seismicity in the vicinity of Puerto Rico, as given by Der-Kiureghian and Ang (1975), and 4 models to describe this seismicity. The boundary of all 6 maps is the same as shown in the upper left. The map at the upper left shows the epicenters of major earthquakes since 1915; the map at the upper right shows events with magnitude greater than  $4\frac{1}{4}$  which occurred between 1964 and 1971. The estimated seismicity rates in each zone of the 4 models (A,B,C,D) are in Table 6.4-1. These zones are the projections of the dipping planar source region for the risk estimates. Models are for the site shown by a solid triangle.

Model B assumes that the major seismic activity in the next 50 years will continue to occur where the major activity of the past was recorded. The map is divided into three zones: I, II and III. Zones I and II are subregions while zone III is again the whole region. As in Model A, the overall seismicity is first assigned to the whole region (zone III), and additional seismicity is then assigned to the two subregions (zones I and II). This model emphasizes the data on smaller events as recorded in recent years.

Model C assumes that the entire seismic activity is associated with an active plate margin, and makes no differentiation between the western portion which has a history of large events and the eastern portion which does not have that history. There is thus only one uniform zone for the whole region.

Model D consists of two zones: zone I for the western region and zone II for the eastern region. It assumes that because, as Kelleher et al. (1975) point out, the eastern region (zone IV) has not had any large historic earthquakes, that this portion of the plate margin must be considered a more likely candidate for a large earthquake in the future. The western region (zone I) was assigned the seismicity which is lower than the historic rates on the assumption that some of the strains there were already relieved by the past events, and would take some time to accumulate to a triggering level again.

The estimated seismicities in each zone of the four models (A,B,C and D) are given in Table 6.4-1. These models will be used to calculate the uniform risk spectra at a site shown in Figure 6.4.1.

TABLE 6.4-1  
 Number of Earthquakes assigned to the source zones of Figure 2.14  
 for the Puerto Rico applications.

Case	Zone	Area $10^4 \text{ km}^2$	Magnitude												
			3.0	3.5	4.0	4.5	5.0	5.5	6.0	6.5	7.0	7.5	8.0	8.5	
A	I	3.83	91	59	38	25	16	10	7	4	3	2	1	0	
	II	2.80	23	17	12	9	6	5	3.3	2.4	1.7	1.3	0.9	0	
	III	2.56	58	35	22	13	8	5	3	2	0	0	0	0	
	IV	1.78	83	44	23	12	6	3	2	1	0	0	0	0	
	V	32.61	107	54	28	14	7	4	2	1	0	0	0	0	
B	I	3.02	3583	1095	319	146	44	29	13	7	5	3	0.5	0	
	II	14.44	13555	4142	1209	554	166	111	50	0	0	0	0	0	
	III	32.62	20779	6350	1852	0	0	0	0	0	0	0	0	0	
C	I	16.33			66	40	23	13	6	5	3	2	1		
D	I	6.83			501	178	63	22	8	3	1	0	0		
	II	10.26			889	315	112	40	14	5	3	1.5	0		

In calculating the uniform risk spectra for the site, variations of each of these models have been considered:

Variation 1 assigns each of the zones of each model to be a diffuse region on the surface. To allow for comparison of the present model with the previous ones, the length of rupture is not included here as in Anderson and Trifunac (1977). This means that each event will be assumed to have rupture length zero, or equivalent, each event is assumed to be a point source, with equal probability of occurring anywhere within the specified zone.

Variation 2 assigns each of the zones of each model to be a diffuse region on a plane dipping south from the northern edge of the region at an angle of 35 degrees. This variation is probably more realistic in describing the geometry of the seismic zone. In the old model of "EQRISK," as was pointed out in Anderson and Trifunac (1977), an approximate extension of the model for attenuation was made for this case. This was done by replacing the epicentral distance with the hypocentral distance. It was emphasized then that this is an approximation. In the present new model of "NEQRISK," as we noted in Section 3.2, a frequency dependent attenuation function,  $\mathcal{A}tt(\Delta, M, T)$  is employed and a new function  $\Delta = \Delta(S, H, R)$ , (equation 3.2.2), known as the "representative distance" from the earthquake source of size  $S$ , at depth  $H$  and epicentral distance  $R$  from the recording site is used.

Figures 6.4.2 and 6.4.3 show uniform risk spectra for the seismicity models for variations 1 and 2, calculated using the old "EQRISK" program. Figures 6.4.4 and 6.4.5 present the uniform risk spectra for the same seismicity models but for variations 1 and 2 calculated using the new "NEQRISK" program, with the new frequency dependent attenuation function  $\mathcal{A}tt(\Delta, M, T)$  and the new "representative" source-to-station distance  $\Delta$ .

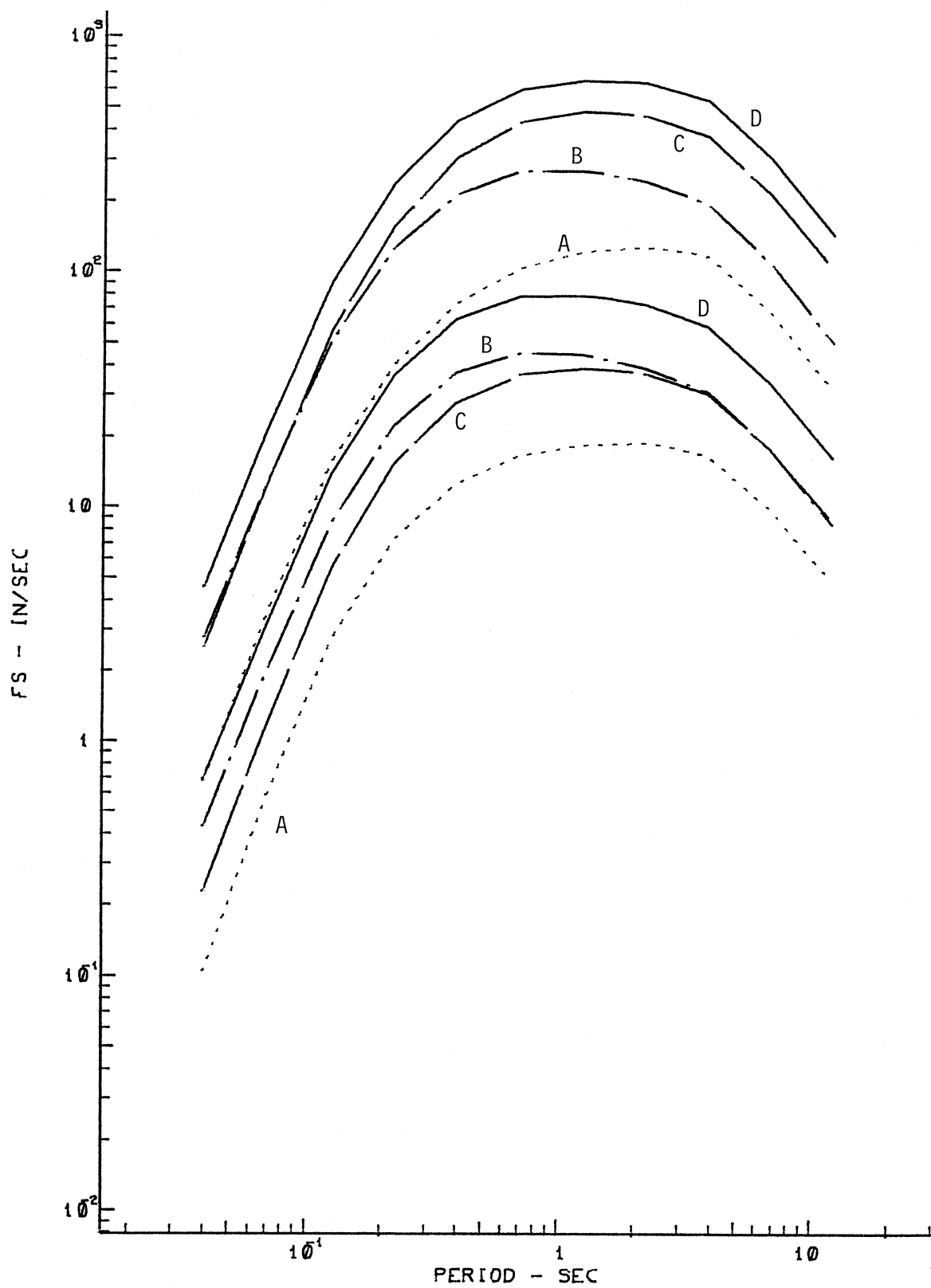


Figure 6.4.2

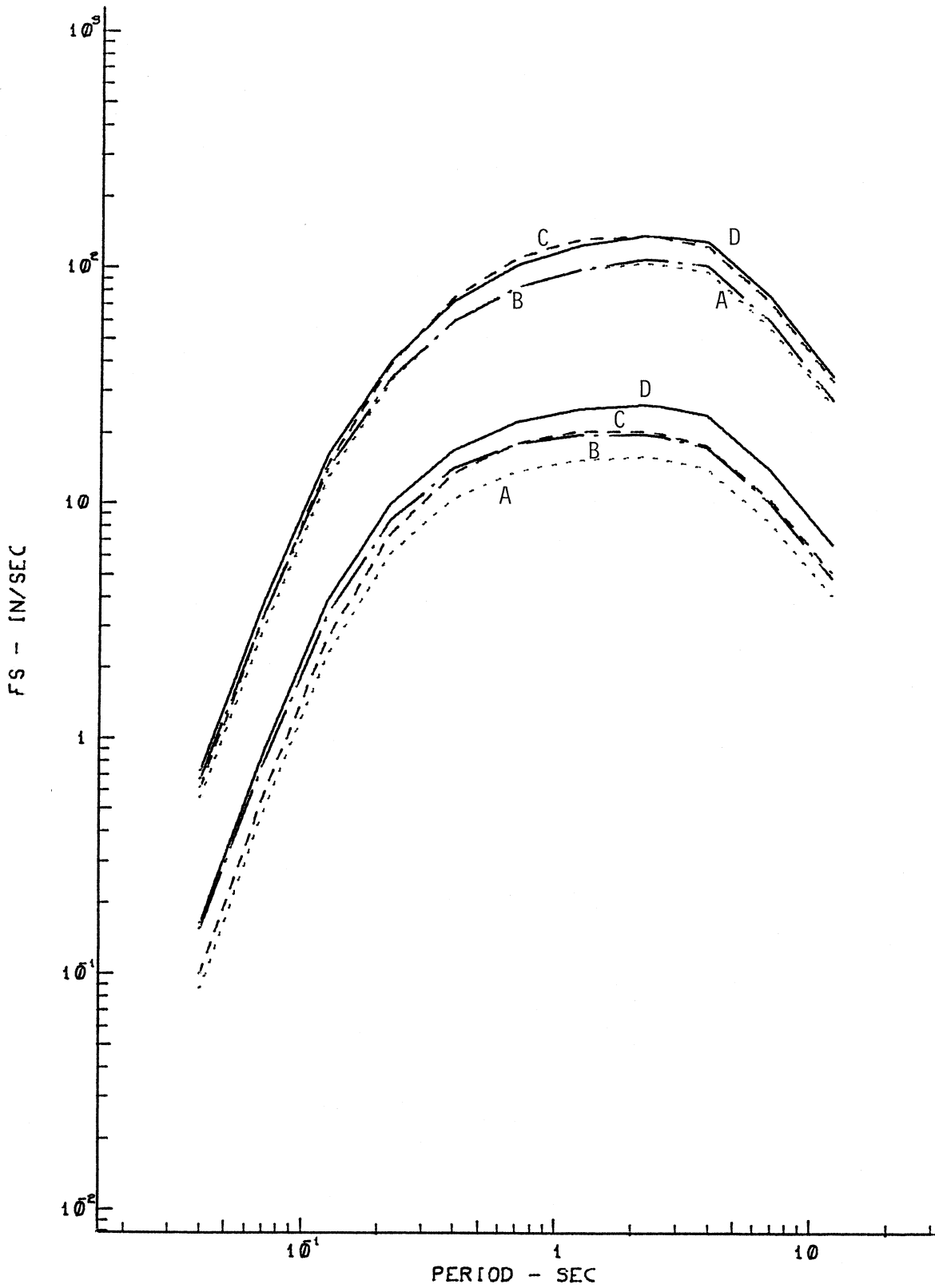


Figure 6.4.3

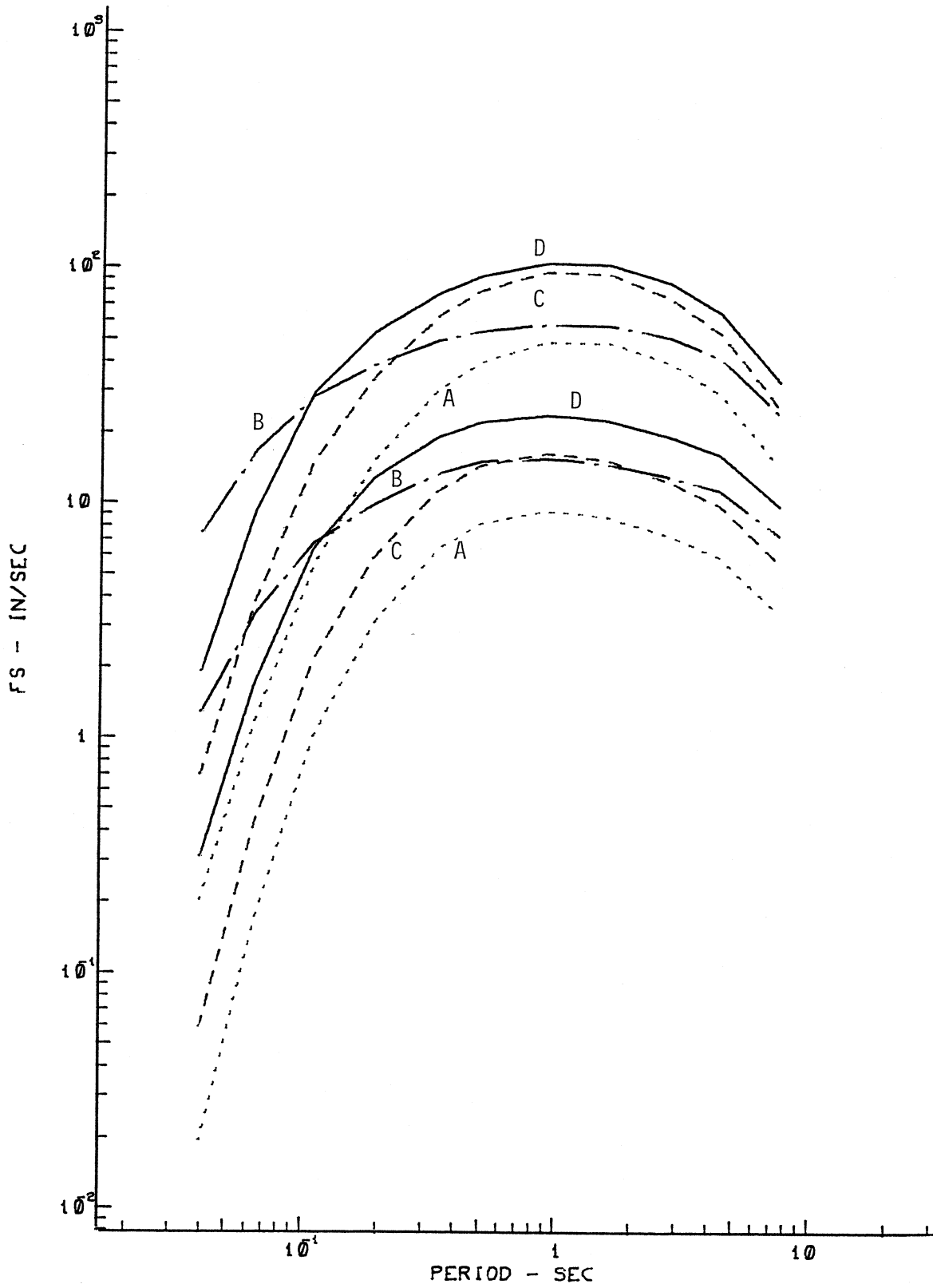


Figure 6.4.4



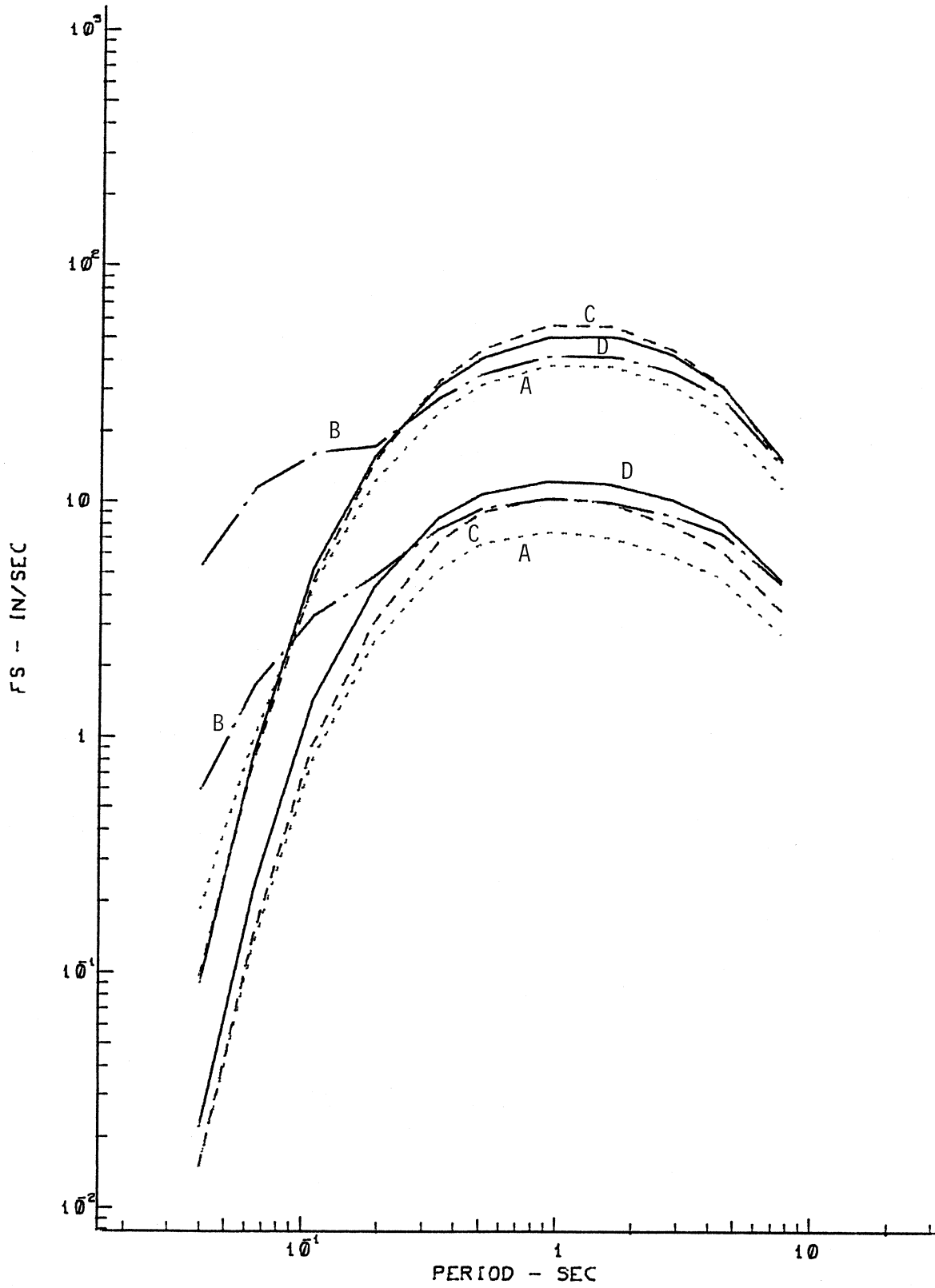


Figure 6.4.5

Several observations can be made about the spectra in the four figures 6.4.2 through 6.4.5. First, in the spectra for the old scaling with the "EQRISK" program (Figures 6.4.2 and 6.4.3), the differences between the spectral amplitudes resulting from cases A-D for a given probability level are considerably greater for the diffuse source, Variation 1, than for the dipping plane source, Variation 2. This is due to the fact that the large events, which contribute most to the spectral amplitudes, are in a wider distance range when they are placed on the surface (Variation 1) than when they are placed on the dipping plane (Variation 2). Similar observations can be made about the spectra in Figure 6.4.4 and 6.4.5, for the same seismicity models, for Variations 1 and 2, but calculated by the new "NEQRISK" program.

In using the old attenuation function, it is noted that Model A is depleted in spectral amplitudes of intermediate and high frequencies relative to the other three models (Figures 6.4.2 and 6.4.3), in particular for Variation 1. This is because Model A assumes a small number of small events close to the site. In using the new frequency dependent attenuation function, the similar observation can be made about Model A (Figures 6.4.4 and 6.4.5). It is also noted that Model B has large amplitudes in the high frequency range beyond 10 Hz, when compared to the amplitudes of Models A, C and D. Model B is unique, compared with other models, in that the expected number of small events in the region close to the site is substantially higher for this than for all other models (Table 6.4-1). The new attenuation function  $A(\Delta, M, T)$  attenuates faster than the Richter's attenuation function in the distance range below 50 to 100 km and for high frequencies. This results in Model B having risk spectra with higher amplitudes in that period range and from small nearby earthquakes.

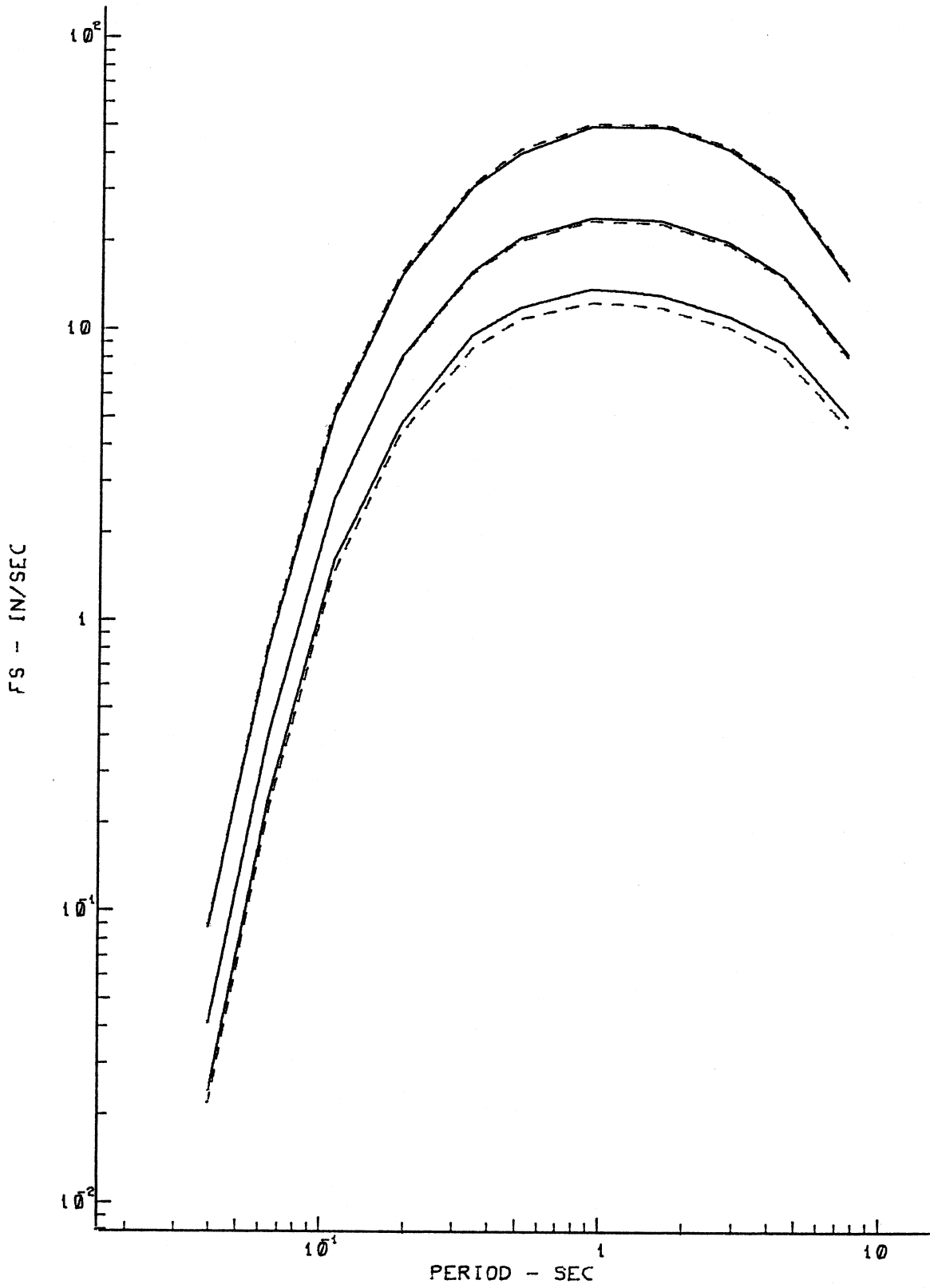


Figure 6.4.6

Finally, a variation of Model D is considered. Recall that for this it is assumed that since its eastern region (region II) did not have any large historic earthquakes, that that portion of the plate margin might be considered as a more likely candidate for a large earthquake in the future. One possible example is to assume then that the expected number of earthquakes in this eastern region (region II) will be literal, while leaving the expected earthquake occurrence rates of the western region (region I) to be Poissonian. Figure 6.4.6 shows the uniform risk spectra for this model at the 10, 50 and 90% probability levels of exceedance. The solid lines represent the risk spectra with the seismicity in the eastern region assumed to be literal while the dashed lines represent the assumption that all the seismicity in all the regions (I and II) is Poissonian.

## ACKNOWLEDGEMENTS

This work was supported in part by a contract from the U.S. Nuclear Regulatory Commission through SEEC and by grants from the National Science Foundation.

## REFERENCES

1. Algermissen, S. T. and Perkins, D. M. (1976). "A Probabilistic Estimate of Maximum Acceleration in Rock in the Contiguous United States," Department of the Interior Geological Survey, Open File Report 76-416.
2. Anderson, J. G. and Trifunac, M. D. (1977). "On Uniform Risk Functionals which Describe Strong Earthquake Ground Motion: Definition, Numerical Estimation and an Application to the Fourier Amplitude of Acceleration," Report No. CE 77-02, Civil Engineering Department, University of Southern California, Los Angeles.
3. Anderson, J. G. (1978). "Program EQRISK: A Computer Program for Finding Uniform Risk Spectra of Strong Earthquake Ground Motion," Report No. CE 78-11, Civil Engineering Department, University of Southern California, Los Angeles.
4. Anderson, J. G. (1979a). "Estimating the Seismicity from Geological Structure for Seismic-Risk Studies," Bull. Seism. Soc. Am., 69, pp. 135-158.
5. Anderson, J. G. (1979b). "On the Attenuation of Modified Mercalli Intensity with Distance in the United States," Appendix D, in Methods for Prediction of Strong Earthquake Ground Motion, U.S. Nuclear Regulatory Commission, NUREG/CR-068
6. Brune, J. (1970). "Tectonic Stress and the Spectra of Seismic Shear Waves from Earthquakes," J. Geophys. Res., 75, pp. 4997-5009.
7. Cornell, C. A. (1968). "Engineering Seismic Risk Analysis," Bull. Seism. Soc. Amer., 58, pp. 1583-1606.
8. Dalal, J. G. (1973). "Probabilistic Seismic Exposure and Structural Risk Evaluation," Ph.D. Dissertation, Stanford University.
9. DeCapua, N. J. and Liu, S. C. (1974). "Statistical Analysis of Seismic Environment in New York State," Fifth Symposium on Earthquake Engineering, Roorkee, India, pp. 389-396.
10. Der-Kiureghian, A. and Ang, A. H-S (1975). "A Line Source Model for Seismic Risk Analysis," University of Illinois, Urbana.
11. Der-Kiureghian, A. and Ang, A. H-S (1977). "Risk Consistent Earthquake Response Spectra," Proc. Sixth World Conference on Earthquake Engineering, New Delhi, India.
12. Der-Kiureghian, A. (1977). "Analysis of Uncertainties in Seismic Risk Evaluation," Proc. 2-nd ASCE EMD Specialty Conference, N. Carolina State Univ., N. Carolina, pp. 320-323.

13. Douglas, B. M. and Ryall, A. (1975). "Return Periods for Rock Acceleration in Western Nevada, Bull. Seism. Soc. Amer., 65, pp. 15-99-1611.
14. Gusev, A. A. (1983). "Descriptive Statistical Model of Earthquake Source Radiation and its Application to an Estimation of Short-Period Strong Motion," Geophys. J. Royal Astr. Soc., 74, pp. 787-808.
15. Kelleher, J., Sykes, L. and Oliver, J. (1973). "Possible Criteria for Predicting Earthquake Locations and their Application to Major Plate Boundaries of the Pacific and the Caribbean, J. Geophys. Res., 78, pp. 2547-2585.
16. Lee, V. W. and Trifunac, M. D. (1984). "Current Developments in Data Processing of Strong Motion Accelerograms," Report No. 84-01, Civil Engineering Department, University of Southern California, Los Angeles.
17. Lee, V. W. and Trifunac, M. D. (1985). "Attenuation of Modified Mercalli Intensity for Small Epicentral Distance in California, Report No. 85-01, Civil Engineering Department, University of Southern California, Los Angeles.
18. Liu, S. C. and Fagel, L. W. (1972). "Earthquake Environment for Physical Design: A Statistical Analysis," The Bell System Technical Journal, 51, pp. 1957-1982.
19. McGuire, R. K. (1974). "Seismic Structural Response Risk Analysis, Incorporating Peak Response Regressions on Earthquake Magnitude and Distance," Department of Civil Engineering, Massachusetts Institute of Technology, Cambridge MA.
20. Milne, W. G. and Davenport, A. G. (1969). "Distribution of Earthquake Risk in Canada," Bull. Seism. Soc. Amer., 59, pp. 729-754.
21. Oetken G., Parks, T. W. and Schuster, H. W. (1975). "New Results in the Design of Digital Interpolators," IEEE Trans. on Acoustics, Speech and Signal Processing, ASSP-23, No. 3, June.
22. Richter, C. F. (1958). "Elementary Seismology," Freeman Publishing Company, San Francisco.
23. Trifunac, M. D. (1976). "Preliminary Empirical Model for Scaling Fourier Amplitude Spectra of Strong Ground Motion in terms of Earthquake Magnitude, Source to Station Distance, and Recording Site Conditions," Bull. Seism. Soc. Amer., 66, pp. 1343-1373.
24. Trifunac, M. D. (1977). "Forecasting the Spectral Amplitudes of Strong Earthquake Ground Motion," Proc. Sixth World Conference on Earthquake Engineering, New Delhi, India.
25. Trifunac, M. D. and Anderson, J. G. (1977). "Preliminary Empirical Models for Scaling Absolute Acceleration Spectra," Civil Engineering Department, Report No. 77-03, University of Southern California, Los Angeles.

26. Trifunac, M. D. and Anderson, J. G. (1978a). "Preliminary Empirical Models for Scaling Pseudo Relative Velocity Spectra," Civil Engineering Department, Report No. 78-04, University of Southern California, Los Angeles.
27. Trifunac, M. D. and Anderson, J. G. (1978b). "Preliminary Empirical Models for Scaling Relative Velocity Spectra," Civil Engineering Department, Report No. 78-05, University of Southern California, Los Angeles.
28. Trifunac, M. D. and Lee, V. W. (1978). "Dependence of the Fourier Amplitude Spectra of Strong Motion Acceleration on the Depth of Sedimentary Deposits," Civil Engineering Department, Report No. 78-04, University of Southern California, Los Angeles.
29. Trifunac, M. D. (1979). "Preliminary Empirical Model for Scaling Fourier Amplitude Spectra of Strong Motion Acceleration in Terms of Modified Mercalli Intensity and Geologic Site Conditions," Int. J. Earthquake Engr. and Struc. Dyn., 1, pp. 63-79.
30. Trifunac, M. D. and Lee, V. W. (1979). "Dependence of Pseudo Relative Velocity Spectra of Strong Motion Acceleration on the Depth of Sedimentary Deposits," Civil Engineering Department, Report No. 79-02, University of Southern California, Los Angeles.
31. Trifunac, M. D. and Lee, V. W. (1985a). "Frequency Dependent Attenuation of Strong Earthquake Ground Motion," Civil Engineering Department, Report No. 85-02, University of Southern California, Los Angeles.
32. Trifunac, M. D. and Lee, V. W. (1985b). "Preliminary Empirical Model for Scaling Fourier Amplitude Spectra of Strong Ground Acceleration in Terms of Earthquake Magnitude, Source to Station Distance, Site Intensity and Recording Site Conditions: Second Paper," Civil Engineering Department, Report No. 85-03, University of Southern California, Los Angeles.
33. Trifunac, M. D. and Lee, V. W. (1985c). "Preliminary Empirical Model for Scaling Pseudo Relative Velocity Spectra of Strong Earthquake Acceleration in Terms of Earthquake Magnitude, Source to Station Distance, Site Intensity and Recording Site Conditions," Civil Engineering Department, Report No. 85-04, University of Southern California, Los Angeles.